MMM--3691-47

228

6/5/69

826

uc-33

unclass

MASTER

LKK 6/10/69

SNAP-21 PROGRAM, PHASE II

DEEP SEA RADIOISOTOPE-FUELED THERMOELECTRIC GENERATOR POWER SUPPLY SYSTEM

QUARTERLY REPORT NO. 11

P1553

Space and Defense Products
ELECTRICAL PRODUCTS GROUP
3-M CENTER, ST. PAUL, MINN. 55101, PH 633-9400
3M COMPANY

SNAP-21 PROGRAM, PHASE II

DEEP SEA RADIOISOTOPE-FUELED THERMOELECTRIC GENERATOR POWER SUPPLY SYSTEM

QUARTERLY REPORT NO. 11

Space and Defense Products
ELECTRICAL PRODUCTS GROUP
3-M CENTER, ST. PAUL, MINN. 55101, PH 633-9400
3M COMPANY

DISCLAIMER

Report No. MMM 3691-47

AEC RESEARCH AND DEVELOPMENT REPORT

This report has been prepared under Contract AT(30-1)3691
with the U.S. Atomic Energy Commission

SNAP-21 PROGRAM, PHASE II

DEEP SEA RADIOISOTOPE-FUELED THERMOELECTRIC GENERATOR POWER SUPPLY SYSTEM

QUARTERLY REPORT NO. 11

Period Covered

January 1, 1969 to March 31, 1969

Prepared by

SNAP-21
Technical Staff

Approved by

J. A. Brandt

J. Brandt
Manager,
SNAP-21 Program

Issued by

Space and Defense Products

MINNESOTA MINING AND MANUFACTURING COMPANY

ST. PAUL, MINNESOTA 55101

Blank page

LEGAL NOTICE

This report was prepared as an account of Government sponsored work. Neither the United States, nor the Commission, nor any person acting on behalf of the Commission:

A. Makes any warranty or representation, expressed or implied, with respect to the accuracy, completeness, or usefulness of of the information contained in this report, or that the use of any information, apparatus, method, or process disclosed in this report may not infringe privately owned rights; or

B. Assumes any liabilities with respect to the use of, or for damages resulting from the use of any information, apparatus, method, or process disclosed in this report.

As used in the above, "person acting on behalf of the Commission" includes any employee or contractor of the commission, or employee of such contractor, to the extent that such employee or contractor of the Commission, or employee of such contractor prepares, disseminates, or provides access to, any information pursuant to his employment or contract with the Commission, or his employment with such contractor.

DISTRIBUTION LIST

	No. of Copies
U.S. Atomic Energy Commission Division of Reactor Development and Technology Washington, D.C. 20545 Attn: S.J. Seiken	5
U.S. Atomic Energy Commission New York Operations Office 376 Hudson Street New York, New York 10014 Attn: L. Wasser	2
U.S. Atomic Energy Commission NY Patents Group Upton, New York 11973	1
Director, Nuclear Engineering Division Naval Facilities Engineering Command Washington, D.C.	1
U.S. Atomic Energy Commission RDT Site Office, 3M Company 2501 Hudson Road Space Center, Building 551 St. Paul, Minnesota 55119 Attn: John J. Stefano	1
Isotopes Development Center ORNL Post Office Box X Oak Ridge, Tennessee 37830 Attn: R.A. Robinson	2
Hittman Associates, Inc. Technical Information Department 9190 Red Branch Road Columbia, Maryland 21043	1

TID-4500
Category UC-33

Blank page

TABLE OF CONTENTS

TABLE OF CONTENTS (Continued)

LIST OF FIGURES

LIST OF FIGURES (Continued)

LIST OF TABLES

Blank page

1.0 SUMMARY

1.0 SUMMARY

The most significant technical accomplishments on the SNAP-21 Program during this period are:

- Heat-up of system S10D3 was initiated.
- System S10D3 Shipping Container Environmental test was performed.
- System S10D2 continued on long-term test.
- Completed Stable Reference Performance test for systems S10P1 and S10P2.
- Completed successful hydrostatic testing of systems S10P1, S10P2, and S10P3.
- Completed dynamic testing of systems S10P1, S10P2, and S10P3.
- Insulation system B10DL5 was incorporated into S10P3.
- Completed assembly and test of insulation system B10DL6.
- Completed processing of materials for insulation systems B10DL7 and B10DL8.
- Insulation system B10DL6 was integrated with the thermoelectric generator, A10P1, for long-term test.
- Continued testing of Phases I and II thermoelectric generators and power conditioners.
- Completed design of handling adapter for the Phase I stainless steel pressure vessel.
- Preliminary planning and scheduling was started in anticipation of Task II.

2.0 TASK I – 10-WATT SYSTEM

2.0 TASK I - 10-WATT SYSTEM

2.1 SYSTEMS

2.1.1 Electrically Heated Systems

2.1.1.1 System S10D2

System S10D2 continued on long-term performance test. There have been some changes in the system temperature. This is due to the one watt decrease in power input. One watt is equivalent to approximately 8°F on the hot side. Figure 2-1 shows thermoelectric generator and system power output. For this report period the performance for the system has been stable. Table 2-1 shows the thermoelectric generator and system electrical performance. Table 2-2 shows the thermal performance data for the system. Figure 2-2 shows system instrumentation. The normalized thermoelectric generator performance data is presented in Figure 2-3. It can be seen that the thermoelectric generator and system performance have been stable.

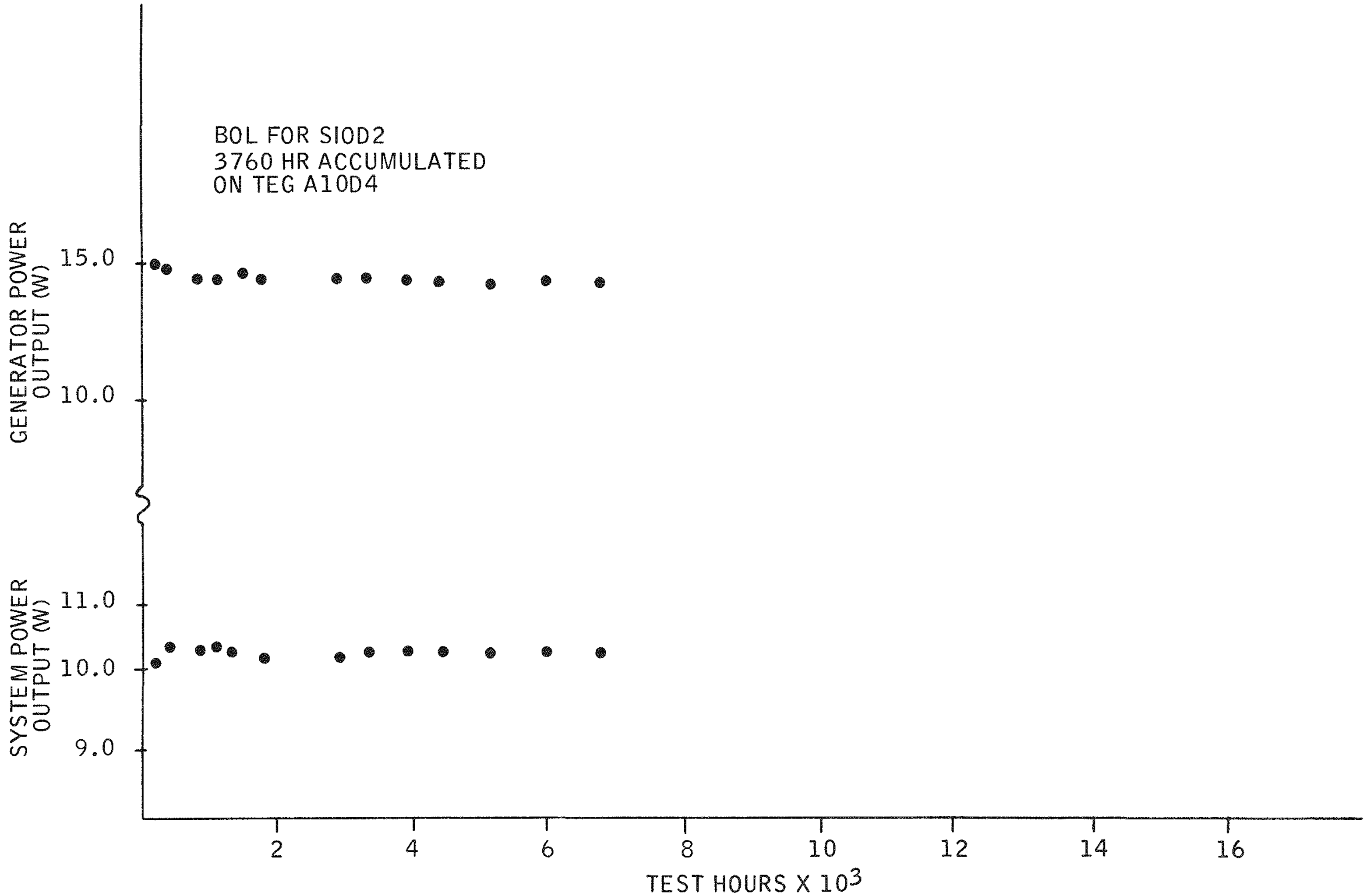

Figure 2-1. System S10D2 Performance

Table 2-1. System S10D2 Electrical Performance

Item	4/24/68	9/4/68	11/15/68	2/24/69
System Power Input (corrected-watts)	218	220	220	219
Generator Primary Load Voltage (vdc)	5.32	5.29	5.30	5.30
Generator Bias Load Voltage (vdc)	0.739	0.734	0.736	0.736
Generator Primary Load Current (amperes)	2.89	2.80	2.78	2.75
Generator Bias Load Current (amperes)	0.142	0.138	0.136	0.136
Generator Primary Power Output (watts)	15.30	14.81	14.73	14.57
Generator Bias Power Output (watts)	0.105	0.101	0.100	0.100
Generator Total Power Output (watts)	15.405	14.91	14.83	14.67
Conditioner Primary Voltage Input (vdc)	5.31	5.26	5.27	5.27
Conditioner Bias Voltage Input (vdc)	0.734	0.724	0.726	0.726
Conditioner Primary Current Input (amperes)	2.89	2.80	2.78	2.75
Conditioner Bias Current Input (amperes)	0.142	0.138	0.136	0.136
Conditioner Primary Power Input (watts)	15.25	14.73	14.65	14.49
Conditioner Bias Power Input (watts)	0.104	0.099	0.098	0.098
Conditioner Total Power Input (watts)	15.35	14.82	14.74	14.58
System Load Voltage (vdc)	24.6	24.5	24.48	24.48
System Load Current (amperes)	0.428	0.426	0.426	0.426
System Load (ohms)	57.48	57.38	57.5	57.5
System Power Output (measured) (watts)	10.53	10.46	10.43	10.43
Test Hours	233	1771	3502	6798
Primary Open Circuit (volts)	9.46	9.40	9.30	9.22
Primary Load Voltage (volts)	5.32	5.29	5.30	5.30
Primary Load Current (amps)	2.87	2.80	2.78	2.75
Bias Open Circuit (volts)	1.39	1.37	1.37	1.35
Bias Load Voltage (volts)	0.739	0.734	0.736	0.736
Bias Load Current (amps)	0.142	0.138	0.136	0.136
Internal Resistance (ohms)	1.43	1.46	1.43	1.41
Total Power Output (watts)	15.40	14.91	14.83	14.67

Table 2-2. System S10D2 Temperature Profile in Water

Thermocouple Location (See Figure 2-2)	Identification	Pre-Dynamic Test 4/28/68 (°F)	Post-Hydro Test 9/4/68 (°F)	Long-Term Test	
				11/15/68	2/24/69
1	Segmented Ring at Pressure Vessel Wall	39	43	45	40
2	TEG Mounting Plate (inner)	50	54	56	50
3	TEG Cold Frame Center (external)	58	63	65	59
4	TEG Hot Frame Center (external)	1042	1040	1041	1028
5	TEG Hot Frame Edge (external)	1047	1046	1046	1035
6	Emitter Center	1254	1277	1278	1267
7	Emitter Midway	1262	1287	1287	1276
8	Emitter Edge	1305	1332	1332	1321
9	Insulation System Upper	97	103	103	99
10	TEG Cold Frame Outer (external)	53	59	60	54
11	TEG Mounting Plate Male	42	47	49	42
12	Heater Block Bottom	1435	1470	1471	1458
13	Power Conditioner Base	44	41	-	-
14	Pressure Vessel, Cover Upper	40	40	41	40
15	Pressure Vessel, Cover Center	40	41	40	40
16	Pressure Vessel Body Lower	40	41	40	40
	TEG Hot Frame (internal) – Edge	1012	1014	1009	1002
	TEG Hot Frame (internal) – Center	999	998	993	985
	Hot Electrode – Edge	999	1001	996	990
	Hot Electrode – Center	976	976	971	963
	Cold Electrode – Edge	95	98	96	94
	Cold Electrode – Center	91	94	93	91
	Cold Frame (internal) – Edge	82	83	82	80
	Cold Frame (internal) – Center	74	72	72	70
	Follower – Edge	81	84	83	81
	Follower – Center	80	81	81	80
17	Water – Top	40	40	39	40
18	Water – Middle	40	40	39	40
19	Water – Bottom	39	40	39	40

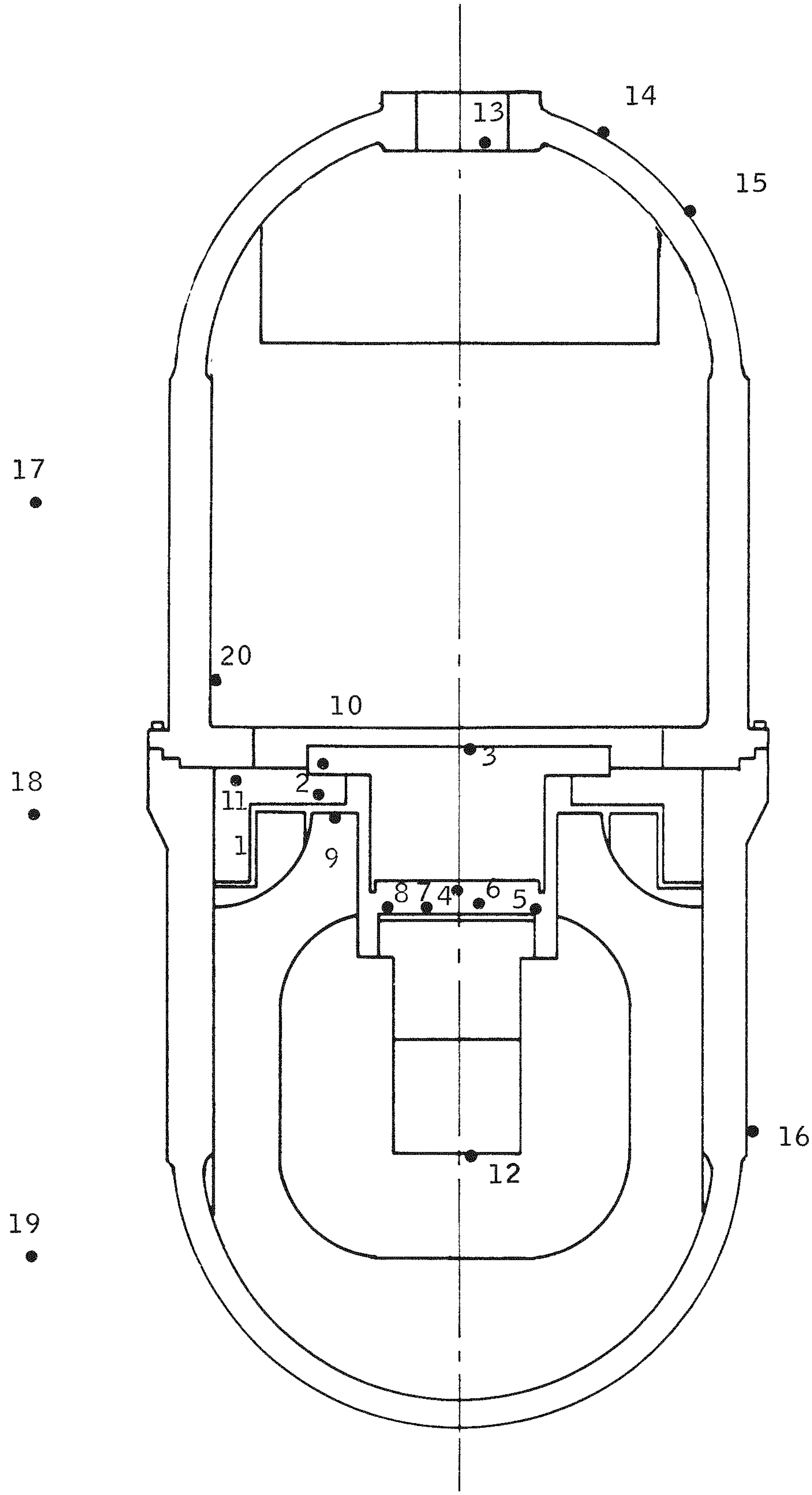

Figure 2-2. System S10D2 Instrumentation

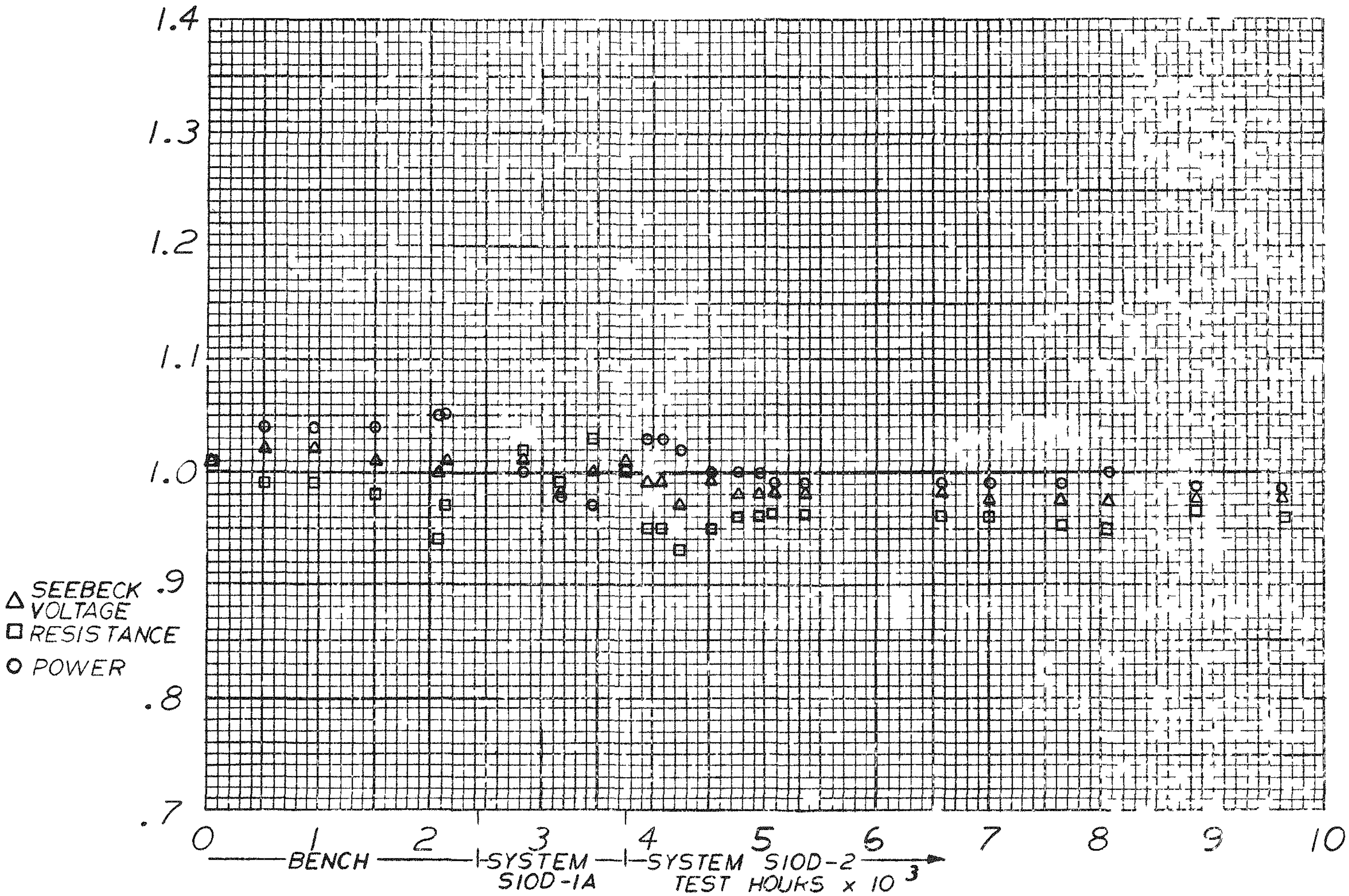

Figure 2-3. SNAP-21 Thermoelectric Generator A10D4 Normalized Data

2.1.1.2 System S10D3

On January 31, 1969, heat-up procedures began on system S10D3. After stabilizing with a power input of 214 watts, the temperature difference between the emitter and hot frame was about 300°F (see Table 2-3). Based on previous system data, this temperature difference should be between 190°F and 220°F. Because of this, the system was taken off test on February 4, 1969 for disassembly.

The high thermal drop across the emitter/hot frame gap indicated a strong possibility of Min-K in the gap. To verify this, the system was inverted without its pressure vessel cover. When the generator was removed upside down, the Min-K remained in the hot frame depression (Figure 2-4), thus verifying the original assumption.

The insulation probably reached the gap during packing of the Min-K into the annulus (between the generator long case and neck tube). Because measurements to determine the potential emitter/hot frame gap dimension had been accomplished during the initial build, this step was not carried out during the rebuild. To perform the measurement, the segmented centering ring was first compressed to move into contact with the pressure vessel wall (the position it will occupy during the life of the system). The generator mounting plate, a part of the centering ring, is lowered toward the emitter plate. Although the spring compression is relieved prior to installing the generator on the mounting plate, the plate does not rebound to nearly the height it would occupy if the segmented centering ring had not first been compressed. If this measuring step is performed, the effect is to lower the generator so that the end of its long case makes complete contact with the microquartz pad located about the emitter plate. Since the measurement was not performed during the rebuild, the installed generator was in a slightly elevated position. As a result it did not make 360° contact with the microquartz pad. When the Min-K was packed between the long case and the neck tube, some insulation apparently was forced through a space between the long case and the microquartz pad into the emitter/hot frame gap.

Quality assurance personnel reviewed and approved the process routings for the rebuild of the system. Extensive surveillance was performed by quality assurance personnel during all phases of reassembly.

Table 2-3. System S10D3 Performance Summary

	BOL Conditions 9/24/68	After 1st Rebuild 2/11/69	After 2nd Rebuild 3/13/69	Power Increased to 235 watts (t) 3/18/69
System Power In, watts (t)	214.0	214.0	214.0	235.0
Segmented Ring at Pressure Vessel (°F)	42.0	40.0	37.0	39.0
Cold Frame (°F)	62.0	60.0	55.0	58.0
Hot Frame Center (°F)	996.0	880.0	928.0	1003.0
Hot Frame Edge (°F)	1008.0	898.0	939.0	1015.0
Emitter (°F)	1239.0	1329.0	1170.0	1237.0
Water Temp (°F)	42.0	38.0	38.0	39.0
TEG Bias Current, amps	0.114	0.104	0.114	0.116
TEG Primary Current, amps	2.65	2.15	2.30	2.68
TEG Bias Closed Circuit Voltage, volts	0.676	0.633	0.673	0.680
TEG Primary Closed Circuit Voltage, volts	4.97	4.55	4.87	4.97
TEG Bias Open Circuit Voltage, volts	1.31	1.06	1.16	1.31
TEG Primary Open Circuit Voltage, volts	8.99	7.22	7.98	8.98
TEG Internal Resistance, ohms	1.507	1.24	1.35	1.496
Total TEG Power Out, watts (t)	13.3	9.8	11.3	13.4
System Load Voltage, volts	24.4	22.5	24.1	24.5
System Power Out, watts (e)	10.4	8.8	10.2	10.5
System Load Resistance, ohms	57.41	57.42	57.24	57.38

Figure 2-4. Generator from System S10D3 Showing Min-K on Hot Frame

To keep Min-K out of the gap during the second rebuild, the springs were pre-compressed and maintained in that configuration while the generator was in position and the Min-K was packed. Also, an additional pad of microquartz was placed around the emitter plate periphery. This ensures that both the generator long case and the microquartz pads are making pressure contact for the full 360° while the Min-K is being charged.

During system operation, the spring is held in compression by the pressure vessel cover when it is bolted to the pressure vessel body. To simulate this during the assembly operation, a tool is used as a substitute for the cover. When this tool is removed prior to installation of the cover, some of the spring pressure is relieved. The result is that the generator moves away from the emitter plate. To keep this movement to a minimum, the shoulder bolts in the segmented centering ring generator mounting plate assembly were altered to permit greater initial spring compression. Therefore, in the second rebuild of S10D3, when the tool used to compress the springs was removed, the generator only moved approximately 0.030-0.040 inch away from the emitter plate, but still maintained contact with the microquartz pad at the periphery of the emitter plate.

One other procedure was changed during the assembly operation. The nitrogen purging operation (performed while the pressure vessel cover was mated with the body) had apparently disturbed the Min-K and had blown it into undesirable locations within the system. (Figure 2-5 shows Min-K on the pressure vessel "O" ring.)

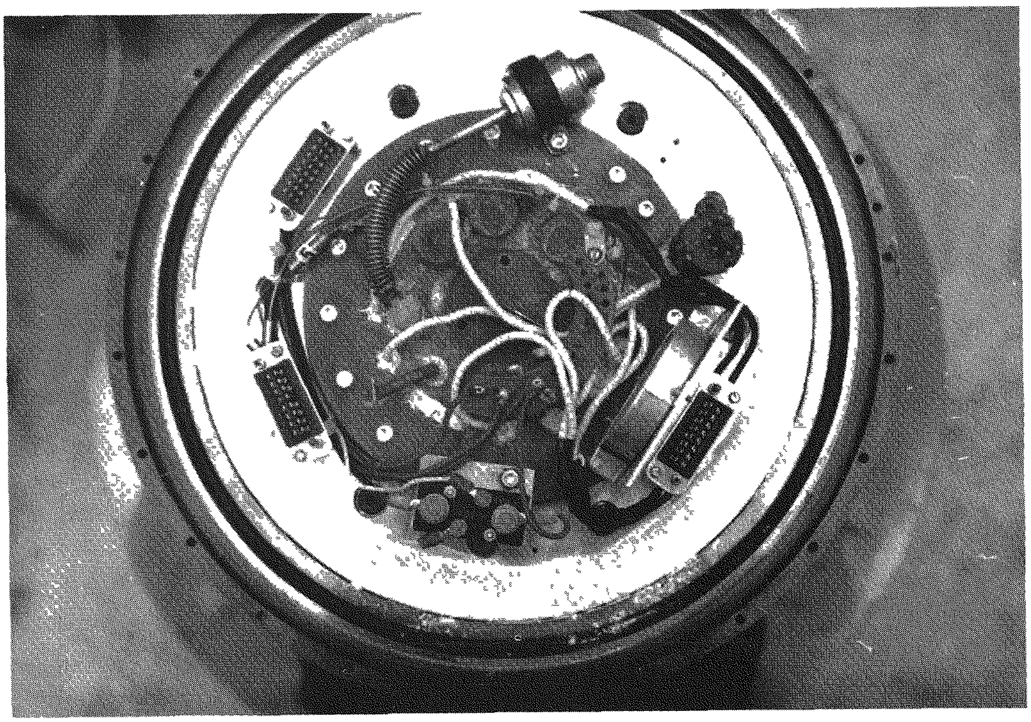

Figure 2-5. System S10D3 Showing Min-K on the Pressure Vessel Flange and the "O" Ring

To prevent this from happening again, the pressure of nitrogen purging was maintained below 2 psig. The tube carrying the gas was introduced only a short distance (1-1/2 to 2 inches) through the polyethylene bag covering the gap between the pressure vessel cover and body.

The system was placed into a tank of water, and heat up was initiated on February 24, 1969. After the system became stable, it was noted that the temperature profile was not correct. The previous power input level of 214 watts was insufficient to bring the system to BOL conditions (see Table 2-3). The power input was increased to 235 watts. This was sufficient to bring the system to approximate BOL conditions. Even though the exact cause for this change in power input is not known, it appears that the added 21 watts input is being lost through the insulation system (possibly caused by a partial loss of vacuum).

It was decided to conduct the Shipping Container Environmental test using system S10D3. Qualification of shipping containers for the SNAP-21 System requires that the container be capable of functioning in temperatures ranging from -65° to 130°F. A Test and Inspection Routing was generated that adequately provides a method of verification with the technical specification. A Quality Control engineer participated in all phases of the evaluation (providing inputs to the procedures, monitoring of the test data, and verifying the specification requirements while the test was performed).

The test was completed during the latter part of this report period. The data will be presented in the next quarterly report. A cursory evaluation indicates that the shipping container satisfactorily passed the 130°F ambient temperature test.

As described in the Quarterly Report Number 10, part of the radiation disk insulation seal consists of a double wrap of microquartz around the bottom of the generator. The microquartz is held in place during assembly by cotton thread which burns away when the system reaches operating temperature. This allows the microquartz to "spring out" and keep the powdered Min-K from entering the radiation gap during vibration.

A brief investigation was conducted to determine if the decomposition byproducts of cotton thread will have any effect on metal parts in the system or on electrical contacts.

The maximum length of cotton thread used is six feet. The weight of six feet of thread is ~200 milligrams. Of this total weight, approximately one-half of it is wrapped around the outside diameter of the microquartz wrap, the other half is stretched across the bottom (hot frame) of the generator. Since the inside of the system is purged with dry nitrogen prior to closing, the exact composition of gas remaining in the system is unknown; however, it is safe to assume that the oxygen content will be considerably lower than normally found in air. The products of decomposition of the cord in this atmosphere at 1300°F will probably be a combination of keytones, aldehydes, alcohol, carbon dioxide, carbon monoxide, water, carbon, and methylene.

The solid decomposition products of that portion of the thread stretched across the bottom of the generator will remain trapped in the radiation gap. The material exposed to the by-products in the radiation gap is 347 stainless steel that has been oxidized in air at temperatures in excess of 1500°F. The portion of the thread wrapped around the microquartz will be close to the inside of the Hastelloy-X inner liner of the insulation system.

A technical representative of the Stellite Division of Union Carbide Corporation was contacted to see if the thread residue would be detrimental to the Hastelloy-X. He felt that there will be no problem because of the relatively low temperature and the small quantity of residue. The 347 stainless steel will also be unaffected by the residue. Insofar as the gaseous byproducts of decomposition are concerned, they are in such small quantities that it is difficult to postulate a situation where they could have any detrimental effect on the electrical contacts and connections in the system. Further, the only path for the gases to escape is through a tightly packed three-inch column of powdered Min-K 1999. The temperature gradient in this column varies from ~1300°F at the hot end to ~55°F at the cold end. Since the powdered Min-K 1999 is absorbent, it will absorb some of the gases, thereby further reducing the possibility of any potential problems due to these gases.

In view of these findings, it is concluded that the cotton thread is not a problem in the system and that further investigation is not warranted.

2.1.2 Fueled Systems

The first three SNAP-21 fueled systems (S10P1, S10P2, and S10P3) were tested this past quarter. All environmental testing has been completed except System Load and Environmental Characteristics testing on S10P3. Shown in Figures 2-6 and 2-7 are a picture and drawing of the System Load and Environmental Characteristics test set-up for systems S10P1 and S10P2. At the present time,

Figure 2-6. System Load and Environmental Characteristic Test Set-Up

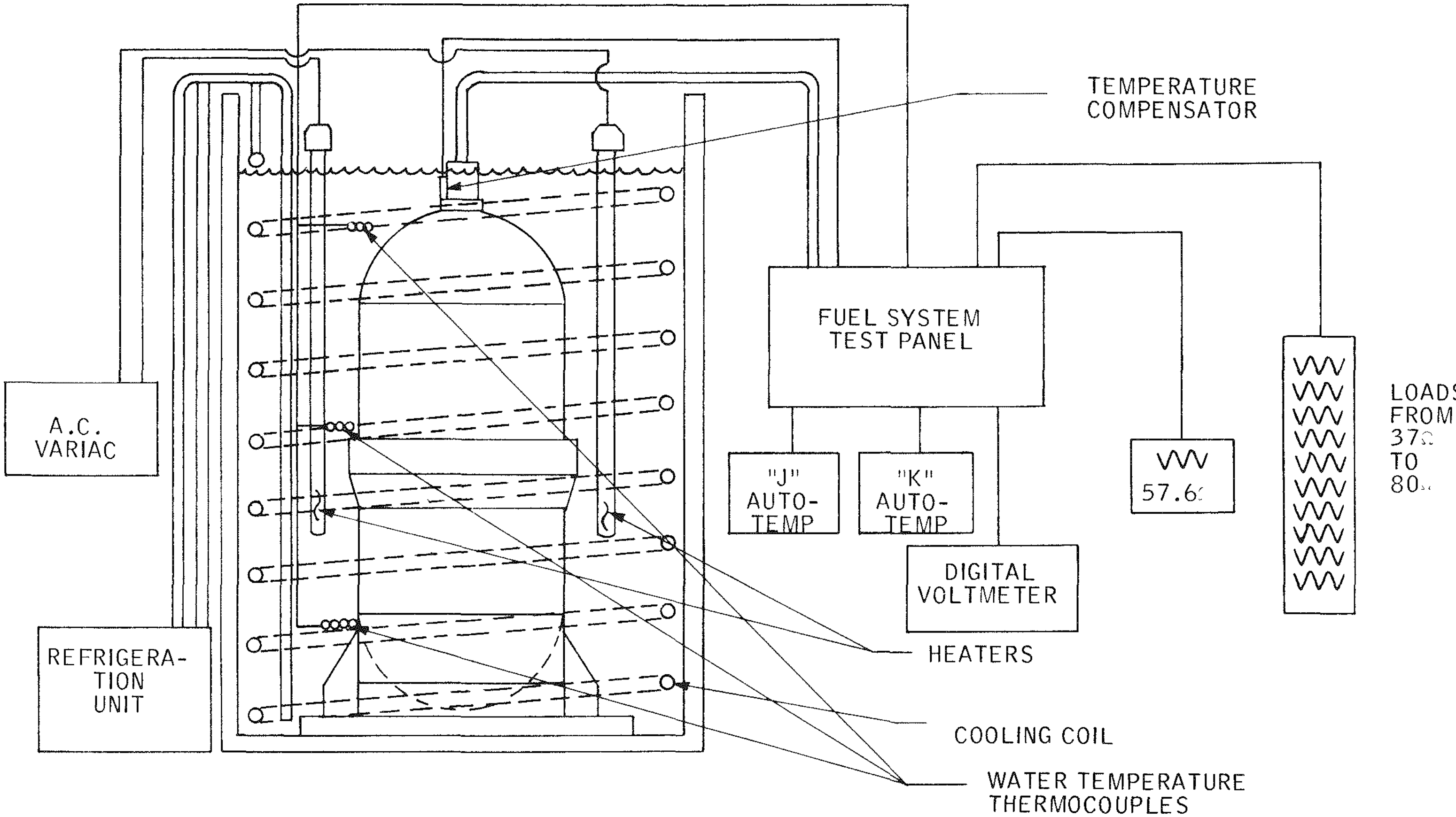

Figure 2-7. Schematic of the Set-Up for Fueled System Load and Environmental Characteristic Test

systems S10P1 and S10P2 are in a hold stage awaiting final preparations for shipment to NRDL. System S10P3 is presently in the water tank and will undergo System Load and Environmental Characteristics testing.

Figure 2-8 shows the decay rate for strontium 90 in the fuel capsules for each system. This graph will be used for future analysis of the systems.

The wire resistance of the system and test console is used for accurate calculation of the performance data of the system. Following, in Table 2-4, are the lead losses for systems S10P1, S10P2 and S10P3. These values will be used with the following expressions to calculate the power conditioner power input:

$$V_{cb} = V_{gbL} - [I_b R_b + (I_p + I_b) R_{p2}]$$

$$V_{cp} = V_{gpL} - [I_p R_{p1} + (I_p I_b) R_{p2}]$$

Table 2-4. Lead Resistance for System S10P1 (ohms)

Lead	System Alone	Pre-Environmental BOL	Shock and Vibration	SRP	Hydro Test	Post Environmental BOL
R_{p1} = Power Conditioner Negative Lead	7×10^{-3}	7×10^{-3}	7×10^{-3}	7×10^{-3}	7×10^{-3}	7×10^{-3}
R_{p2} = Power Conditioner Positive Lead	3×10^{-3}	3×10^{-3}	3×10^{-3}	3×10^{-3}	3×10^{-3}	3×10^{-3}
R_b = Power Conditioner to Receptacle Pins 3 and 7	12×10^{-3}	0.15	0.15	0.206	0.294	0.126

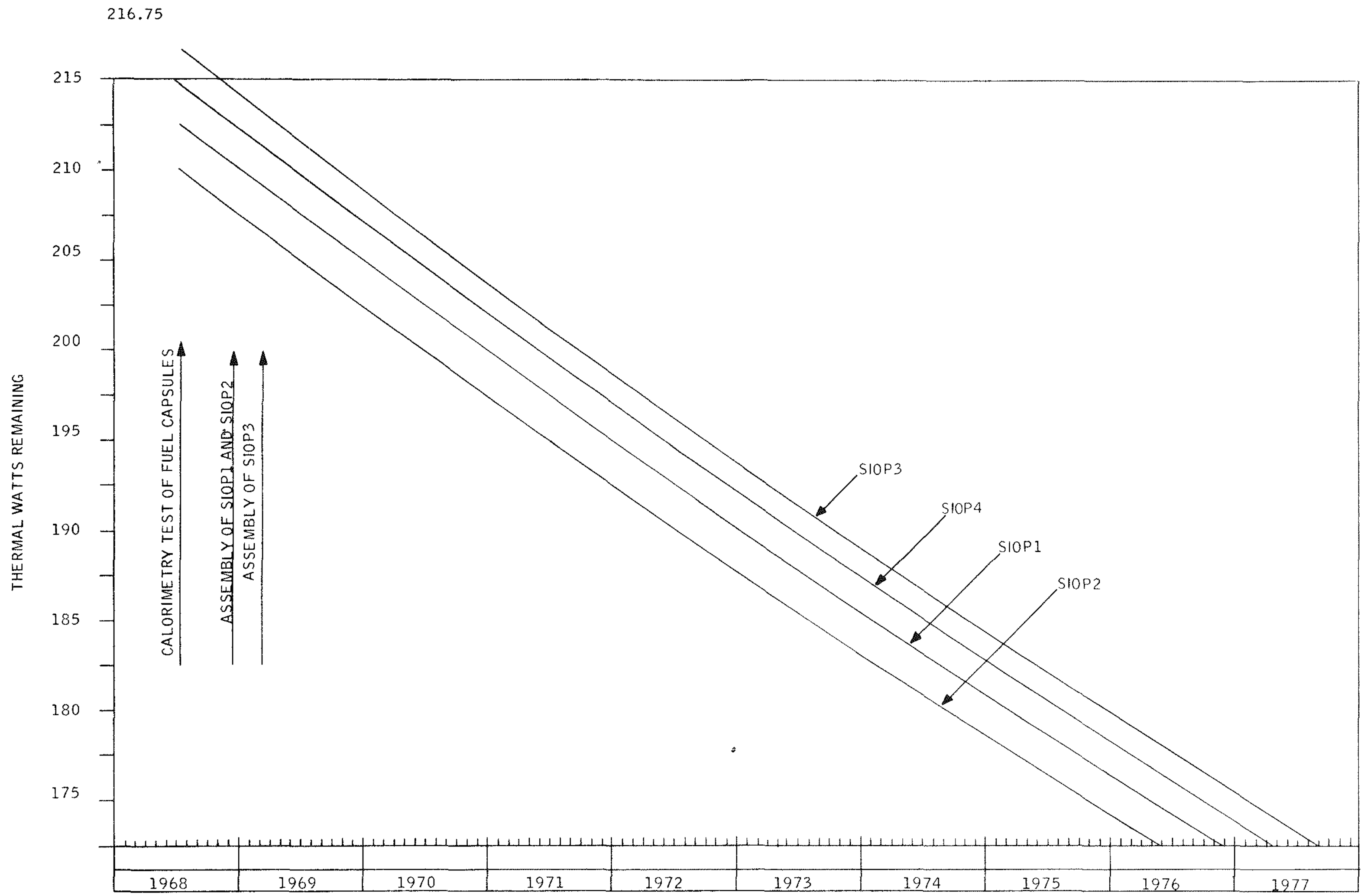

Figure 2-8. SNAP-21 Fuel Decay

The performance for the systems has been stable. The only exception to this is the blue ribbon connector incident (see section 2.1.2.2) on system S10P2, but this has been remedied. The following comments can be made with regard to the performance of the systems (see Tables 2-5, 2-7, and 2-9). Exceptions to this will be noted as necessary.

- Because of decreasing internal resistance, the power output from the thermoelectric generator has increased.
- In comparing the Pre-Environmental BOL Performance and the first Stable Reference Performance tests, the temperature difference across the legs decreased, but the Seebeck voltage increased. This is due to the Seebeck coefficient of the cold segments of the legs, which also accounts for the higher Seebeck voltage for the Stable Reference Performance tests.
- The temperature distributions do not correlate with the changes in ambient temperature for the various Stable Reference Performance tests. This is because of the slight differences in the attachment of the fins and to the manner of controlling the ambient temperatures. The Stable Reference Performance is used as an indication of a change in over-all performance.
- Comparison of Pre-Environmental BOL Performance (12/10/68) and BOL Performance tests (3/5/69) for system S10P1 shows that the hot frame decreased approximately 18°F while the emitter stayed the same. This increased the ΔT between the emitter and hot frame. The exact cause for this is not known, but it appears to have little effect on the system performance. A similar event happened on S10D2 (SNAP-21 Program, Phase II, Quarterly No. 8, MMM 3691-0035). It should be noted that system S10D2 has continued on test with no significant change in performance (see section 2.1.1.1).
- Correlation of the Hydro Test and BOL Performance tests for systems S10P1 and S10P2 indicates some error on the cold end temperature for the hydrostatic testing (in particular, the

temperature drop between the pressure vessel and water). This error is due to the difference in test set-up and earlier analysis (SNAP-21 Program, Phase II, Quarterly No. 9, MMM 3691-39). The set-up for both BOL Performance tests is conducted with a compensator, while during hydro test the temperatures are referenced to water. It appears that there is about a 4°F temperature drop between the water and pressure vessel.

- By comparing the Pre-Environmental BOL Performance Test (1/2/69) to the Post-Environmental BOL Performance Test (3/7/69) of S10P2, the hot frame temperature decreased approximately 16°F while the emitter temperature decreased approximately 6°F. Although the exact cause of this change is not known at this time, the overall performance does compare satisfactorily.
- The temperature for the center external hot frame for system S10P2 is an estimate. The thermocouple degraded at the start of test. It was checked during the disassembly at SWRI and found to be open.

2.1.2.1 System S10P1

Following assembly at ORNL in December 1968, the fueled systems S10P1 and S10P2 were shipped to Sandia Test Labs for dynamic testing. These tests were performed during the period January 13 through January 22, 1969.

Surveillance of all phases of the dynamic testing was made by a representative of Quality Assurance from 3M Company. Included were documenting of procedures and emphasis on calibration controls.

A Quality Assurance representative was also present during all phases of the test equipment equalization.

Calibration of equipment, used to control all testing phases, was within the required frequency periods.

a) Shock and Vibration

The dynamic testing of system S10P1 was completed on January 17, 1969. On arrival at the test facility, the system and equipment were inspected for transportation damage. The temperature recorder and impactograph on the shipping container were inspected and dated. A Stable Reference Performance test was conducted on the system prior to removal from the shipping container.

During the Stable Reference Performance period, a dummy system of equivalent system size and weight was placed in the shock and vibration fixture and attached to the vibration machine. Vibration control instrumentation was calibrated and adjusted to give the optimum pulse for shock testing. This information was recorded on tape to be played back during the system shock testing. This calibration was conducted in the three test axes.

The vibration equipment was given an operational checkout by conducting one sweep at the required input levels and duration.

Maximum acceleration (g) was measured and recorded during an emergency automatic shut-down, by causing the amplifier to go into automatic shut-down at a frequency of 6 Hz. The maximum shock pulse recorded was 9g at 1 ms, which is less than the energy imparted to a unit in a normal shock pulse.

Following equipment capability verification, the fueled system S10P1 was placed into the shock and vibration fixture; the cooling ring was attached; and the system was allowed to stabilize.

The system was subjected to the required levels and durations for vibration and shock, as indicated below:

Vibration

5-5-1/2 Hz at 0.8 inch DA displacement

5-1/2-26 Hz at 1.3g peak acceleration

26-40 Hz at 0.036 inch DA displacement

40-50 Hz at 3.0g peak acceleration

Sweep three times 5-50-5 Hz in three axes in a period of 45 minutes per axis.

Shock

Terminal peak sawtooth wave pulse with a magnitude of 6g and a duration of 6 ms.

Three shock pulses in each direction of the three major axes (total 18 shocks).

System performance readings were taken before and after each sweep of vibration and after each of the three shock pulses. See Table 2-5 for a summary of system performance data.

System S10P1 successfully completed the vibration and shock requirements and was removed from the shock and vibration fixture. Cooling fins were attached, and the system was placed into the shipping container.

During the entire time the two fueled systems were at the Sandia Test Laboratories, the systems were monitored at least once daily for a radiation hazard by the Sandia Health/Physics Department. No changes in radiation levels were found on either system throughout the dynamic testing.

Following the dynamic test, the Stable Reference Performance test was conducted. The systems were placed into a short circuit condition and then shipped to Southwest Research Institute for Hydrostatic Pressure testing.

Sandia is presently preparing a complete test report on the shock and vibration testing.

b) Hydrostatic Testing

After shock and vibration at Sandia, system S10P1 was shipped to Southwest Research Institute (SWRI) for hydrostatic testing. The system and related equipment arrived at SWRI on January 24, 1969, in good condition. System S10P1 was immediately set up for Stable Reference Performance (SRP) test. Upon completion of this test, the system was placed into the pressure tank on the 29th of January.

Table 2-5. Performance Data for Fueled System S10P1

Parameter	Pre-Environmental BOL Performance	Stable Reference Performance	Stable Reference Performance	Pre-Z-Axis Shock and Vibration	Post-Z-Axis Shock and Vibration	Post-Y-Axis Shock and Vibration	Post-X-Axis Shock and Vibration	Stable Reference Performance	Stable Reference Performance	Hydrostatic Pressure Test	Stable Reference Performance	Stable Reference Performance	Post-Environmental BOL Performance	Thermocouple No. Per Figure 2-9
Date Month/Day/Year	12/10/68	12/11/68	1/14/69	1/16/69	1/17/69	1/17/69	1/17/69	1/20/69	1/29/69	1/30/69	2/24/69	3/3/69	3/5/69	
System Fuel Input, watts (t)	210.4	210.4	210.0	209.9	209.9	209.9	209.9	209.8	209.7	209.7	209.3	209.2	209.2	
Generator Primary Open Circuit (volts)	9.58	9.84	9.95	9.84	9.79	9.78	9.78	9.93	9.89	9.58	9.79	9.84	9.42	
Generator Bias Open Circuit (volts)	1.41	1.43	1.45	1.44	1.43	1.43	1.43	1.44	1.44	1.39	1.43	1.43	1.37	
Generator Primary Load Voltage (vdc)	4.98	4.97	5.01	5.01	5.01	5.01	5.01	4.99	4.98	5.00	4.96	4.97	4.97	
Generator Bias Load Voltage (vdc)	0.695	0.686	0.691	0.697	0.696	0.695	0.696	0.688	0.687	0.692	0.686	0.687	0.698	
Generator Primary Load Currents (amps)	2.88	2.83	2.85	2.93	2.93	2.90	2.90	2.85	2.80	3.00	2.85	2.83	2.95	
Generator Bias Load Current (amps)	0.116	0.124	0.124	0.122	0.122	0.122	0.122	0.124	0.124	0.116	0.124	0.124	0.118	
Generator Primary Power Output, watts (e)	14.3	14.0	14.3	14.7	14.7	14.5	14.5	14.2	13.9	15.0	14.1	14.1	14.7	
Generator Bias Power Output, watts (e)	0.081	0.085	0.086	0.085	0.085	0.085	0.085	0.085	0.085	0.080	0.085	0.085	0.082	
Generator Total Power Output, watts (e)	14.4	14.1	14.4	14.8	14.8	14.6	14.6	14.3	14.0	15.1	14.2	14.2	14.7	
Generator Internal Resistance (ohms)	1.59	1.713	1.72	1.64	1.62	1.63	1.63	1.72	1.74	1.52	1.68	1.71	1.50	
Conditioner Total Power Input, watts (e)	14.3	14.1	14.3	14.7	14.7	14.6	14.6	14.3	14.0	15.1	14.2	14.1	14.7	
System Load Voltage (vdc)	24.6	24.4	24.6	24.7	24.6	24.6	24.6	24.6	24.5	24.5	24.4	24.5	24.4	
System Load Current (amps)	0.426	0.426	0.430	0.431	0.430	0.430	0.430	0.428	0.427	0.428	0.424	0.424	0.424	
System Power Output, watts (e)	10.5	10.4	10.6	10.6	10.6	10.6	10.6	10.5	10.5	10.5	10.4	10.4	10.4	
System Load Resistance (ohms)	57.7	57.3	57.2	57.3	57.2	57.2	57.2	57.5	57.4	57.2	57.6	57.8	57.5	
Seg. Ret. Ring at Pressure Vessel Wall (°F)	44	86	87	61	61	61	61	87	94	34	87	95	43	1
Seg. Ret. Ring Inner (°F)	56	98	99	75	75	75	75	99	106	44	97	105	53	2
TEG Cold Frame Center (Ext) (°F)	64	106	107	85	84	85	84	107	113	53	106	113	62	3
TEG Hot Frame Center (Ext) (°F)	1050	1084	1078	1065	1061	1061	1060	1081	1079	1032	1072	1079	1033	4
TEG Hot Frame Edge (Ext) (°F)	1066	1098	1091	1077	1073	1072	1073	1093	1093	1047	1086	1093	1047	5
Emitter Plate Center (°F)	1249	1270	1272	1266	1265	1264	1266	1275	1270	1242	1272	1275	1249	6
Reference (°F)	41	88	87	67	65	66	67	86	96	34	87	97	39	7
Water Top (°F)	40	--	--	--	--	--	--	--	--	35	--	--	39	8
Water Center (°F)	40	--	--	--	--	--	--	--	--	34	--	--	39	9
Water Bottom (°F)	40	--	--	--	--	--	--	--	--	32	--	--	39	10
Average Cold Junction (Estimated) (°F)	92	134	135	113	112	113	112	135	141	82	134	141	90	
Average Hot Junction (Estimated) (°F)	999	1032	1026	1012	1008	1008	1008	1028	1027	980	1020	1027	981	
Ambient (°F)	--	72	67	73	69	73	73	65	80	79	79	76	72	
Test Hours	135	168	975	1027	1046	1051	1052	1122	1334	1367	1960	2127	2177	

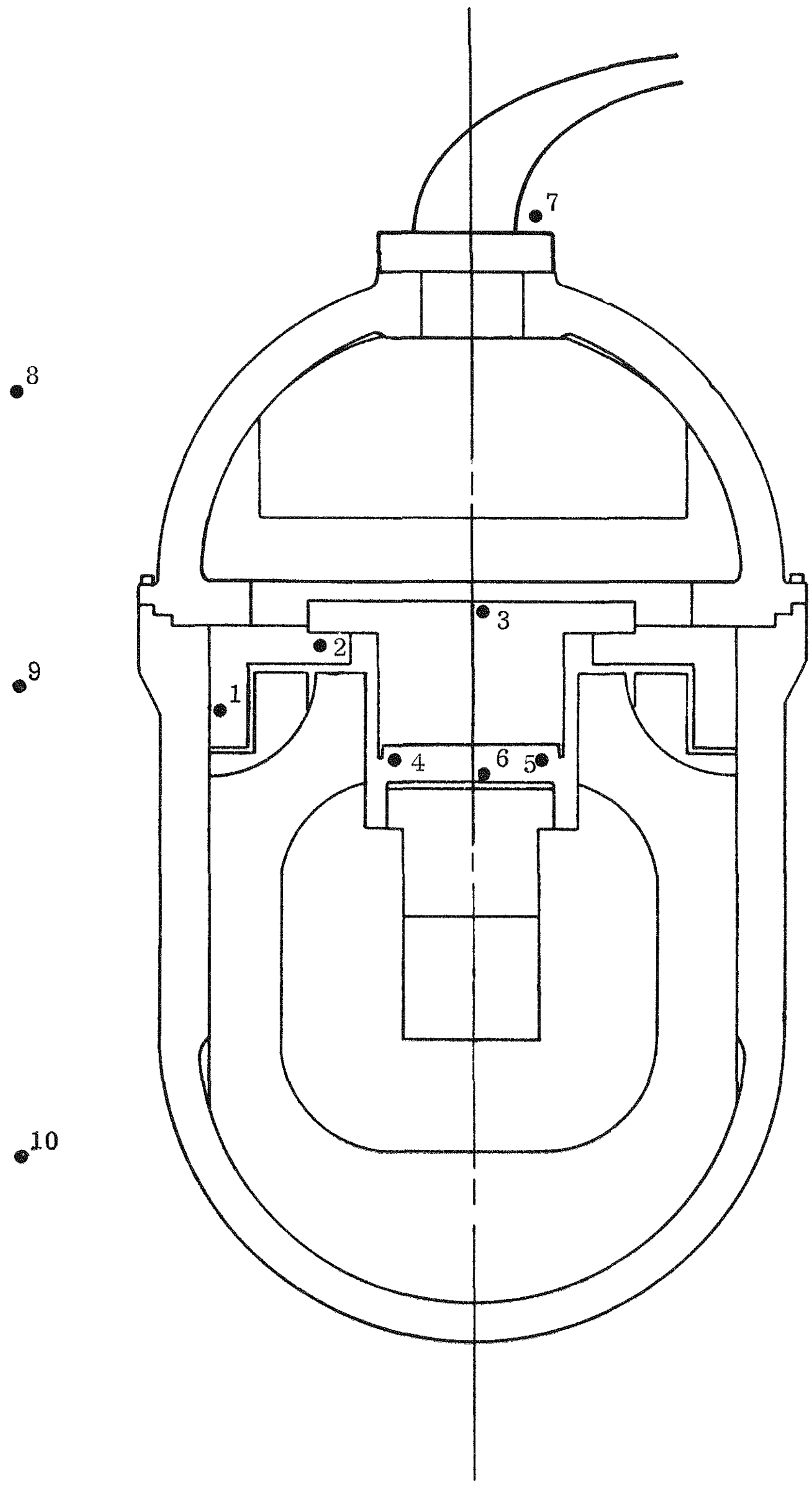

Figure 2-9. General System Instrumentation

Hydrostatic testing of system S10P1 was accomplished on January 30, 1969. Hydro testing was done in simulated sea water at 34-42°F. Pressurization was done at 2000 psi increments with a 10-minute hold period at each step. The hydro test pressure of 10,000 $^{+200}_{-0}$ psi was held for a minimum of 5 hours. During the pressurization and 5-hour hold period, system performance was monitored and recorded. After the 5-hour hold period, depressurization of the chamber was done at a rate of 1000 psi/min. Table 2-5 gives performance data for the system. It can be seen that the performance for the system was satisfactory, and that the system successfully passed the hydrostatic test.

Because of the trouble with system S10P2 (see section 2.1.2.2b), system S10P1 experienced more than the required 5 hours at 10,000 psi. This was necessary in order to ascertain the difficulties with S10P2. The system was at 10,000 psi for a total of 6.5 hours and was subjected to a total of 5 cycles from ambient to 10,000 psi. Figure 2-10 shows removal of the system from the hydrostatic test chamber.

This system, along with system S10P2, was left at SWRI until shipment on 24 February 1969. The final Stable Reference Performance test was taken on 24 February 1969. After the systems arrived at 3M Company on 28 February 1969, final tests began on this system in March.

A Quality Assurance representative was at Southwest Research during preparations for and hydrostatic testing of fueled system S10P1.

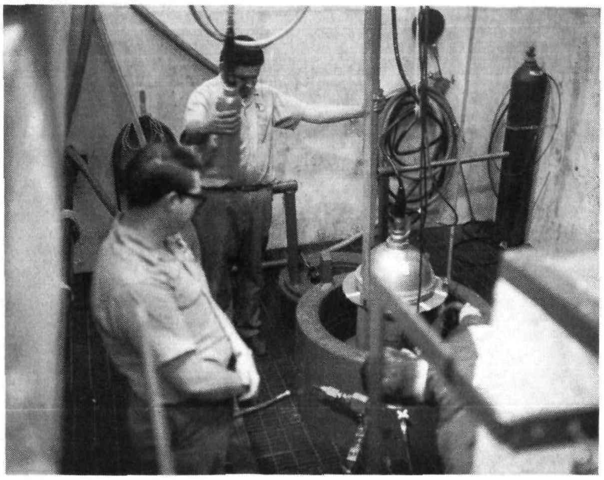

Figure 2-10. SNAP-21 System Being Removed from Test Chamber after Hydrostatic Test

c) BOL Performance Test

Following the dynamic and hydrostatic testing of S10P1, a BOL Performance Test was conducted to determine its various electrical characteristics.

The system and related equipment arrived at 3M Company on February 28, 1969 in good condition. The system was immediately set upfor Stable Reference Performance Test. See Table 2-5.

After the fins were removed from the system, it was noted that some black material formed on the pressure vessel. Investigation showed that the pressure vessel became slightly etched where the fins were on the system. It was determined that a reaction had taken place between the pressure vessel, salt water used in hydro test and the heat transfer grease used on the fins. Although the system was wiped with alcohol, it appears that this was not sufficient.

It was decided to wash future systems with fresh water, then wipe with alcohol after hydro test. When this was done on system S10P3, no reaction took place. Most of the material was removed from systems S10P1 and S10P2 by rubbing with alcohol and copper polish.

Upon completion of the SRP testing, the system was removed from the shipping container and placed into a water tank. The water temperature was controlled to 41 ± 3°F.

After a stabilization period, system S10P1 was subjected to a System Performance test. This test was done to determine various system characteristics. As specified in the engineering specification the requirements and results of this test are as follows:

(a) Generator Open Circuit Voltage – The generator open circuit voltage shall be 9.10 vdc minimum when the power conditioner is electrically disengaged from the circuit.

Result: S10P1 - 9.42 vdc

(b) Generator Output Voltage — The generator output voltage shall be 4.83 ± 0.14 vdc when a variable load resistance placed across the system output terminals is varied from infinity to rated load (57.6 ohms).

Result: S10P1 - 4.97 vdc

(c) Voltage Regulation — The system output voltage shall be 24.0 ± 0.6 vdc when a variable load resistance placed across the system output terminals is varied from infinity to rated load (57.6 ohms).

Result: S10P1 - 24.4 vdc

(d) Generator Power — The minimum generator power output shall be 13.4 watts when rated load 57.6 ± 0.5 ohms is applied to the system output terminals.

Result: S10P1 - 14.74

(e) Power Conditioner Efficiency — The minimum power conditioner efficiency shall be 88 percent. This is determined by adjusting the system load resistance until the system output voltage is 24 ± 0.02 vdc. The system voltage and current measured under these conditions is then used in the following equation to obtain power conditioner efficiency:

$$\text{Efficiency} = \frac{\text{Power System Output}}{\text{Power Conditioner Input}}$$

Result: S10P1 - 90.3 percent

(f) Cold End Temperature Drop — The difference between the test tank water temperature and the cold frame center temperature shall not be greater than 35°F.

Result: S10P1 -	Cold Frame	62°F
	Water	38°F
	Temp. Difference	24°F

(g) Output Ripple — The system output voltage shall have a ripple less than 0.10 volt peak-to-peak when the system load resistance is varied from infinity to 45 ohms.

Result: S10P1 - Less than 0.10 volts peak-to-peak

(h) Starting Capability — The system open circuit shall be 24 ± 1 vdc after being short circuited for a minimum of 5 minutes.

Result: S10P1 - 24.4 volts open circuit after a minimum of 5 minutes at short circuit.

System S10P1 successfully completed the BOL Performance test.

d) System Environmental and Characterization Tests

The system was characterized for various system resistive loads at 40°F - 60°F and 80°F environmental water temperatures. At the present time, the data is being compiled and used with computer programs to predict annual characterization curves. The following parameters will be used to define the performance: generator power voltage, current, cold junction temperature and hot junction temperature each as a function of system resistance load at each environment water condition, system power out, current and voltage as a function of resistance load at each environmental water condition, and generator cold and hot junction temperatures as a function of time.

These data are being prepared for submission to the AEC and will be a part of the data package accompanying each fueled system. Table 2-6 presents the data collected during the test. An analysis and plots of all predicted data will be presented in the next quarterly report.

2.1.2.2 System S10P2

Following assembly at ORNL in December 1968, the fueled systems S10P1 and S10P2 were shipped to Sandia Test Labs for dynamic testing. These tests were performed during the period January 13 through January 22, 1969.

Table 2-6. System Environmental and Characteristics Test – S10P1

Water Temperature	System Load	Thermoelectric Generator: Hot Frame Temperature °F	Thermoelectric Generator: Cold Frame Temperature °F	Thermoelectric Generator: Primary Load Voltage (V)	Thermoelectric Generator: Primary Load Current (A)	Thermoelectric Generator: Resistance (Ω)	Thermoelectric Generator: Primary Power Out (W)	System: Load Voltage (V)	System: Load Current (A)	System: Power Out (W)
40°F	37.0Ω	1032	64	4.50	3.18	1.51	14.3	21.8	0.588	12.8
	42.0Ω	1036	64	4.80	3.03	1.50	14.5	23.5	0.556	13.1
	47.0Ω	1037	63	4.97	2.93	1.50	14.6	24.4	0.530	12.9
	51.1Ω	1037	61	4.97	2.93	1.50	14.6	24.4	0.530	11.5
	57.6Ω	1037	61	4.96	2.93	1.50	14.5	24.4	0.424	10.4
	65.0Ω	1037	61	4.97	2.93	1.50	14.6	24.5	0.387	9.5
	80.0Ω	1037	61	4.97	2.93	1.50	14.6	24.4	0.306	7.5
60°F	37.0Ω	1050	84	4.46	3.15	1.58	14.1	21.7	0.582	12.6
	42.0Ω	1054	83	4.76	3.00	1.58	14.3	23.3	0.551	12.8
	47.0Ω	1055	80	4.96	2.87	1.58	14.3	24.4	0.516	12.6
	51.1Ω	1055	80	4.97	2.87	1.58	14.3	24.4	0.475	11.6
	57.6Ω	1055	82	4.98	2.87	1.57	14.3	24.5	0.425	10.4
	65.0Ω	1055	82	4.96	2.87	1.58	14.3	24.4	0.375	9.6
	80.0Ω	1055	81	4.96	2.87	1.58	14.3	24.4	0.306	7.5
80°F	37.0Ω	1066	101	4.44	3.12	1.64	13.9	21.5	0.577	12.4
	42.0Ω	1069	100	4.73	2.98	1.64	14.1	23.2	0.546	12.7
	47.0Ω	1072	100	4.97	2.85	1.64	14.2	24.5	0.516	12.6
	51.1Ω	1072	99	4.97	2.85	1.64	14.2	24.4	0.475	11.6
	57.6Ω	1072	100	4.96	2.85	1.65	14.1	24.4	0.425	10.4
	65.0Ω	1072	101	4.98	2.85	1.64	14.2	24.5	0.375	9.2
	80.0Ω	1073	101	4.98	2.85	1.64	14.2	24.5	0.305	7.5

Surveillance of all phases of the dynamic testing was made by a representative of Quality Assurance from 3M Company. Included was documenting of procedures and emphasis on calibration controls.

A Quality Assurance representative was also present during all phases of test equipment equalization.

a) Shock and Vibration

The dynamic testing of system S10P2 was completed on January 21, 1969. After arrival at the test facility, the system and equipment were inspected for transportation damage. The temperature recorder and impactograph on the shipping container were inspected and dated. A Stable Reference Performance Test was conducted on the system prior to removal from the shipping container.

During the Stable Reference Performance period, a dummy system of equivalent system size and weight was placed in the shock and vibration fixture and attached to the vibration machine. Vibration control instrumentation was calibrated and adjusted to give the optimum pulse for shock testing. This information was recorded on tape to be played back during the system shock testing. This calibration was conducted in the three test axes.

The vibration equipment was given an operational checkout by conducting one sweep at the required input levels and duration.

Maximum acceleration (g) was measured and recorded during an emergency automatic shut-down, by causing the amplifier to go into automatic shut-down at a frequency of 6 Hz. The maximum shock pulse recorded was 9g at 1 ms which is less than the energy imparted to a unit in a normal shock pulse.

Following equipment capability verification, the fueled system (S10P2) was placed into the shock and vibration fixture; the cooling ring was attached; and the system was allowed to stabilize.

The system was subjected to the required levels and durations for vibration and shock, as indicated by the following:

Vibration

5 - 5-1/2 Hz at 0.8 inch DA displacement

5-1/2 - 26 Hz at 1.3g peak acceleration

26 - 40 Hz at 0.036 inch DA displacement

40 - 50 Hz at 3.0g peak acceleration

Sweep three times 5-50-5 Hz in three axes in a period of 45 minutes per axis.

Shock

Terminal peak sawtooth wave pulse with a magnitude of 6g and a duration of 6 milliseconds.

Three shock pulses in each direction of the three major axes (total 18 shocks).

System performance readings were taken before and after each sweep of vibration and each three shock pulses. See Table 2-7 for system performance data.

System S10P2 successfully completed the vibration and shock requirements and was removed from the shock and vibration fixture. Cooling fins were attached, and the system was placed into the shipping container.

During the entire time the two fueled systems were at the Sandia Test Laboratories, the systems were monitored at least once daily for a radiation hazard by the Sandia Health/Physics Department. No changes in radiation levels were found on either system throughout the dynamic testing.

Following the dynamic test, the Stable Reference Performance test was accomplished. The systems were then placed into a short circuit condition and shipped to Southwest Research Institute for Hydrostatic Pressure Testing.

Sandia is presently preparing a complete test report on the shock and vibration testing.

Table 2-7. Performance Data for Fueled System – S10P2

Parameter	Pre-Environmental BOL Performance	Stable Reference Performance	Stable Reference Performance	Pre-Z Axis Shock and Vibration	Post-Z Axis Shock and Vibration	Post-Y Axis Shock and Vibration	Post X Axis Shock and Vibration	Stable Reference Performance	Stable Reference Performance	Hydrostatic Pressure Test	Stable Reference Performance	Stable Reference Performance	Post-Environmental BOL Performance	Thermocouple No. Per Figure 2-9
Date Month/Day/Year	1/2/69	1/3/69	1/18/69	1/20/69	1/21/69	1/21/69	1/21/69	1/22/69	1/30/69	2/8/69	2/24/69	3/4/69	3/7/69	
System Fuel Input, watts (t)	207.7	207.7	207.5	207.4	207.4	207.4	207.4	207.3	207.2	207.1	206.8	206.7	206.6	
Generator Primary Open Circuit (volts)	9.33	9.57	9.72	9.53	9.50	9.48	9.48	9.61	9.74	9.32	9.64	9.66	9.25	
Generator Bias Open Circuit (volts)	1.36	1.41	1.42	1.40	1.39	1.39	1.39	1.42	1.42	1.36	1.41	1.41	1.35	
Generator Primary Load Voltage (vdc)	4.96	4.97	4.98	4.98	4.98	4.98	4.98	4.97	4.98	4.97	4.97	4.96	4.95	
Generator Bias Load Voltage (vdc)	0.686	0.681	0.681	0.687	0.686	0.686	0.686	0.681	0.683	0.682	0.680	0.679	0.688	
Generator Primary Load Current (amps)	2.80	2.73	2.73	2.78	2.78	2.78	2.78	2.78	2.75	2.85	2.75	2.75	2.83	
Generator Bias Load Current (amps)	0.118	0.122	0.122	0.120	0.120	0.120	0.120	0.122	0.122	0.114	0.120	0.122	0.118	
Generator Primary Power Output, watts (e)	13.9	13.6	13.6	13.8	13.8	13.8	13.8	13.8	13.7	14.2	13.7	13.6	14.0	
Generator Bias Power Output (watts)	0.081	0.083	0.083	0.082	0.082	0.082	0.082	0.083	0.083	0.078	0.082	0.083	0.081	
Generator Total Power Output, watts (e)	14.0	13.6	13.7	13.9	13.9	13.9	13.9	13.9	13.8	14.2	13.8	13.7	14.1	
Generator Internal Resistance (ohms)	1.55	1.67	1.72	1.62	1.62	1.61	1.61	1.69	1.72	1.52	1.69	1.70	1.51	
Conditioner Total Power Input, watts (e)	13.9	13.6	13.6	13.9	13.9	13.9	13.9	13.9	13.8	14.2	13.7	13.7	14.1	
System Load Voltage (vdc)	24.5	24.5	24.6	24.5	24.6	24.5	24.5	24.5	24.5	24.4	24.5	24.4	24.4	
System Load Current (amps)	0.426	0.426	0.426	0.426	0.427	0.426	0.427	0.425	0.426	0.426	0.427	0.424	0.425	
System Power Output, watts (e)	10.4	10.4	10.5	10.4	10.5	10.4	10.5	10.4	10.4	10.4	10.5	10.4	10.4	
System Load Resistance (ohms)	57.5	57.5	57.8	57.5	57.6	57.5	57.4	57.7	57.5	57.3	57.4	57.6	57.4	
Seg. Ret. Ring at Pressure Vessel Wall (°F)	43	82	88	63	63	65	64	82	89	31	85	91	44	1
Seg. Ret. Ring Inner (°F)	54	94	100	74	74	75	75	93	100	43	94	101	54	2
TEG Cold Frame Center (Ext) (°F)	62	100	107	81	81	82	83	101	106	49	101	108	61	3
TEG Hot Frame Center (Ext) (°F)	1023 Est.	1055 Est.	1059 Est.	1040 Est.	1038 Est.	1039 Est.	1037 Est.	1056 Est.	1058 Est.	1004 Est.	1048 Est.	1053 Est.	1009 Est.	4
TEG Hot Frame Edge (Ext) (°F)	1039	1069	1072	1052	1050	1050	1049	1068	1072	1019	1062	1067	1023	5
Emitter Plate Center (°F)	1231	1250	1253	1241	1241	1238	1238	1254	1255	1214	1250	1253	1225	6
Reference (°F)	40	82	87	60	61	61	62	80	90	31	83	88	40	7
Water Top (°F)	40	--			--	--	--	--	-	32	-	--	39	8
Water Center (°F)	40	--	--	--	--	--	--	--	-	33		--	39	9
Water Bottom (°F)	40	--	--			-	-	-	--	30	--	--	39	10
Average Cold Junction (Estimated) (°F)	90	128	135	109	109	110	111	129	134	77	129	136	88	
Average Hot Junction (Estimated) (°F)	972	1003	1007	987	985	986	984	1003	1006	953	996	1001	958	
Ambient (°F)	--	80	66	65	64	72	73	60	75	77	75	74	75	
Test Hours	139	161	522	569	591	595	597	619	813	1029	1408	1600	1673	

b) Hydrostatic Test

System S10P2 arrived at SWRI on 24 January 1969. System S10P2 was set up for the Stable Reference Performance test on 25 January 1969. The system checked out satisfactorily and was placed into the pressure chamber on January 31, 1969. Hydrostatic testing of the system was started on February 1, 1969.

The hydrostatic testing procedure includes a salt water environment at 34-42°F; pressurization was in 2000 psi increments to $10,000\,^{+200}_{-0}$ psi with a ten-minute hold period at each step. The pressure of $10,000\,^{+200}_{-0}$ psi is to be held for a minimum of 5 hours. During the pressurization and hold periods, system performance is monitored and recorded.

System performance was satisfactory up through 8,000 psi. After holding at 10,000 psi for 15 minutes, the thermoelectric generator bias voltage had dropped from the nominal 682 mv to 673 mv. This is the only change that had taken place. After 4.5 hours of the 5.0-hour hold period, the bias circuit opened completely, and the bias voltage dropped to zero. Measurements of the thermoelectric generator and of the system load voltage indicated an open circuit.

The electrical schematic diagram (Figure 2-11) will aid the reader in the following discussion. The electrical receptacle connector pins are referred to unless otherwise noted.

In attempting to find the trouble, pins No. 6 and No. 3 were shorted together. This started the power conditioner and closed the thermoelectric generator circuit to load. When this shunt was removed from pins No. 6 and No. 3, the power conditioner again stopped, resulting in TEG and system open circuit conditions. After approximately one hour, the bias voltage and system performance returned to normal. The pressure was decreased to ambient, and the system performance was satisfactory.

After holding at ambient pressure for 36 hours, the system was repressurized using a different cable. The system bias remained normal up to 9,200 psi when the bias again dropped to a slightly lower value of 669 mv. The power conditioner remained operating, and the TEG and system were found to be normal. The test console was also changed at this point with no adverse effect. Depressurizing to

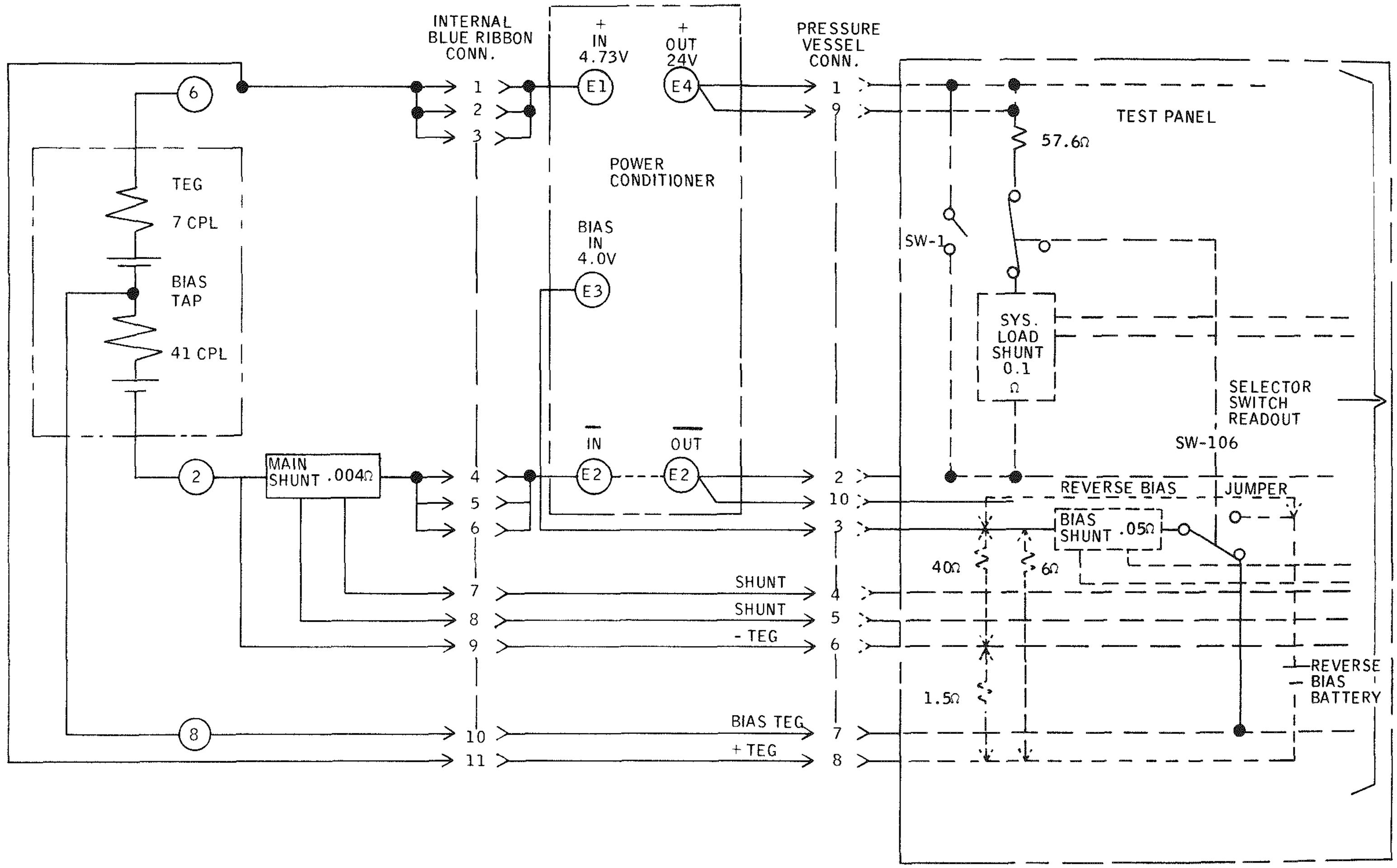

Figure 2-11. SNAP-21 10-Watt Electrical Schematic

7,700 psi caused the bias to go to zero voltage, and stop the power conditioner. The system returned to normal when depressurization stopped. While the depressurization continued, the system opened at approximately 5,000 psi. The TEG voltage was 9.23 vdc "under load". The system voltage was 8.80 vdc with a current of only 155 ma as indicated by the voltage drop across the 0.1 ohm system shunt (external). The difference between TEG and system Seebeck voltage is attributed to internal resistance of the power conditioner.

In order to rule out the possibility that the receptacle on the pressure chamber was the trouble spot, system S10P1 was placed into the pressure chamber and repressurized. Since no problems were encountered, the pressure chamber receptacle was determined satisfactory. System S10P1 was then removed and S10P2 was placed back into the chamber.

Several diagnostic tests were conducted to determine the cause of the open circuit of the bias voltage. The power conditioner was stopped by reversing the bias voltage using two "D" cells jumpered between pins No. 3 and No. 8 (the 0.05 ohm bias shunt was disconnected from lead pin No. 3). A 1.5-ohm resistor was placed across the TEG output (pins No. 6 and 8) to simulate the power conditioner resistance. The power conditioner bias resistance was simulated by placing a 6-ohm resistor in series with the bias resistor (0.05 ohm) across pins No. 7 and 8. The simulated bias current was determined to be 48 ma from the IR drop across the 0.05-ohm bias shunt (2.4 mv). Since the current should be ~112 ma some extraneous resistance was indicated.

Under pressurization (February 5, 1969), the simulated bias readings remained steady until 8,950 psi when the voltage dropped from 2.4 mv to 1.9 mv. The TEG load voltage remained at 4.2 volts. The simulated bias held steady at 1.9 mv until 9,600 psi was reached when it went to 0.1 mv. During depressurizing, the simulated bias remained steady until 7,000 psi when it returned to 2.3 mv. Erratic readings were recorded down to 6,000 psi. At this time, the 6-ohm resistor was removed, and a 40-ohm resistor was placed in series with the bias shunt (0.05 ohm); but instead of being connected to positive pin No. 8, it was connected to negative pin No. 6. The battery-supplied reverse bias was maintained to shut off the power conditioner. As can be seen in the electrical schematic, the current through pin No. 7 was reversed in this test.

The unit was brought up to 10,000 psi pressure (February 6, 1969), with continuous bias voltage and current. The circuit was restored to normal, and the power conditioner and system operated normally. However, when the unit was cycled to approximately 8,200 psi and back to 10,000 psi, the unit opened (usually while the pressure was changing).

The results of these tests indicated that some erratic and extraneous resistance was being introduced into the bias circuit lead (lead No. 7) during pressurization.

It was decided to disassemble the system at SWRI and attempt to take corrective action. The system was disassembled (February 7, 1969); the No. 10 pin (to which lead No. 7 is connected) of the Blue Ribbon connector was found to have a small piece of white, pasty material on it. The majority was on the female portion which was also found to have a scratch in the major contact area. Figure 2-12 shows a scratch on the second pin from the left on the Blue Ribbon connector.

Corrective action consisted of connecting the bias lead from the generator to one of the unused pins (No. 16) of the male part of the Blue Ribbon connector. The corresponding female pin was shunted to the No. 10 pin, the lead of which connects to the No. 7 pin of the electrical receptacle.

Throughout the disassembly, the TEG was short circuited. The system temperatures were monitored to ensure that excessive temperatures were not experienced.

The system process routing procedure was used to reassemble the system. A preliminary check of system performance indicated proper electrical connections had been made.

Upon completion of reassembly, the system was subjected to pressure cycling (February 7, 1969) to determine if the pressure effects had been eliminated.

After the system performed satisfactorily, plans were made to rerun the final pressure test. On February 8, 1969, this test was performed without incident, and the system was made ready for return shipment to 3M.

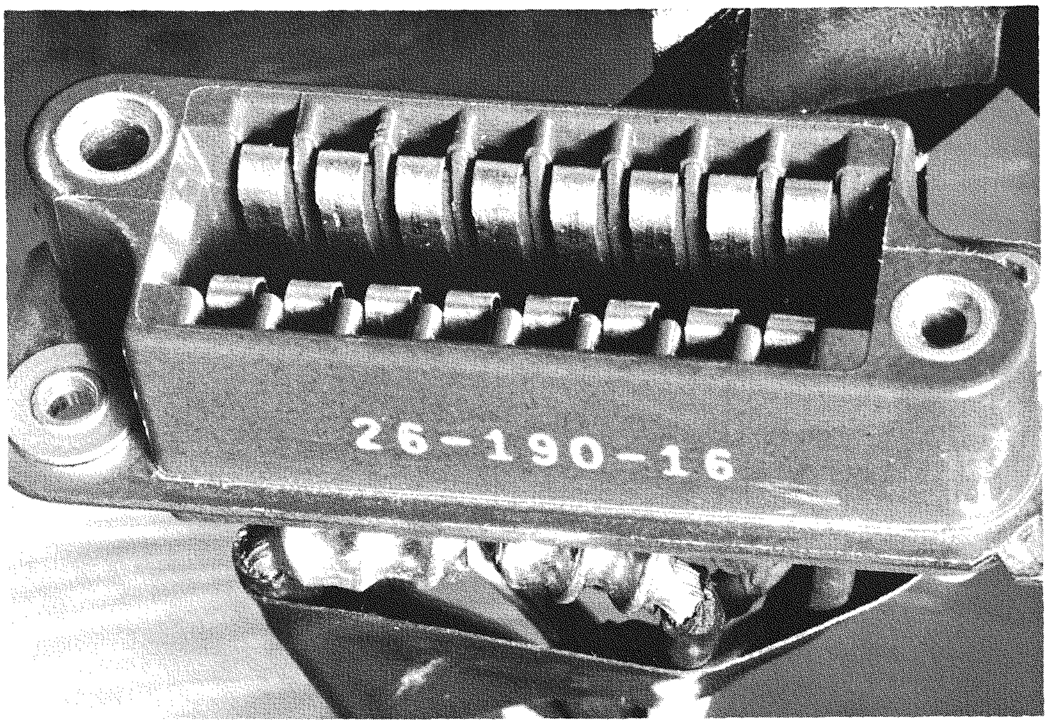

Figure 2-12. Female Half of Blue Ribbon Connector Showing Scratch on Second Pin from Left

System S10P2 was at 10,000 psi for a total of 14 hours. Shown in Table 2-8 is a summary of performance for system S10P2.

The system was left under loaded conditions (Stable Reference Performance test set-up) at SWRI until shipment on the 24th of February to 3M Company. SWRI personnel monitored the system daily until shipment.

A Quality Assurance representative was at SWRI during all preparations for and hydrostatic testing of system S10P2. The diagnostic tests, disassembly, rework, and reassembly were witnessed and documented on a process routing by Quality Assurance personnel. Installation of the fueled system into the shipping container preparatory to system shipping from the hydrostatic test vendor are shown in Figure 2-13.

Table 2-8. System Environmental and Characteristics Test – S10P2

Water Temperature	System Load	Thermoelectric Generator						System		
		Hot Frame Temperature °F	Cold Frame Temperature °F	Primary Load Voltage (V)	Primary Load Current (A)	Resistance (Ω)	Primary Power Out (W)	Load Voltage (V)	Load Current (A)	Power Out (W)
	37.0Ω	1008	62	4.41	3.13	1.50	13.8	21.4	0.575	12.3
	42.0Ω	1010	61	4.70	2.95	1.51	13.9	23.0	0.544	12.5
	47.0Ω	1014	63	4.88	2.85	1.52	13.9	24.1	0.522	12.6
40°F	51.1Ω	1015	62	4.96	2.83	1.50	14.0	24.4	0.470	11.5
	57.6Ω	1014	60	4.96	2.83	1.50	14.0	24.4	0.425	10.4
	65.0Ω	1015	61	4.96	2.83	1.50	14.0	24.5	0.387	9.5
	80.0Ω	1014	62	4.96	2.83	1.50	14.0	24.5	0.305	7.5
	37.0Ω	1025	80	4.38	3.08	1.58	13.5	21.3	0.571	12.2
	42.0Ω	1029	81	4.66	2.93	1.58	13.6	22.7	0.539	12.2
	47.0Ω	1031	81	4.91	2.80	1.58	13.8	24.1	0.513	12.4
60°F	51.1Ω	1031	80	4.96	2.78	1.57	13.8	24.4	0.475	11.6
	57.6Ω	1031	81	4.96	2.78	1.58	13.8	24.5	0.425	10.4
	65.0Ω	1031	80	4.95	2.78	1.58	13.8	24.4	0.373	9.1
	80.0Ω	1031	80	4.96	2.78	1.57	13.8	24.4	0.306	7.5
	37.0Ω	1042	100	4.35	3.07	1.64	13.4	21.0	0.564	11.8
	42.0Ω	1045	99	4.64	2.93	1.64	13.6	22.7	0.535	12.1
	47.0Ω	1050	99	4.89	2.80	1.65	13.7	24.1	0.510	12.3
80°F	51.1Ω	1051	98	4.96	2.75	1.65	13.6	24.5	0.475	11.6
	57.6Ω	1051	99	4.95	2.73	1.66	13.5	24.4	0.425	10.4
	65.0Ω	1052	100	4.95	2.73	1.67	13.5	24.4	0.373	9.1
	80.0Ω	1051	100	4.95	2.73	1.67	13.5	24.4	0.306	7.5

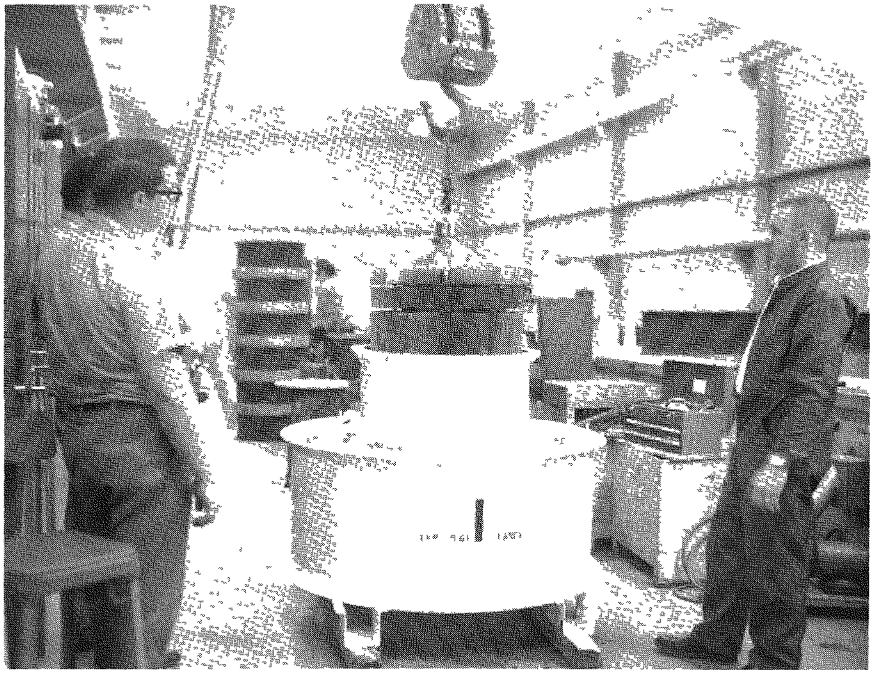

Figure 2-13. Fueled System Installation into Shipping Container

c) BOL Performance Test

Following the dynamic and hydrostatic testing of system S10P2, a BOL Performance Test was conducted to determine the various electrical characteristics.

The system and related equipment arrived at 3M Company on February 28, 1969, in good condition. The system was immediately set up for the Stable Reference Performance test. See Table 2-8.

Upon completion of the SRP testing, the system was removed from the shipping containers and placed into the water tank. The water temperature was controlled to 41 ± 3°F. After a stabilization period, the system was subjected to a System Performance test. This test was done to determine various system characteristics. The requirements and results of this test are as follows:

(a) Generator Open Circuit Voltage — The generator open circuit voltage shall be 9.10 vdc minimum when the power conditioner is electrically disengaged from the circuit.

Result: S10P2 - 9.25 vdc

(b) Generator Output Voltage — The generator output voltage shall be 4.83 ± 0.14 vdc when a variable load resistance placed across the system output terminals is varied from infinity to rated load (57.6 ohms).

Result: S10P2 - 4.95 vdc

(c) Voltage Regulation — The system output voltage shall be 24.0 ± 0.6 vdc when a variable load resistance placed across the system output terminals is varied from infinity to rated load (57.6 ohms).

Result: S10P2 - 24.4 vdc

(d) Generator Power — The minimum generator power output shall be 13.4 watts when rated load 57.6 ± 0.5 ohms is applied to the system output terminals.

Result: S10P2 - 14.09

(e) Power Conditioner Efficiency — The minimum power conditioner efficiency shall be 88 percent. This is determined by adjusting the system load resistance until the system output voltage is 24 ± 0.02 vdc. The system voltage and current measured under these conditions is then used in the following equation to obtain power conditioner efficiency:

$$\text{Efficiency} = \frac{\text{Power of System Output}}{\text{Power of Conditioner Input}}$$

Result: S10P2 - 90.0 percent

(f) Cold End Temperature Drop — The difference between the test tank water temperature and the cold frame center temperature shall not be greater than 35°F.

Result:	S10P2 -	Cold Frame	61°F
		Water	39°F
		Temp. Difference	22°F

(g) Output Ripple — The system output voltage shall have a ripple less than 0.10 volt peak-to-peak when the system load resistance is varied from infinity to 45 ohms.

Result: S10P2 - Less than 0.10 volts peak-to-peak

(h) Starting Capability — The system open circuit shall be 24 ± 1 vdc after being short circuited for a minimum of 5 minutes.

Result: S10P2 - 24.4 volts open circuit after a minimum of 5 minutes at short circuit

System S10P2 successfully completed the BOL Performance test.

d) System Environmental and Characterization Tests

The system was characterized for various system resistive loads at 40°F - 60°F and 80°F environmental water temperatures. At the present time, the data is being compiled and used with computer programs to predict annual characterization curves. The following parameters will be used to define the performance: generator power voltage, current, cold junction temperature and hot junction temperature each as a function of system resistance load at each environment water condition, system power out, current and voltage as a function of resistance load at each environmental water condition, and generator cold and hot junction temperatures as a function of time.

These data are being prepared for submission to the AEC and will be a part of the data package accompanying each fueled system.

2.1.2.3 System S10P3

Following assembly at ORNL in February 1969, the fueled system S10P3 was shipped to SWRI for hydrostatic testing. An opening in the schedule occurred at Sandia; it proved advantageous to ship the system to Sandia for dynamic testing, then return it to SWRI for hydrostatic testing.

A Quality Assurance representative was at ORNL during the period (11 through 13 February 1969) for the assembly, fueling, BOL test, preparations for shipping, and actual shipping operations of system S10P3. Modifications to the process routings for the assembly procedure were made to provide more comprehensive inspection to prevent the problems found in system S10P2.

A Quality Assurance representative was at Sandia during the period 25 through 28 February 1969 to witness equalization of the test equipment, preparation of fueled system S10P3 for dynamic testing, and actual testing operations. A thorough surveillance of methods and procedures with emphasis on calibration controls was made by the 3M Quality Control engineer.

a) Shock and Vibration

The shock and vibration testing was completed on fueled system S10P3 on March 4, 1969. The required tests to specifications were successfully conducted with no change in system performance.

Upon arrival at the test facility in February 1969, the system and equipment were inspected for transportation damage. The temperature recorder and impactograph on the shipping container were inspected and dated.

A Stable Reference Performance test was conducted on the system prior to removal from the shipping container.

During the Stable Reference Performance period, a dummy load equal to system weight was placed in the shock and vibration fixture and attached to the vibration machine. The recorded shock pulses used on fueled systems S10P1 and S10P2 were utilized on the dummy load configuration and found to be identical to previous trials and satisfactory for S10P3 shock testing.

The vibration equipment was given an operational check-out by conducting one sweep at the required input levels and duration.

Maximum acceleration (g) was measured and recorded during an emergency automatic shut-down, by causing the amplifier to go into automatic shut-down at a frequency of 6 Hz.

Following equipment capability verification, system S10P3 was placed into the shock and vibration fixture, the cooling ring was attached, and the system was allowed to stabilize.

The system was subjected to the required levels and durations for vibration and shock, as indicated below:

Vibration

5 - 5-1/2 Hz at 0.8 in DA displacement

5-1/2 - 26 Hz at 1.3g peak acceleration

26 - 40 Hz at 0.036 in DA displacement

40 - 50 Hz at 3.0g peak acceleration

Sweep three times 5-50-5 Hz in three axes in a period of 45-minute per axis.

Shock

Terminal peak sawtooth wave pulse with a magnitude of 6g and a duration of 6 milliseconds.

Three shock pulses in each direction of the three major axes (total 18 shocks).

System performance readings were taken before and after each sweep of vibration and each three shock pulses. See Table 2-9.

During the first Y-axis vibration sweep of the system, the power amplifier experienced a transient on the input voltage and went into automatic shut-down. The shaker dumped at 38 Hz. The shaker imparted a shock pulse of 5g in one millisecond to the input control accelerometer at the base of the test fixture.

The cause of the transient could not be found after a thorough inspection of the amplifier and control equipment. It was felt that the cause was due to the very high winds affecting the power lines outside the test building.

Table 2-9. Performance Data for Fueled System – S10P3

Parameter	Pre Environmental BOL Performance	Stable Reference Performance	Stable Reference Performance	Pre-Z Axis Shock and Vibration	Post Z Axis Shock and Vibration	Post Y Axis Shock and Vibration	Post-X Axis Shock and Vibration	Stable Reference Performance	Stable Reference Performance	Hydrostatic Pressure Test	Stable Reference Performance	Stable Reference Performance	Post Environmental BOL Performance	Thermocouple No Per Figure 2 8
Date Month/Day/Year	2/17/69	2/19/69	2/28/69	3/3/69	3/4/69	3/4/69	3/4/69	3/5/69	3/19/69	3/21/69	3/23/69			
System Fuel Input watts (t)	213 5	213 5	213 3	213 3	213 3	213 3	213 3	213 3	213 1	213 0	213 0			
Generator Primary Open Circuit (volts)	9 73	10 08	10 12	9 89	9 92	9 94	9 98	10 08	10 04	9 84	10 05			
Generator Bias Open Circuit (volts)	1 42	1 47	1 47	1 44	1 44	1 45	1 46	1 47	1 46	1 43	1 46			
Generator Primary Load Voltage (vdc)	4 97	4 97	4 99	4 98	4 98	4 98	4 98	4 97	4 99	5 00	4 99			
Generator Bias Load Voltage (vdc)	0 702	0 698	0 700	0 702	0 701	0 703	0 702	0 695	0 698	0 698	0 698			
Generator Primary Load Current (amps)	2 90	2 85	2 85	2 93	2 93	2 93	2 95	2 85	2 88	3 00	2 88			
Generator Bias Load Current (amps)	0 124	0 126	0 126	0 124	0 122	0 124	0 124	0 124	0 124	0 118	0 124			
Generator Primary Power Output watts (e)	14 4	14 2	14 2	14 6	14 6	14 6	14 7	14 2	14 4	15 0	14 4			
Generator Bias Power Output watts (e)	0 087	0 088	0 088	0 087	0 086	0 087	0 087	0 086	0 086	0 082	0 086			
Generator Total Power Output watts (e)	14 5	14 2	14 3	14 7	14 7	14 7	14 8	14 2	14 5	15 1	14 5			
Generator Internal Resistance (ohms)	1 63	1 78	1 79	1 66	1 67	1 68	1 68	1 78	1 74	1 60	1 75			
Conditioner Total Power Input watts (e)	14 5	14 2	14 3	14 6	14 6	14 6	14 8	14 2	14 4	15 0	14 4			
System Load Voltage (vdc)	24 5	24 5	24 6	24 5	24 5	24 5	24 5	24 5	24 5	24 5	24 5			
System Load Current (amps)	0 428	0 426	0 428	0 428	0 428	0 428	0 428	0 427	0 428	0 428	0 428			
System Power Output watts (e)	10 5	10 4	10 5	10 5	10 5	10 5	10 5	10 5	10 5	10 5	10 5			
System Load Resistance (ohms)	57 2	57 5	57 5	57 2	57 2	57 2	57 2	57 4	57 2	57 2	57 2			
Seg Ret Ring at Pressure Vessel Wall (°F)	44	82	98	64	64	64	64	96	82	37	84			1
Seg Ret Ring Inner (°F)	56	94	110	80	80	80	80	108	94	47	96			2
TEG Cold Frame Center (Ext) (°F)	64	102	117	88	87	88	87	116	102	56	104			3
TEG Hot Frame Center (Ext) (°F)	1056	1090	1095	1070	1071	1073	1077	1095	1081	1044	1083			4
TEG Hot Frame Edge (Ext) (°F)	1072	1106	1010	1086	1086	1088	1092	1110	1097	1061	1098			5
Emitter Plate Center (°F)	1268	1292	1296	1282	1286	1286	1293	1304	1293	1264	1294			6
Reference (°F)	40	83	97	71	72	71	71	96	81	37	85			7
Water Top (°F)	40									41				8
Water Center (°F)	40													9
Water Bottom (°F)	*40*									*30*				*10*
Average Cold Junction (Estimated) (°F)	92	130	145	116	115	116	115	144	130	85	132			
Average Hot Junction (Estimated) (°F)	1004	1038	1044	1019	1020	1022	1025	1044	1030	993	1032			
Ambient (°F)	62	71	75	72	73	3	2	72	67	4	72			
Test Hours	117	161	380	450	473	477	480	499	834	886	931			

The system remained stable following the dump pulse. Since the energy of the pulse was less than a normal shock pulse, the vibration sweep was resumed at 35 Hz with no further incidents occurring in vibration or shock testing.

System S10P3 successfully completed the vibration and shock requirements and was removed from the shock and vibration fixture.

Cooling fins were attached and the system was placed into the shipping container, after which a Stable Reference Performance test was conducted.

During the entire time that the fueled system was at the Sandia Test Laboratories, the system was monitored at least once daily for a radiation hazard by the Sandia Health/Physics Department.

No changes in radiation levels were found on the system throughout the dynamic testing.

Following the post-test Stable Reference Performance test, the system was placed into a short-circuit condition and shipped to Southwest Research Institute for hydrostatic pressure testing.

Sandia is preparing a complete test report on the shock and vibration testing.

b) Hydrostatic Test

System S10P3, and related test equipment, arrived at SWRI on March 17, 1969; visual examination revealed no damage. The test console was connected to the system for SRP and allowed to stabilize until the 19th of March when the SRP was taken on the system. On the same day, the system was placed into the pressure chamber.

A Quality engineer was at the hydrostatic testing facility during all preparations and system testing.

Hydrostatic testing was started on March 20 in simulated sea water at 34-42°F. Pressurization was performed at 2000 psi increments with a 10-minute hold period at each step. The hydro tests consisted of holding a pressure of $10,000\ ^{+200}_{-0}$ psi for a minimum of 5 hours. During the pressurization and 5-hour hold period, system performance was monitored and recorded. After the 5-hour hold period, depressurization of the chamber was done at a rate of 1,000 psi/min. During the first hour of the 5-hour hold period, the pressure chamber developed a leak of 600 lbs/min. It was decided to dump the test and fix the leak in the lower seal of the pressure chamber. To do this, the system had to be placed into a barrel of ice water in a loaded condition. After about three hours, the system was placed back into the pressure chamber.

On the 21st of March, hydrostatic testing was conducted in its entirety. The system performance was satisfactory, and the unit passed the test. Upon completion of the test, the unit was removed from the chamber and set up for SRP. After completion of the SRP on the 23rd of March, the system was made ready for shipment. Shipment of the system back to 3M Company was made on the 24th of March.

A report of condition for corrective action to the hydrostatic testing vendor has been prepared for vendor action.

2.1.2.4 General Quality Control Activities

In order to verify the adequacy of Quality Control Traceability of historical data for program hardware, the following effort is being completed:

A 100 percent traceability of all raw materials, detail parts, subassemblies and assemblies, including software documentation, is being completed for fueled system S10P1. Previous audits of the total traceability system by the RDT Site Representative, SNAP-21 Program Manager, and Quality supervision showed the traceability system and historical data to be valid.

The spherical surface measurement machine used specifically for verifying the critical spherical radius on T/E couple followers has been refurbished and recalibrated by Bendix Corporation, Dayton, Ohio. Calibration of the unit and all accessories is traceable through certificates to the National Bureau of Standards.

2.2 FUEL CAPSULE

The gage used for dimensional inspection of fuel capsules was used for acceptance of the fuel capsules used in fueled systems S10P1, S10P2, and S10P3.

Immediately prior to insertion of the fuel capsules into the systems, the fuel capsules were cooled with water and dimensionally checked with the "go" gage. This procedure was witnessed by a Quality Control engineer from 3M Company as part of the system assembly surveillance by Quality Assurance.

2.3 BIOLOGICAL SHIELD

Shield serial #009 (that has been in a hold status at Linde due to an oversize interface dimension) has been designated for use in HTVIS B10DL7. To compensate for the oversize interface dimension, additional compatibility barrier material will be applied to the spider, and the spider will be ground oversize.

Shield serial #007, from the disassembled HTVIS B10DL1, has been received from Linde and is being refurbished. A detailed processing and inspection procedure has been generated for cleaning, heat treating, and copper flashing. Figure 2-14 shows the dimensional inspection of the biological shield after heat treating and copper flashing. Quality assurance will participate in all phases of the refurbishing, including vendor selections. This shield is tentatively designated for HTVIS B10DL8.

2.4 INSULATION SYSTEM

2.4.1 Inner Liner Fabrication

During the Engineering Analysis of High Temperature Vacuum Insulation System (HTVIS) B10D4, it was found that the metallurgical properties of the neck tube portion of the inner liner were not as good as was desired. A study was therefore initiated to investigate fabrication techniques which would provide better metallurgical properties of the neck tube. Appendix A provides a brief background history of the inner liner development, the fabrication methods investigated, the development work which was performed on the selected fabrication technique, and the results, conclusions and recommendations arrived at as a result of this study.

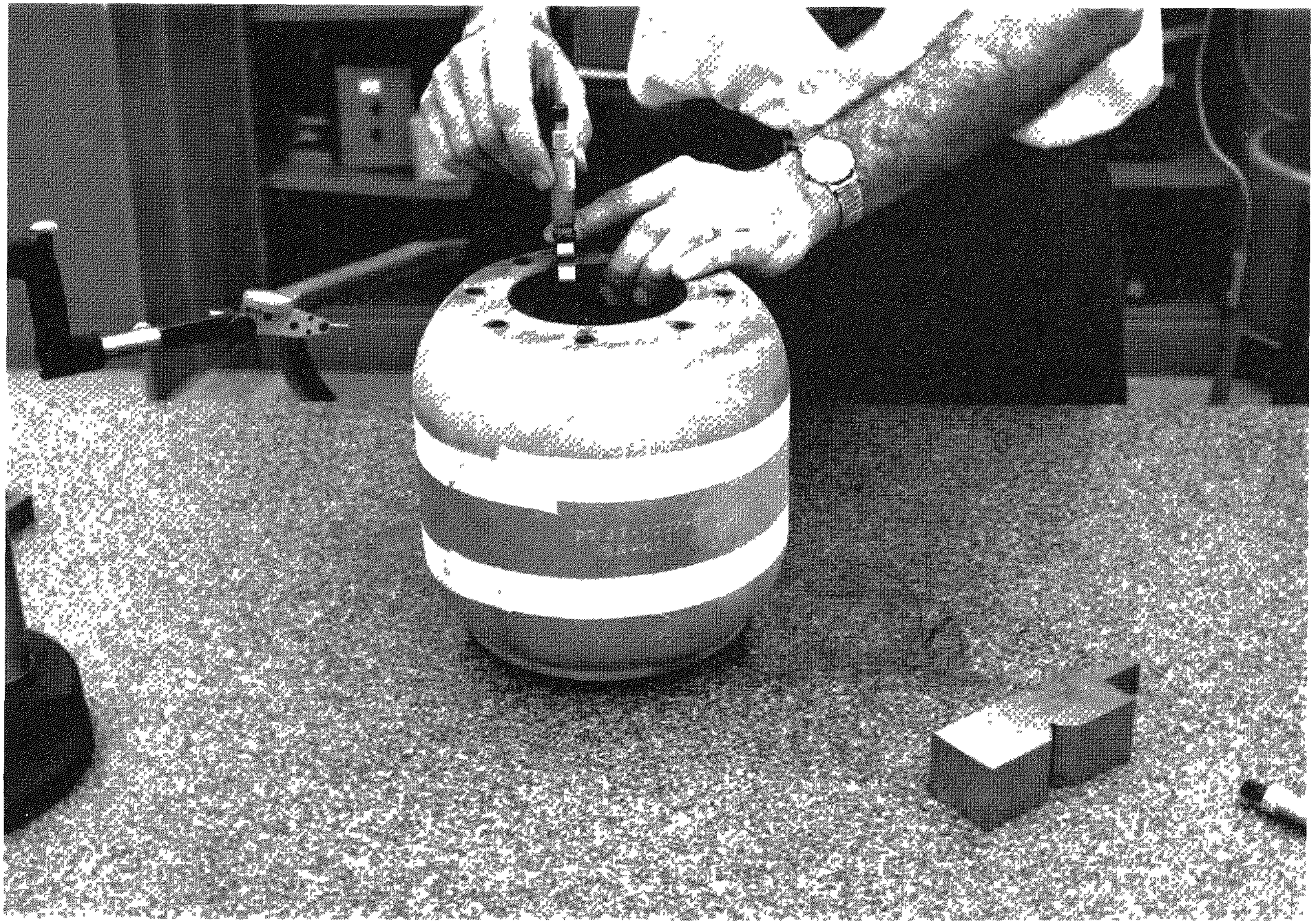

Figure 2-14. Dimensional Inspection, Biological Shield after Light Treat and Copper Flashing

Metallographic samples of the weld development sections were made to correlate the findings in the development x-rays. The metallographic samples confirmed the results of the x-rays. Sixteen 12" diameter Hastelloy-X circles in three separate thicknesses (0.093, 0.112, and 0.125) were ordered and received from the Haynes Stellite Division of Union Carbide. Five circles of each size were hydroformed at the Deep Draw Co. It was observed that a significant difference in surface finish occurred in the 0.112 size stock. Metallographic examination of this material confirmed that the grain size was larger than specified. The 0.112 parts were rejected, and the 0.125 parts were used instead. Fabrication of the hydroformed inner liners was completed, inspected by Quality Control, and accepted.

2.4.2 Disassembly of B10DL1

The spider, biological shield, and molybdenum washers (salvaged from unit B10DL1) will be used in the assembly of unit B10DL8.

Upon return of unit B10DL1 by common carrier truck from Ogden Technological Laboratories in Deer Park, Long Island, New York, disassembly was performed to salvage reusable components. The unit was mounted on an assembly shaft and installed in a unit handling fixture to facilitate the work. The tension rod seal-off plugs were milled out, and the female tension rods were removed from the unit. It was noted that female rod number 2 was broken near the threaded end. Next the bottom enclosure head was cut off with a seam grinder, thus exposing the insulation. The insulation over the spider was removed and the spider bolt was threaded out of the shield without difficulty. The spider was removed with a few gentle taps with a leather mallet.

The inner liner was cut off and the upper enclosure head was removed, followed by the removal of the insulation on the inner liner end of the shield. The inner liner bolts were loosened to remove the inner liner; however, five bolts were broken off during removal with only three being threaded out. The inner liner was easily lifted out of the radiation shield without cooling. The shield was oxidized with only traces of the copper flash coating remaining.

All the parts were surveyed for radioactive contamination and cleaned as required. The inner liner, shield, and spider were dimensionally inspected in the fit regions with the results presented in Table 2-10.

Table 2-10. Dimensional Inspection of Unit B10DL1 Components

	Measure at Unit Assembly (5/23/68)	Measure at Unit Salvage (3/18/69)	
Shield #007			
Overall Length	7.9967 7.9971	7.9954 7.9961	7.9963 7.9959
Spider Fit Dia.	4.4981 4.4993	4.4990 4.4983	4.4981 4.4981
Liner Fit Dia.	4.0368 4.0371	4.0397 4.0391	4.0393 4.0397
Spider #006			
Fit Dia.	4.4980 } (5/17/68) 4.4987 }	4.4982 4.4978	4.4981 4.4980
Liner #006			
Fit Dia.	4.0365 4.0369	4.0360 4.0362	4.0356 4.0355

Following the dimensional inspection the radiation shield, spider, inner liner, bolts and washers were shipped to 3M Company for rework to make these components suitable for use in unit B10DL8.

2.4.3 Completion of B10DL5

Wrapping of the insulation material on this unit was completed. The top enclosure head was welded to the neck tube, and the bottom enclosure head was aligned with the top enclosure head; the automatic girth weld was performed. The tension tie rods were installed, and the closure and leak check was completed. The thermal conditioning and thermal test were performed. The unit heat loss is 50.8 watts which exceeds specifications by 8.2 watts. The getter was installed and the final seal-off was made. The unit was placed in its shipping container, shipped to ORNL, and incorporated into system S10P3. 3M Quality Control personnel witnessed the final assembly of this system.

2.4.4 Assembly and Test of B10DL6

Unit B10DL6 was assembled using insulation system B10Q1. The instrumentation wires were removed, and the original bottom head was replaced by a new one. The tension tie rods were installed.

During the first leak check of unit B10Q1 prior to conducting the first thermal force cycle of the B10D4 Engineering Analysis, a small leak was located just below the neck tube edge weld. The presence of the leak was determined by helium leak check methods employing both a spray of helium and the helium filled bag technique. The absolute leak rate was not determined.

The leak was repaired by the application of epoxy in the leaking area for approximately 3/8 inch in length. The unit was releak checked, and no leakage was observed when spraying the epoxied area with helium. A bag leak test of the entire unit was performed, and the unit leak rate was acceptable.

Since this repair in June 1968, the unit has been subjected to four heat-cool cycles during the conduct of the thermal force cycle work. It has been decided to overhaul this unit to a delivery unit status and rename the unit B10DL6. Prior to the start of the overhaul work, the unit was evacuated. The neck tube was found to be less than 1×10^{-10} atm. cc. air/sec which is the minimum detectable leak rate of the leak detector. Visual observation could not detect any of the previously applied epoxy.

Because the unit has been built to the final delivery configuration, it was decided to apply a nickel plate to the neck tube similar to the one applied to B10DL2. Because the original leak could not be located circumferentially, the entire circumference was plated with nickel from the top of the neck tube one-half inch down using the equipment purchased for the B10DL2 repair.

Coatalyte 310B (Bright nickel, the material used for the rework) is certified, and certifications and analyses are on file in QC traceability files.

The unit was instrumented for conditioning as described in the Acceptance Test Plan. The unit was evacuated and heated to 1400°F. and held at this temperature for 48 hours to provide the required conditioning. Following the conditioning, the unit was cooled to operating temperature; the pressure rise rate was determined to be 0.15 microns per hour. The maximum allowable pressure rise rate for the delivery units is 2.42 microns per hour.

Following the pressure rise test, 15 grams of regular getter were installed in the unit.

After the unit was sealed off, the thermal performance test was conducted. It was found that a corrected power input of 61.8 watts was required to maintain the unit at a nominal 1285°F operating temperature. The subtractable heat loss due to the Min-K insulation, heater and thermocouple wires, and power lead loss is 14.1 watts. This yields a total unit heat loss of 47.7 watts. The required loss at test conditions (equivalent to the specification heat loss of 45 watts) is 42.6 watts. This unit, therefore, has a heat loss in excess of specifications of 5.1 watts.

Following the thermal performance test, the unit was fast cooled. After cooldown, the unit was installed in a HTVIS shipping container and shipped by Linde to 3M Company.

All work was performed under the surveillance of the Linde Quality Control organization.

Insulation system B10DL6 was put on long-term test the latter part of this report period. This HTVIS was integrated with thermoelectric generator A10P1 for long-term testing. Shown in Figure 2-15 is the instrumentation layout for this test. Shown in Figure 2-16 is a photograph of the test set-up. This arrangement closely simulates the actual system and is identical to the efficiency fixture test set-up. See section 2.5.2 for thermoelectric generator A10P1 performance. Thermal analysis of the insulation system will be completed when heat-up and stabilization are complete.

2.4.5 Insulation Systems B10DL7 and B10DL8

A Quality Control representative supported development of the inner liner (hydroformed thin wall section) by providing non-destructive testing and in-process

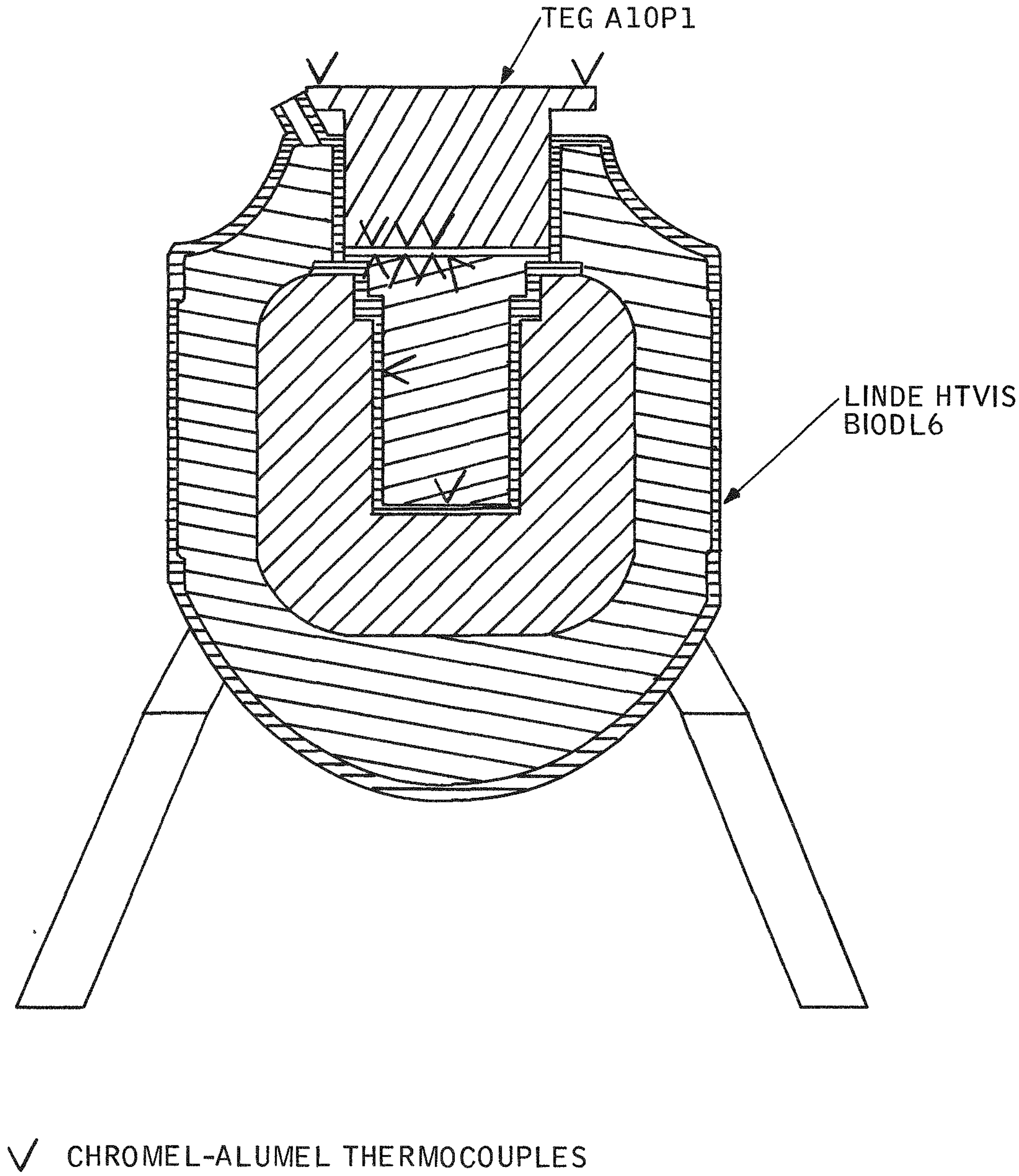

Figure 2-15. Instrumentation for HTVIS B10DL6 and TEG A10P1

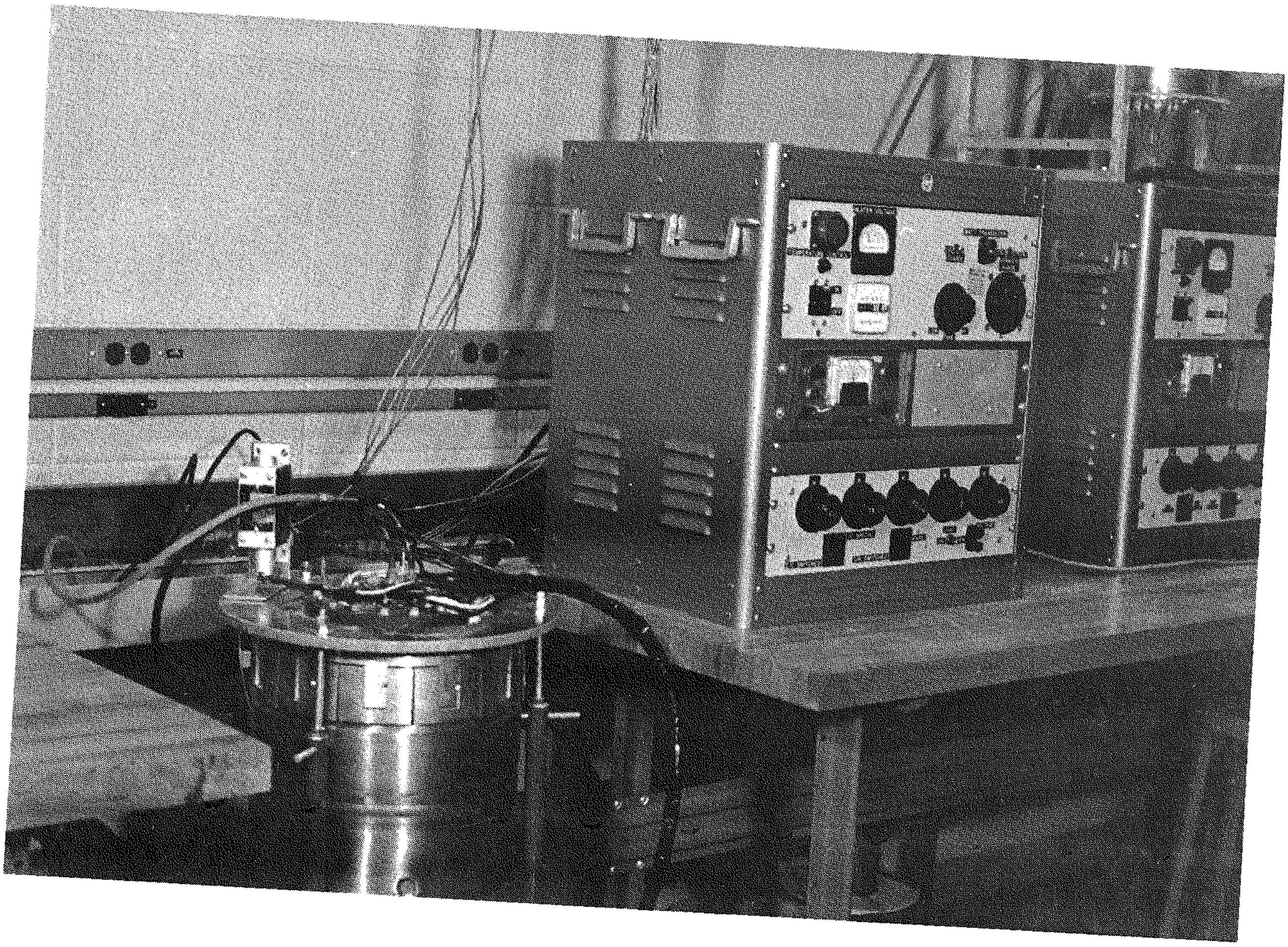

Figure 2-16. HTVIS B10DL6 and TEG A10P1 Test Set-Up

inspection activity. Weld integrity was evaluated by radiography. A 3M approved vendor (Larpen Industries, Milwaukee, Wisc.) was selected to perform the radiography. The vendor used a 1MEV x-ray unit for the analysis. The inner liners used in HTVIS B10DL7 and designated for HTVIS B10DL8 were inspected as detail parts (including x-ray and dye penetrant inspection of welds) and were plasma sprayed with aluminum oxide. One liner was ground for interface with the biological shield and used in insulation system B10DL7. Figure 2-17 shows the equipment and the method used for inspection of the inner liners.

The biological shield for this system is serial #009. The spider (serial #006) removed from destructed HTVIS B10DL1, has been reworked, re-sprayed with aluminum oxide, and re-ground to interface with shield serial #009. The spider was inspected and accepted while in-process and after final operations.

Figure 2-18 is a photo showing top view of the spider as sprayed and prior to grinding. A 3M Quality engineer was at Linde during the inspection and early stages of assembly of the system.

The insulation materials for systems B10DL7 and B10DL8 were pre-processed. As much pre-assembly of the insulation system as possible was performed to reduce the schedule time for unit fabrication to a minimum. Personnel were trained in the insulation application technique to ensure timely delivery of the final two units. Three men are now qualified to apply insulation during fabrication of units B10DL7 and B10DL8.

For unit B10DL7, the Linde and 3M supplied components were quality control inspected, and the spider sockets were lapped with the support rods male end.

The biological shield (#007) for system B10DL8 is being refurbished at 3M prior to shipment to Linde.

A summary of the thermal performance of all insulation systems built to date is shown in Table 2-11.

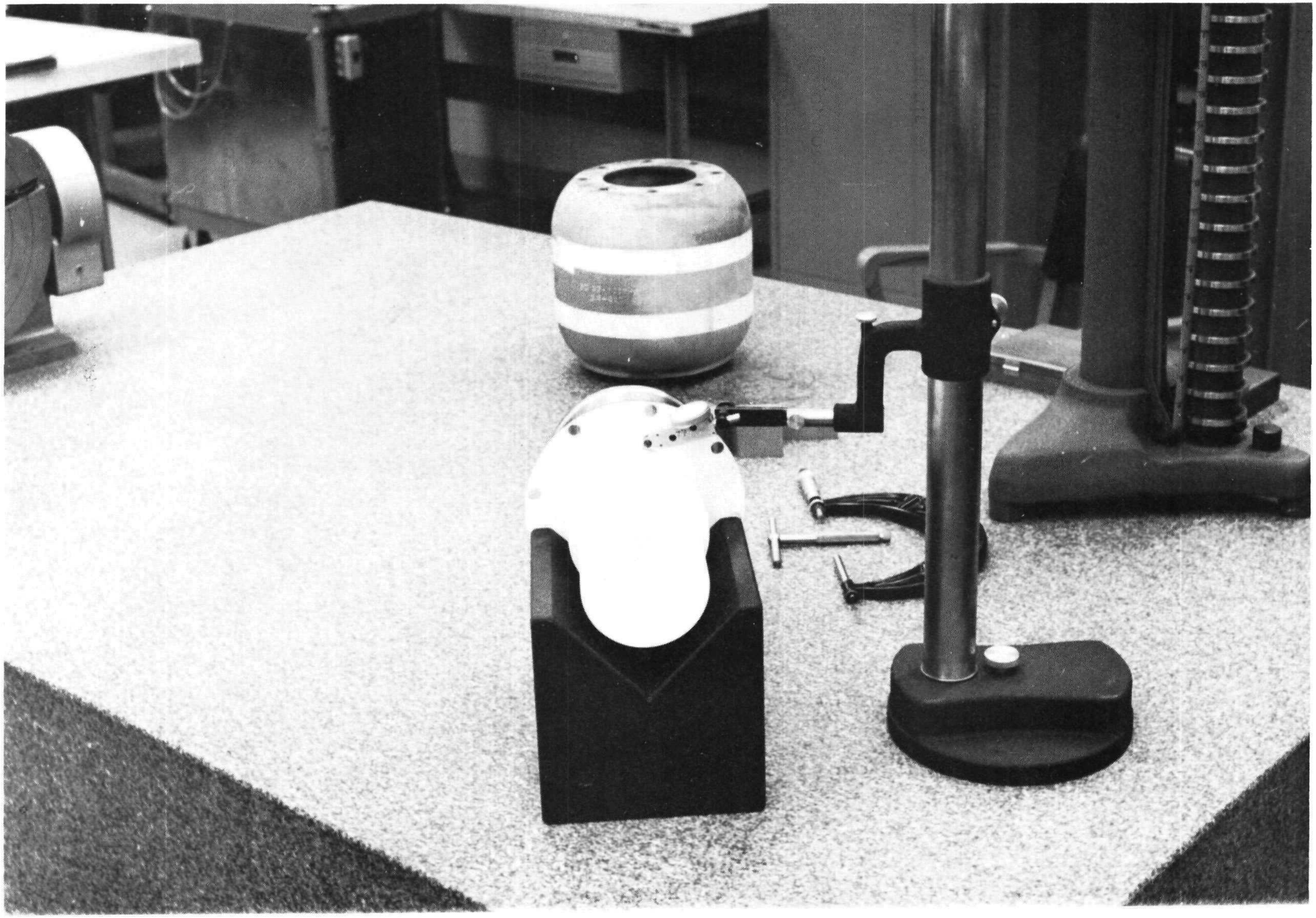

Figure 2-17. Inspection of Inner Liner

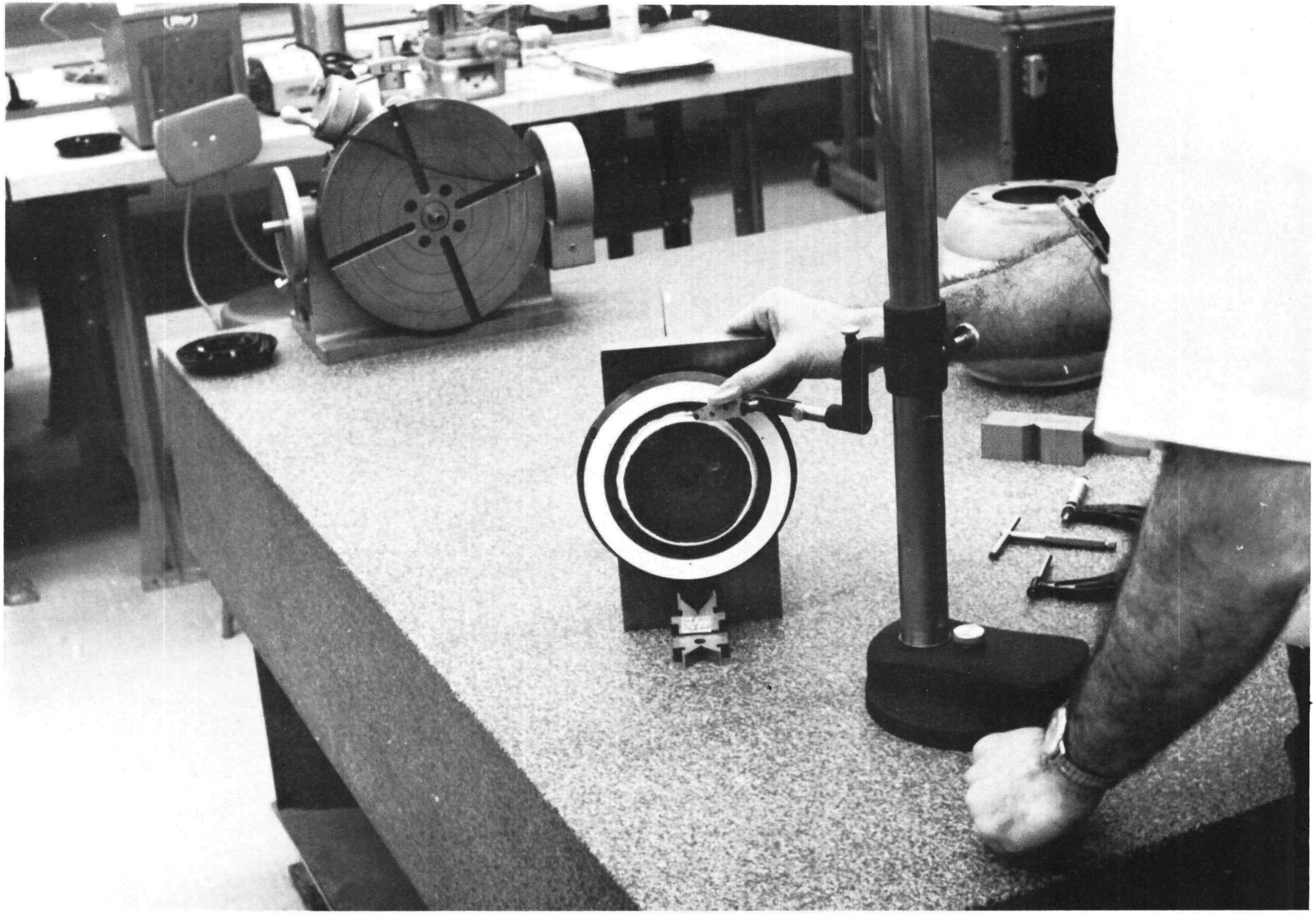

Figure 2-18. Inspection of the Spider, as Plasma Spray with Aluminum Oxide, Prior to Grinding for Interface with the Biological Shield

Table 2-11. Summary of HTVIS Unit Thermal Performance

Unit Number	Corrected Total Power To Unit (Watts)	Subtractibles (Watts)	Unit Heat Loss (Watts)
B10D1	61.1 **	10.9	50.2
B10D2	71.8 **	24.2	47.7
B10D3	71.3 **	24.3	47.0
B10D4	67.8 **	24.9	42.9
B10DL1	62.2	14.1*	48.1
B10DL2	63.2	14.1*	49.1
B10DL3	64.7	14.1*	50.6
B10DL4	68.0	14.1*	53.9
B10DL5	64.9	14.1*	50.8
B10DL6	61.8	14.1*	47.7

* Includes 0.9 watt I^2R loss of power wire between meters and heaters.

** Corrected for I^2R loss of power wire between meters and heaters and for test meter calibration. Delivery unit corrected total power is corrected only for test meter calibration.

2.5 THERMOELECTRIC GENERATOR

2.5.1 Phase I

Data collection and analysis of the Phase I 6-couple modules and prototype generators continued during this quarter. Performance data for 6-couple modules A1, A3, and A4 is given in Table 2-12 and Figures 2-19 through 2-21. Data from prototypes P5, P6, and P7 are given in Tables 2-13 through 2-15 and Figures 2-22 through 2-24.

Performance for 6-couple modules A1 and A3 remained stable this past quarter.

At the start of this report period, 6-couple module A4 started to increase in resistance. Eventually the resistance increased to such a value (~18.8Ω) that it appeared as an open circuit. Investigation showed that the open circuit was in the vicinity of couple #1 (see Figure 2-25). Because of the instrumentation, the exact location could not be pinpointed. Possible causes for this are: a broken lead internal to the unit, poor contact at the hot end, or a cracked leg.

At the present time, couple #1 is shorted out through the iron thermocouple lead of the P-leg of couple #2 and the current lead from couple #1.

A major cause for the power degradation was from the near open circuit condition across the couple #1 in the thermopile. The power output of the remaining five couples is presently at 0.38 watt, significantly less than the 1.5 watts BOL operating condition for the thermopile.

It is recommended that this thermopile be allowed to continue operating in the present five-couple status for the following reasons:

a. Degradation appears to have been curtailed. There is an indication of an improvement in power output for the five couples since the electrical by-pass.

b. It is believed that little information can be obtained from tearing down this module at this time. This module has had large output power fluctuations since BOL, which are not typical of the other modules built during the same period (1964).

Table 2-12. Performance Data of SNAP-21 6-Couple Modules

Module	Date	T_h (°F, est)	T_c (°F)	E_o (volts)	E_L (volts)	I_L (amps)	P_o (watts)	R (milliohms)	P_I (watts)	Hours
A1	8-13-68	1040	115	1.29	0.64	1.75	1.12	371	32.0	35,543
	8-27-68	1040	114	1.28	0.63	1.73	1.10	373	32.0	35,879
	9-6-68	1040	115	1.28	0.63	1.73	1.10	373	32.0	36,119
	9-16-68	1040	116	1.27	0.63	1.73	1.09	369	32.0	36,359
	10-9-68	1040	115	1.27	0.63	1.72	1.08	373	32.0	36,911
	10-21-68	1040	114	1.27	0.63	1.73	1.09	369	32.0	37,199
	11-7-68	1040	114	1.27	0.63	1.72	1.09	371	32.0	37,607
	11-25-68	1040	115	1.27	0.63	1.72	1.09	370	32.0	38,039
	12-9-68	1040	115	1.27	0.63	1.71	1.08	374	32 0	38,375
	12-9-68			Power Input Reduced						
	12-11-68	1020	116	1.24	0.62	1.67	1.03	374	35.0	38,423
	12-16-68	1020	115	1.24	0.61	1.67	1.03	375	35.0	38,543
	1-7-69	1020	115	1.24	0.62	1.71	1.06	362	35.0	39,071
	1-17-69	1020	115	1.24	0.62	1.71	1.06	363	35.0	39,311
	2-10-69	1020	116	1.24	0.63	1.69	1.06	364	35.0	39,887
	2-26-69	1020	117	1.25	0.62	1.67	1.03	380	35.0	40,271
	3-11-69	1020	115	1.24	0.62	1.69	1.05	367	35.0	40,583
	3-18-69	1020	116	1.24	0.62	1.69	1.05	367	35.0	40,751
A3	8-13-68	1040	117	1.30	0.65	1.76	1.14	372	46.5	34,211
	8-27-68	1040	119	1.30	0.64	1.77	1.14	371	46.5	34,547
	9-6-68	1040	119	1.30	0.64	1.76	1.13	374	46.5	34,787
	9-16-68	1040	119	1.29	0.64	1.76	1.13	367	46.5	35,027
	10-9-68	1040	118	1.30	0.64	1.76	1.13	373	46.5	35,579
	10-21-68	1040	119	1.31	0.64	1.77	1.14	376	46.5	35,867
	11-7-68	1040	118	1.31	0.65	1.77	1.14	375	47.0	36,275
	11-25-68	1040	119	1.31	0.65	1.76	1.14	378	47.0	36,707
	12-9-68	1040	120	1.30	0.65	1.77	1.14	370	47.0	37,043
	12-9-68			Power Input Reduced						
	12-11-68	1020	117	1.28	0.63	1.74	1.10	371	45.5	37,091
	12-16-68	1020	117	1.28	0.63	1.74	1.10	372	45.5	37,211
	1-7-69	1020	117	1.28	0.63	1.74	1.10	372	45.5	37,739
	1-17-69	1020	117	1.28	0.63	1.74	1.10	372	45.5	37,979
	2-10-69	1020	117	1.28	0.64	1.71	1.09	374	45.5	38,555
	2-26-69	1020	116	1.28	0.64	1.71	1.09	374	45.5	38,939
	3-11-69	1020	116	1.28	0.64	1.72	1.10	371	45.5	39,251
	3-18-69	1020	116	1.28	0.64	1.71	1.09	375	45.5	39,419

Table 2-12. Performance Data of SNAP-21 6-Couple Modules (Continued)

Module	Date	T_h (°F, est)	T_c (°F)	E_o (volts)	E_L (volts)	I_L (amps)	P_o (watts)	R (milliohms)	P_I (watts)	Hours
A4	8-13-68	1040	117	1.24	0.62	2.28	1.42	271	39.5	33,571
	8-27-68	1040	118	1.23	0.61	2.28	1.39	272	39.5	33,707
	9-6-68	1040	119	1.24	0.61	2.28	1.39	276	39.5	33,947
	9-16-68	1040	118	1.24	0.61	2.28	1.40	275	39.5	34,187
	10-9-68	1040	119	1.24	0.61	2.20	1.33	288	39.5	34,739
	10-21-68	1040	119	1.24	0.61	2.20	1.33	288	39.5	35,027
	11-7-68	1040	119	1.25	0.60	2.20	1.32	296	39.5	35,435
	11-25-68	1040	118	1.25	0.59	2.20	1.31	298	39.5	35,867
	12-9-68	1040	117	1.24	0.56	2.04	1.15	332	39.5	36,203
	12-9-68			Power Input Reduced						
	12-11-68	1020	112	1.22	0.56	2.03	1.13	327	38.8	36,251
	12-16-68	1020	112	1.23	0.55	2.00	1.10	341	38.5	36,371
	1-7-69	1020	115	1.23	0.55	1.62	0.896	418	37.5	36,899
	1-17-69	1020	115	1.22	0.61	1.44	0.871	427	37.5	37,139
	2-10-69	1020	115	1.23	0.61	1.37	0.836	453	37.5	37,715
	2-26-69	1020	115	1.23	0.45	0.993	0.450	782	37.0	38,099
	3-11-69	1020	115	1.22	0.04	0.081	0.003	14,590	37.0	38,411
	3-18-69	1020	115	1.22	0.03	0.061	0.002	18,880	37.0	38,579
	4-9-69	1020	115	1.05	0.51	0.743	0.378	730	37.0	39,107

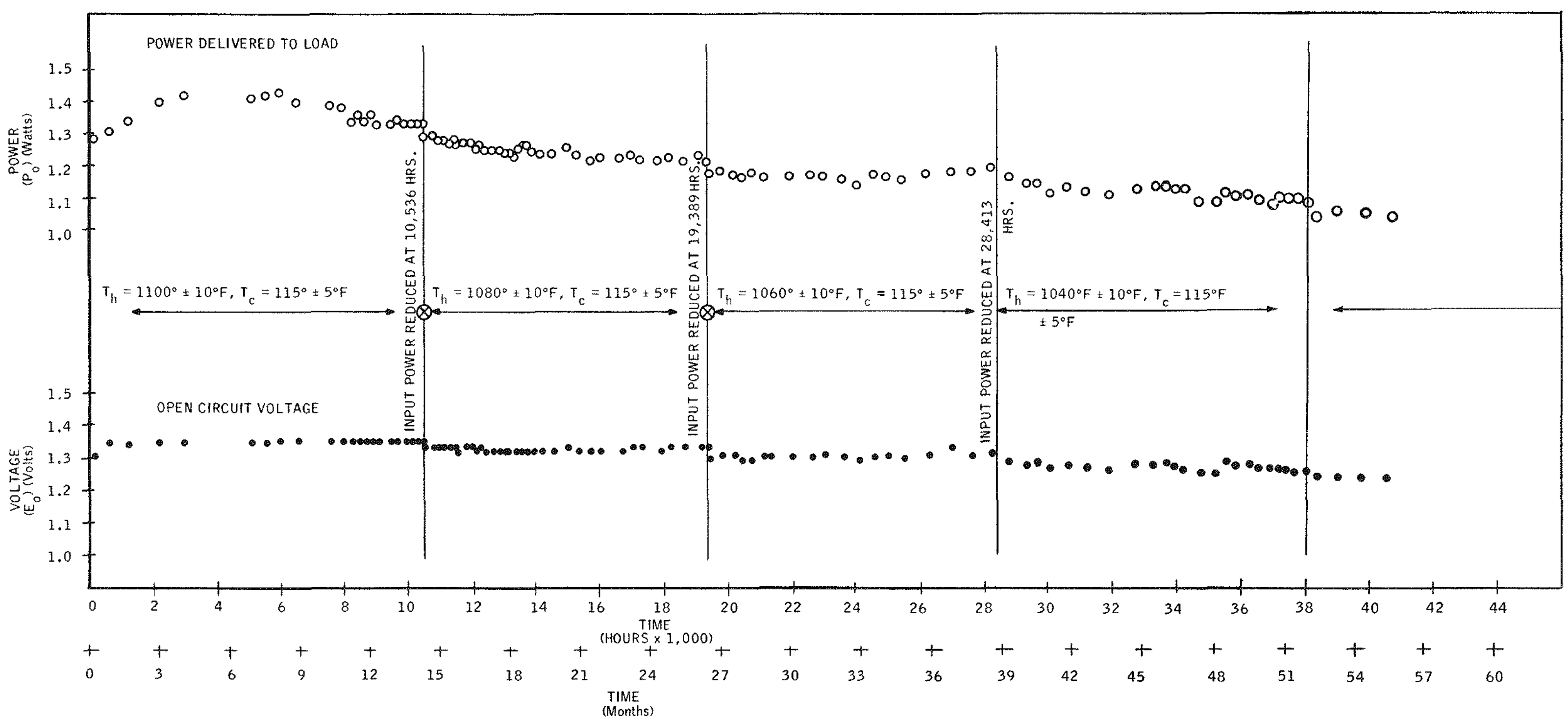

Figure 2-19. SNAP-21B 6-Couple Module A1

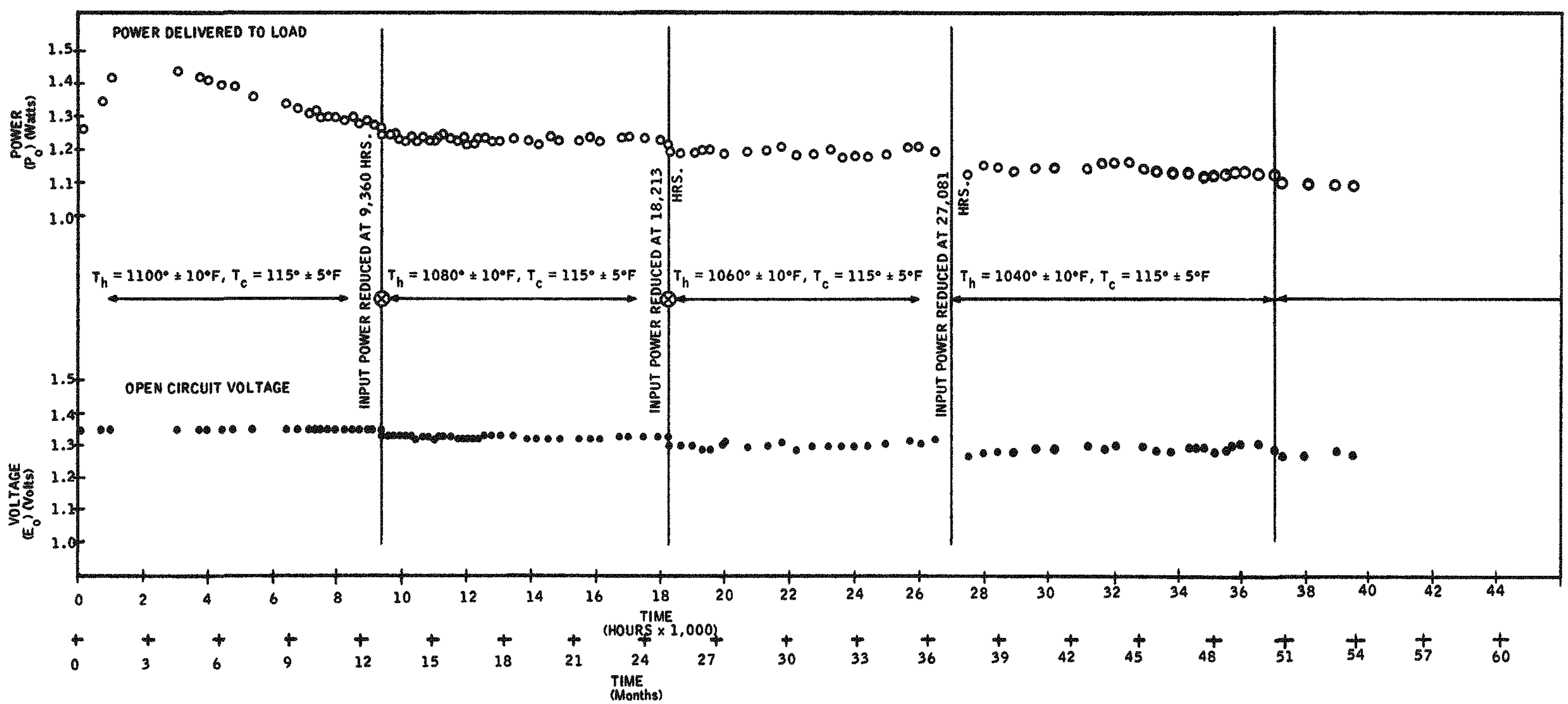

Figure 2-20. SNAP-21B 6-Couple Module A3

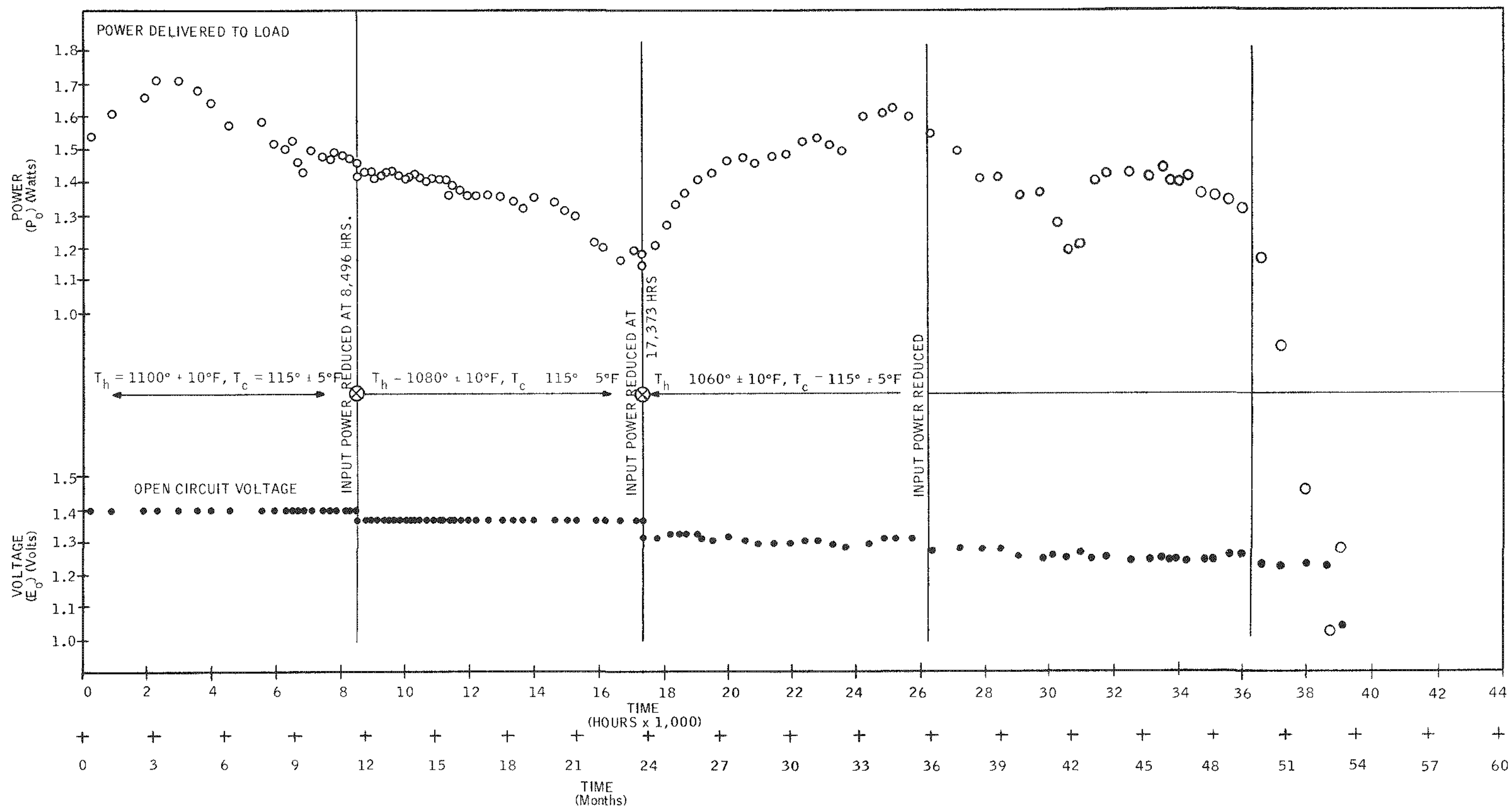

Figure 2-21. SNAP-21B 6-Couple Module A4

Table 2-13. Typical Performance Data SNAP-21B Prototype P5*

Date	T_h[1] (°F)	T_c[2] (°F)	E_o (volts)	F_L (volts)	I_L (amp)	P_o (watts)	R (ohms)	P_I (watts)	E_x/E_c	R_x/R_c	P_x/P_c	Hours on Test
4-19-65	1112	117	11.20	5.60	2.04	11.42	2.74	-	0.99	1.26	0.78	24
5-12-65	1115	127	10.92	5.46	2.00	10.92	2.73	--	0.97	1.24	0.77	576
6-30-65	1097	135	10.65	5.32	2.02	10.74	2.64	176	0.97	1.20	0.78	1,320
7-26-65	1097	142	10.68	5.34	2.01	10.72	2.66	176	0.98	1.21	0.79	1,944
9-10-65	1095	144	10.60	5.30	2.06	10.92	2.57	--	0.97	1.17	0.81	3,048
10-26-65	1097	147	10.56	5.28	2.05	10.81	2.58	180	0.97	1.16	0.82	4,152
12-1-65	1102	151	10.58	5.29	2.10	11.11	2.52	--	0.98	1.13	0.84	5,016
1-28-66	1094	149	10.56	5.28	2.14	11.30	2.47	180	0.98	1.11	0.86	6,408
3-28-66	1094	152	10.54	5.27	2.16	11.38	2.44	180	0.98	1.10	0.87	7,821
4-28-66	1074	151	10.20	5.10	2.19	11.17	2.33	176	0.97	1.07	0.87	8,565
6-21-66	1073	151	10.24	5.00	2.18	10.90	2.40	174	0.97	1.10	0.86	9,834
8-12-66	1078	161	10.15	5.07	2.20	11.15	2.30	178	0.97	1.04	0.89	11,081
9-14-66	1075	161	10.16	5.07	2.19	11.10	2.32	175	0.97	1.06	0.89	11,873
12-27-66	1077	153	10.22	5.11	2.19	11.19	2.33	184	0.97	1.07	0.87	14,369
1-31-67	1073	159	10.12	5.06	2.20	11.13	2.30	179	0.96	1.05	0.90	15,209
4-1-67	1074	148	10.20	5.10	2.24	11.42	2.28	175	0.97	1.05	0.89	16,649
5-24-67	1076	150	10.28	5.14	2.20	11.31	2.34	179	0.97	1.08	0.88	17,921
6-30-67	Power Failure, Emergency Power Came On at 8:28 PM to 10:30 PM											
7-1-67	1067	159	10.00	5.00	2.19	10.95	2.28	175	0.95	1.00	0.88	18,833
8-5-67	1069	164	10.01	5.00	2.22	11.10	2.26	170	0.95	1.01	0.90	19,673
9-26-67	1068	160	10.04	5.02	2.17	10.89	2.31	172	0.96	1.05	0.88	20,921
11-6-67	1067	158	10.08	5.04	2.19	11.04	2.30	174	0.96	1.00	0.89	21,953
12-29-67	1066	150	10.20	5.10	2.22	11.32	2.30	175	0.97	1.06	0.90	23,225
1-15-68	Power Failure, Emergency Power Came On for One Hour											
1-30-68	1070	151	9.90	4.95	2.21	10.94	2.26	175	0.94	1.01	0.87	23,993
2-17-68	Power Failure, Emergency Power Came On for Five Hours											
2-19-68	1068	149	10.10	5.05	2.17	10.96	2.33	177	0.96	1.00	0.87	24,473
3-14-68	1052	156	9.96	4.98	2.19	10.91	2.27	177	0.98	1.03	0.90	25,049
5-22-68	1077	154	10.02	5.02	2.22	11.14	2.25	176	0.95	1.04	0.87	26,705
6-17-68	1042	157	9.92	4.96	2.14	10.61	2.32	171	0.98	1.06	0.90	27,329
6-17-68	Reduced Input Power											
8-13-68	1044	166	9.80	4.90	2.09	10.24	2.34	169	0.98	1.14	0.87	28,697
9-16-68	1050	164	9.82	4.90	2.09	10.24	2.35	169	0.97	1.14	0.86	29,513
11-6-68	1052	162	9.76	4.88	2.10	10.25	2.32	170	0.97	1.13	0.87	30,737
12-16-68	1052	152	9.86	4.93	2.15	10.60	2.29	170	0.97	1.13	0.86	31,697
1-16-69	1052	151	9.88	4.94	2.12	10.47	2.33	170	0.97	1.13	0.87	32,441
1-27-69	Regulator Failure Power Increased for 12 Hours											
2-10-69	1052	149	9.88	4.94	2.21	10.92	2.24	171	0.97	1.10	0.88	33,041
3-10-69	1050	154	9.85	4.89	2.21	10.83	2.24	172	0.96	1.09	0.89	33,713

*Begin test on 4-19-65
Turned off from 5-20-65 to 6-7-65

1 Based on average of two N leg Seebeck voltages
2 Based on average of four cold electrode thermocouples

Table 2-14. Typical Performance Data SNAP-21B Prototype P6*

Date	T_h [1] (°F)	T_c [2] (°F)	E_o (volts)	E_L (volts)	I_L (amp)	P_o (watts)	R (ohms)	P_I (watts)	$\frac{E_x}{E_c}$	$\frac{R_x}{R_c}$	$\frac{P_x}{P_c}$	Hours on Test
6- 2-65	1095[1]	132	10.88	5.44	2.58	14.03	2.10	204	1.03	1.02	1.02	24
6-30-65	1095[2]	145	10.88	5.44	2.34	12.73	2.32	206	1.04	1.11	0.96	720
7-29-65	1095[2]	157	10.88	5.44	2.28	12.40	2.38	--	1.04	1.13	0.96	1,416
9- 1-65	1095[2]	162	10.80	5.40	2.20	11.88	2.45	201	1.04	1.16	0.93	2,184
9-30-65	1095[2]	166	10.72	5.36	2.19	11.74	2.45	198	1.04	1.15	0.93	2,880
11-17-65	1095[2]	169	10.80	5.40	2.16	11.66	2.50	201	1.05	1.16	0.94	4,032
12-28-65	1095[2]	171	10.78	5.39	2.18	11.75	2.47	200	1.05	1.15	0.95	5,016
2- 5-66	1095[2]	171	10.74	5.37	2.14	11.49	2.51	197	1.04	1.17	0.93	5,952
3-28-66	1095[2]	171	10.74	5.39	2.13	11.44	2.52	197	1.04	1.17	0.92	7,173
4-28-66	1095[2]	172	10.76	5.38	2.11	11.35	2.55	201	1.04	1.19	0.92	7,941
8-12-66	1075[2]	181	10.52	5.23	2.05	10.72	2.58	191	1.05	1.20	0.92	10,452
9-14-66	1075[2]	182	10.53	5.24	2.06	10.79	2.57	190	1.05	1.20	0.93	11,244
12-27-66	1075[2]	176	10.82	5.41	2.09	11.28	2.59	192	1.07	1.22	0.95	13,740
1-27-67	1075[2]	176	10.84	5.42	2.10	11.38	2.58	199	1.08	1.22	0.96	14,484
3-13-67	1075[2]	173	10.86	5.43	2.09	11.35	2.60	198	1.08	1.23	0.95	15,564
4-27-67	1075[4]	168	10.38	5.19	2.07	10.72	2.51	194	1.03	1.20	0.89	16,524
6-16 67	1075[4]	176	10.58	5.29	2.05	10.84	2.58	194	1.05	1.23	0.90	17,844
6-22-67	Power Input Reduced							186				17,988
6-30-67	1055[4] Bldg Power Failure, Emergency Power for Approx. 2 Hours											
7- 1-67	1055[4]	172	10.10	5.05	2.04	10.28	2.48	184	1.03	1.20	0.88	18,204
8- 4-67	1055[4]	178	9.95	4.98	2.03	10.11	2.45	185	1.02	1.18	0.90	19,020
9-26-67	1055[4]	175	10.08	5.04	2.02	10.18	2.50	186	1.03	1.21	0.88	20,292
11- 6-67	1055[4]	172	10.08	5.04	2.02	10.18	2.50	185	1.03	1.21	0.87	21,324
11-30-67	1055[4]	166	10.00	5.00	2.04	10.20	2.45	190	1.02	1.20	0.86	21,900
1-15-68	Bldg. Power Was Off—Emergency Power Came On for One Hour											
1-17-68	1055[4]	166	10.04	5.02	2.03	10.19	2.47	192	1.02	1.20	0.86	23,052
2-17-68	Bldg. Power Was Off—Emergency Power Came On for 5 Hours											
3-14-68	1055[4]	171	10.02	5.01	2.04	10.22	2.46	192	1.02	1.19	0.88	24,420
5- 9-68	1055[4]	169	10.00	5.00	2.04	10.20	2.45	192	1.01	1.19	0.87	25,764
7-10-68	1035[4]	173	9.76	4.88	1.97	9.61	2.48	188	1.03	1.23	0.87	27,252
8-13-68	1035[4]	182	9.76	4.88	1.99	9.71	2.45	188	1.04	1.21	0.89	28,068
9-16-68	1035[4]	175	9.76	4.88	1.98	9.66	2.46	188	1.03	1.22	0.87	28,884
5-9-68	1055	169	10.00	5.00	2.04	10.20	2.45	192	1.01	1.19	0.87	25,764
6-17-68	Reduced Input Power											
7-10-68	1035[4]	173	9.76	4.88	1.97	9.61	2.48	188	1.03	1.23	0.87	27,252
8-13-68	1035[4]	182	9.76	4.88	1.99	9.71	2.45	188	1.04	1.21	0.89	28,068
9-16-68	1035[4]	175	9.76	4.88	1.98	9.66	2.46	188	1.03	1.22	0.87	28,884
11-6-68	1035[4]	174	9.80	4.89	1.99	9.73	2.47	188	1.04	1.22	0.88	30,108
12-16-68	1035[4]	165	9.80	4.89	2.00	9.78	2.46	188	1.03	1.23	0.87	31,068
1-16-69	1035[4]	165	9.83	4.90	2.00	9.80	2.47	188	1.03	1.24	0.87	31,812
1-27-69	Regulator Failure Power Increased for 12 Hours											
2-10-69	1035[4]	164	9.83	4.91	2.05	10.07	2.40	188	1.03	1.20	0.89	32,412
3-10-69	1035[4]	166	9.86	4.92	2.06	10.14	2.40	190	1.04	1.20	0.90	33,084

*Begin test 6-1-65

1 Based on average of two hot electrode thermocouples
2 Based on hot frame thermocouple referenced to 6-2-65
3 Based on average of two cold electrode thermocouples
4 Based on average input power from 6-5-66 to 12-27-66

Table 2-15. Typical Performance Data SNAP-21B Prototype P7*

Date	T_h[1] (°F)	T_c[2] (°F)	E_o (volts)	E_I (volts)	I_I (amp)	P_o (watts)	R (ohms)	P_I (watts)	$\frac{E_x}{E_c}$	$\frac{R_x}{R_c}$	$\frac{R_x}{P_c}$	Hours on Test
6-8-65	1099[1]	127	10.80	5.40	2.44	13.17	2.21	200	1.01	1.08	0.95	168
7-14-65	1098[1]	142	10.80	5.40	2.21	11.95	2.44	194	1.01	1.18	0.88	1,032
8-24-65	1100[3]	152	10.82	5.41	2.13	11.52	2.54	192	1.03	1.21	0.88	1,968
10-12-65	1100[3]	156	10.86	5.43	2.11	11.47	2.57	194	1.04	1.22	0.82	3,144
11-17-65	1095[3]	158	10.80	5.40	2.08	11.23	2.60	188	1.04	1.23	0.87	4,008
12-28-65	1095[3]	159	10.78	5.39	2.07	11.16	2.60	191	1.04	1.23	0.88	4,992
2-10-66	1095[3]	158	10.82	5.41	2.06	11.14	2.63	191	1.04	1.24	0.88	6,048
3-28-66	1095[3]	160	10.80	5.40	2.05	11.07	2.63	191	1.04	1.24	0.87	7,149
5-16-66	1095[3]	163	10.82	5.41	202	10.93	2.68	189	1.04	1.26	0.86	8,324
6-4-66	Reduced Input Power											
6-21-66	1075[3]	158	10.72	5.40	1.99	10.75	2.67	186	1.06	1.28	0.87	9,181
6-28-66	Moved Test from T.C.A. to Space Center											
8-12-66	1075[3]	173	10.56	5.26	1.96	10.31	2.55	188	1.05	1.26	0.86	10,428
10-3-66	1075[3]	178	10.62	5.31	1.95	10.35	2.72	185	1.05	1.27	0.89	11,676
12-28-66	1075[4]	165	10.70	5.35	1.94	10.37	2.76	186	1.05	1.31	0.84	13,760
1-31-67	1075[4]	171	10.70	5.35	1.96	10.49	2.73	186	1.06	1.30	0.86	14,576
3-13-67	1075[4]	173	10.60	5.30	1.94	10.26	2.74	186	1.06	1.29	0.86	15,560
5-13-67	1075[4]	175	10.61	5.30	1.91	10.11	2.78	186	1.06	1.31	0.85	17,024
6-22-67	Input Power was Reduced							180				
6-23-67	1055[4]	171	10.30	5.15	1.91	9.84	2.70	180	1.05	1.31	0.84	18,008
6-30-67	Bldg. Power Failure, Emergency Power was on for Approx. 2 Hours											
7-1-67	1055[4]	165	10.30	5.15	1.86	9.58	2.77	180	1.05	1.35	0.81	18,192
8-8-67	1055[4]	182	10.19	5.10	1.92	9.79	2.65	178	1.05	1.27	0.86	19,110
9-26-67	1055[4]	166	10.26	5.13	1.92	9.85	2.67	179	1.04	1.30	0.83	20,286
10-20-67	1055[4]	171	10.14	5.07	1.91	9.68	2.65	176	1.03	1.29	0.83	21,091
1-15-68	Bldg. Power was off - Emergency Power came on for One Hour											
1-17-68	1055[4]	169	10.40	5.20	1.92	9.98	2.71	177	1.06	1.32	0.85	23,203
2-17-68	Bldg. Power was off - Emergency Power came on for about 5 Hours											
2-19-68	1055[4]	164	10.20	5.10	1.92	9.79	2.66	180	1.04	1.30	0.83	23,997
3-20-68	1055[4]	169	10.28	5.14	1.92	9.87	2.68	181	1.05	1.30	0.85	24,717
4-18-68	1055[4]	177	10.20	5.10	1.93	9.84	2.64	189	1.04	1.28	0.85	25,384
5-9-68	1055[4]	179	10.28	5.14	1.93	9.92	2.66	180	1.06	1.28	0.87	25,917
6-17-68	1055[4]	182	9.94	4.97	1.90	9.44	2.62	176	1.02	1.26	0.83	26,853
8-13-68	1035[4]	177	9.78	4.89	1.91	9.34	2.56	174	1.04	1.27	0.85	28,221
9-16-68	1035[4]	173	9.75	4.88	1.90	9.27	2.56	174	1.03	1.27	0.84	29,037
6-17-68	1055[4]	182	9.94	4.97	1.90	9.44	2.62	176	1.02	1.26	0.83	26,853
6-17-68	Reduced Power Input											
8-13-68	1035[4]	177	9.78	4.89	1.91	9.34	2.56	174	1.04	1.27	0.85	28,221
9-16-68	1035[4]	173	9.75	4.88	1.90	9.27	2.56	174	1.03	1.27	0.84	29,037
11-6-68	1035[4]	170	9.82	4.91	1.87	9.18	2.63	174	1.03	1.30	0.82	30,261
12-16-68	1035[4]	159	9.83	4.93	1.88	9.27	2.61	174	1.03	1.30	0.82	31,221
1-16-69	1035[4]	159	9.88	4.94	1.92	9.48	2.57	174	1.04	1.30	0.84	31,965
1-27-69	Regulator Failure Power Increased for 12 Hours											
2-10-69	1035[4]	158	9.90	4.94	1.96	9.68	2.53	175	1.04	1.28	0.85	32,565
3-10-69	1035[4]	16	9.91	4.94	1.97	9.73	2.52	175	1.04	1.27	0.86	33,237

* Begin test 6-2-65.

1. Based on average of two hot electrode thermocouples.
2. Based on average of two cold electrode thermocouples.
3. Based on hot frame thermocouple referenced to 6-30-65.
4. Based on average input power from 7-13-66 to 11-12-66.

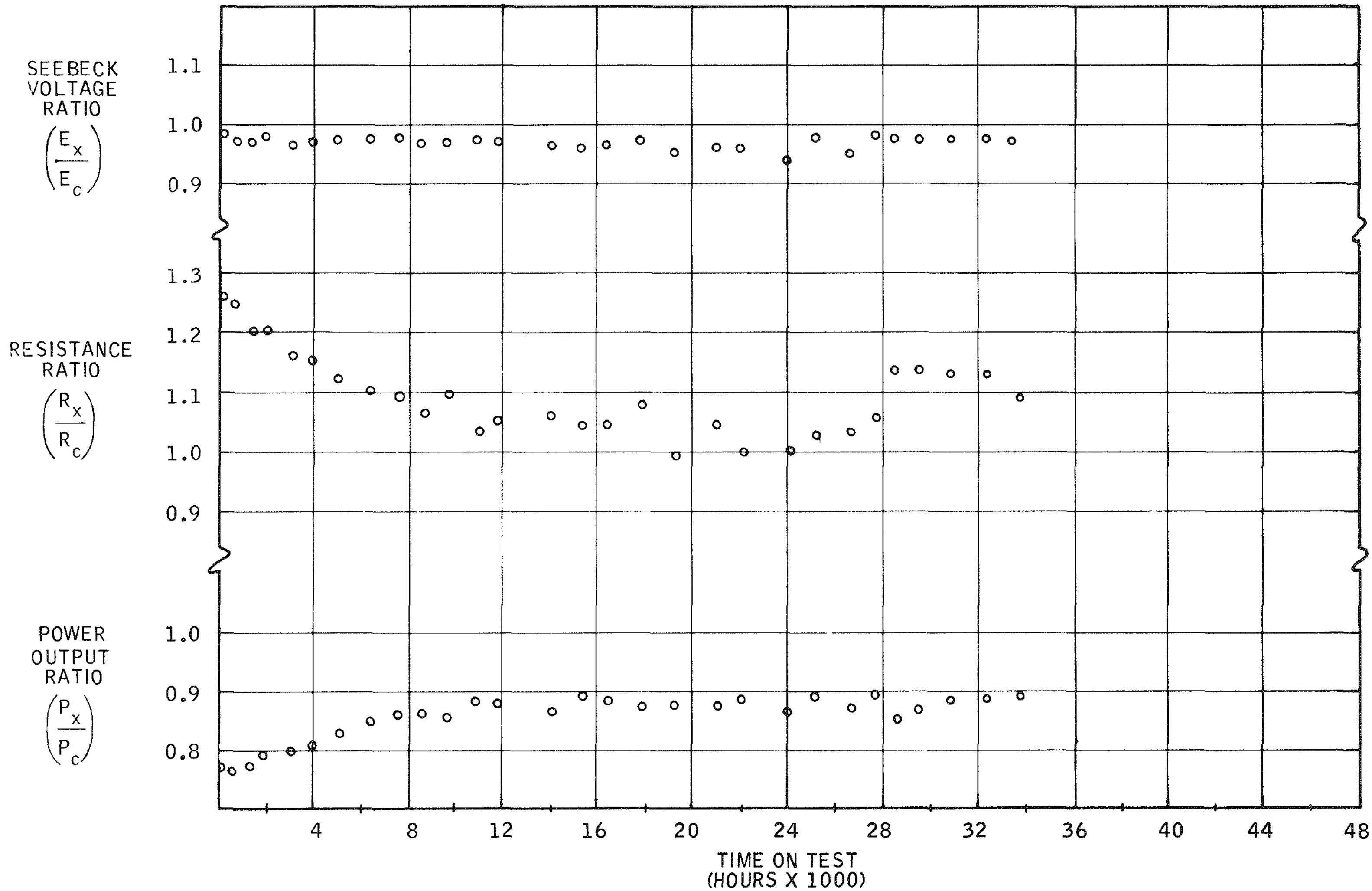

Figure 2-22. SNAP-21B 48-Couple Prototype Generator P5 Performance Ratios (Experimental/Calculated)

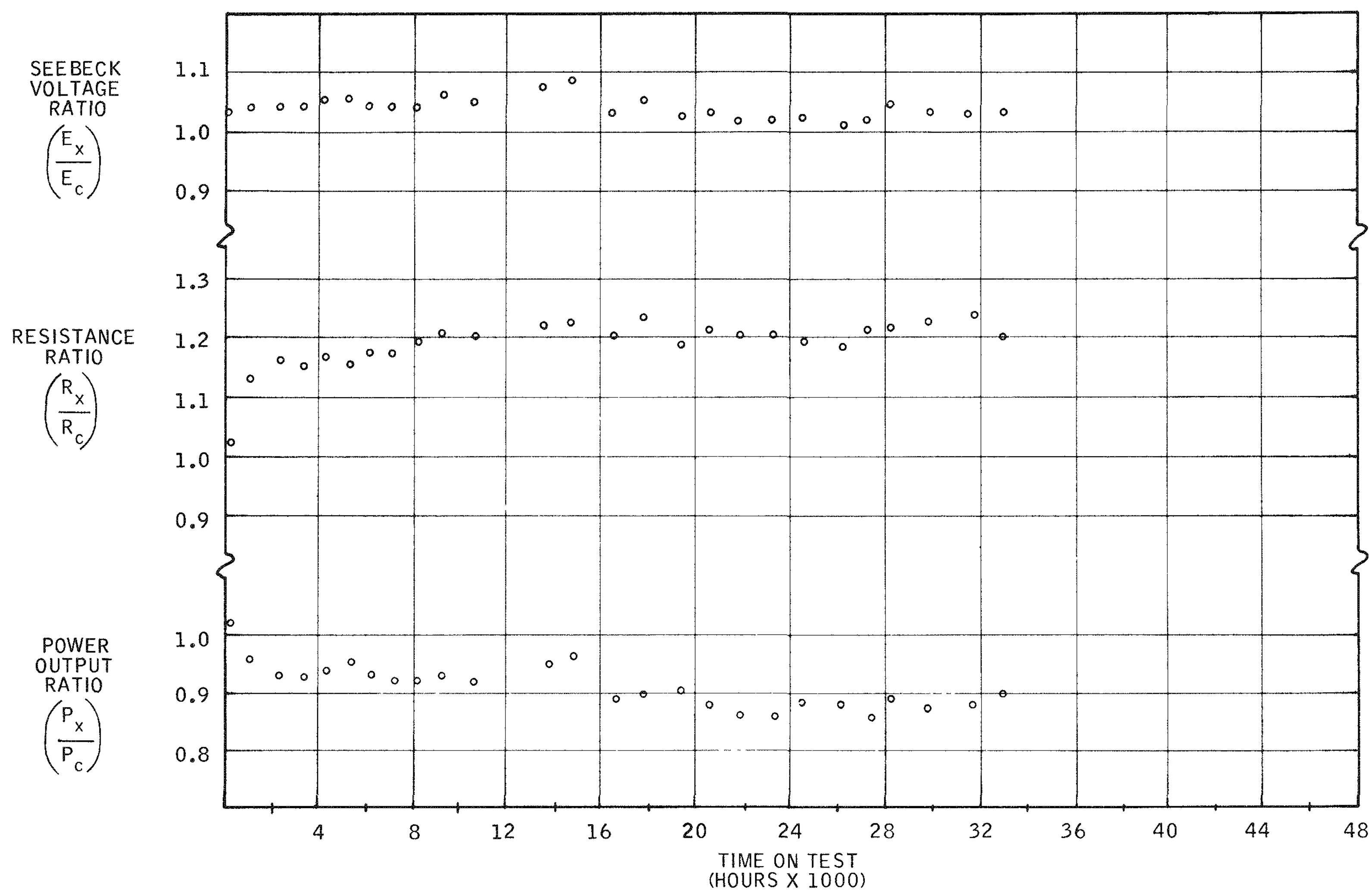

Figure 2-23. SNAP-21B 48-Couple Prototype Generator P6 Performance Ratios (Experimental/Calculated)

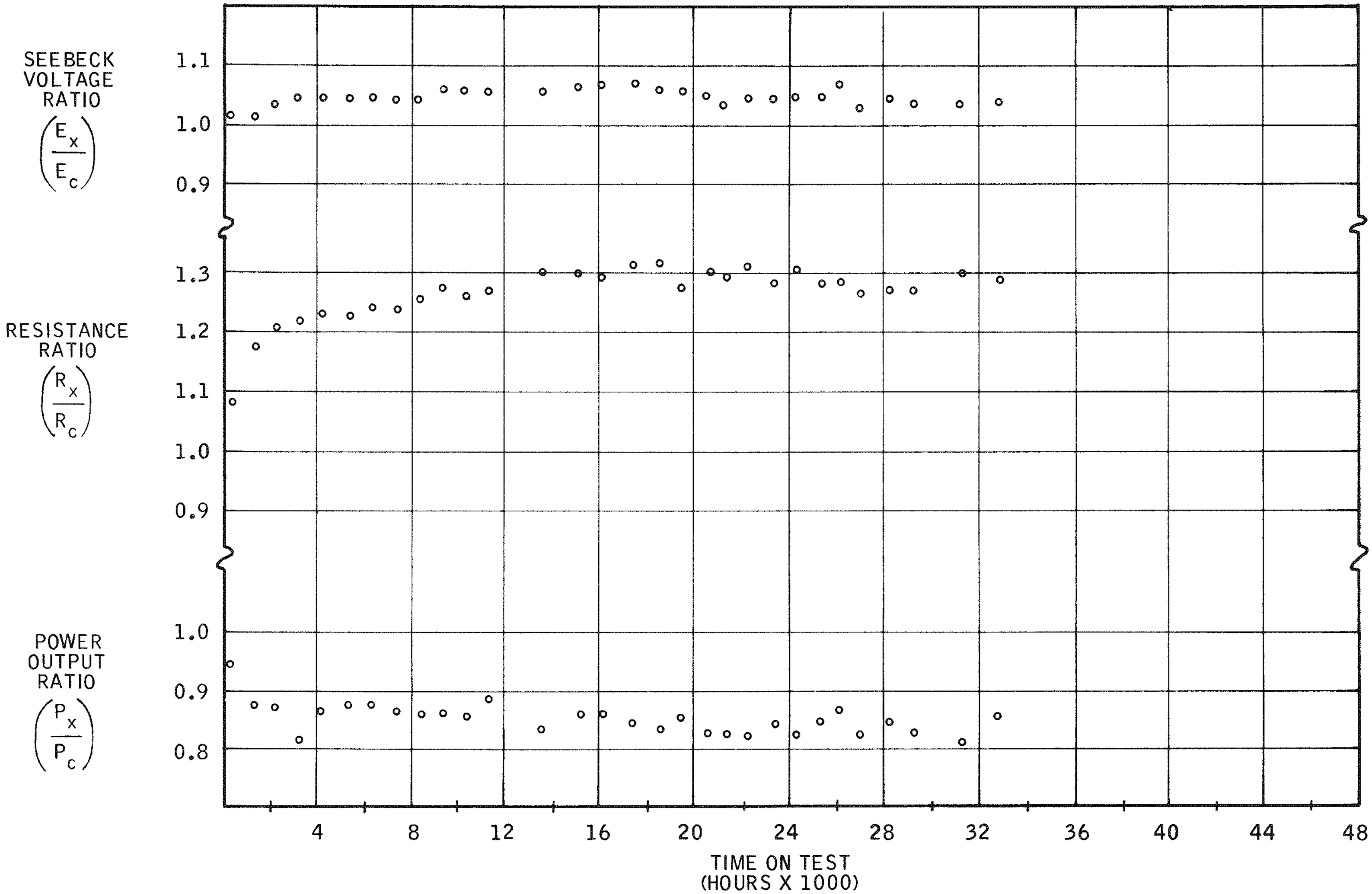

Figure 2-24. SNAP-21B 48-Couple Prototype Generator P7 Performance Ratios (Experimental/Calculated)

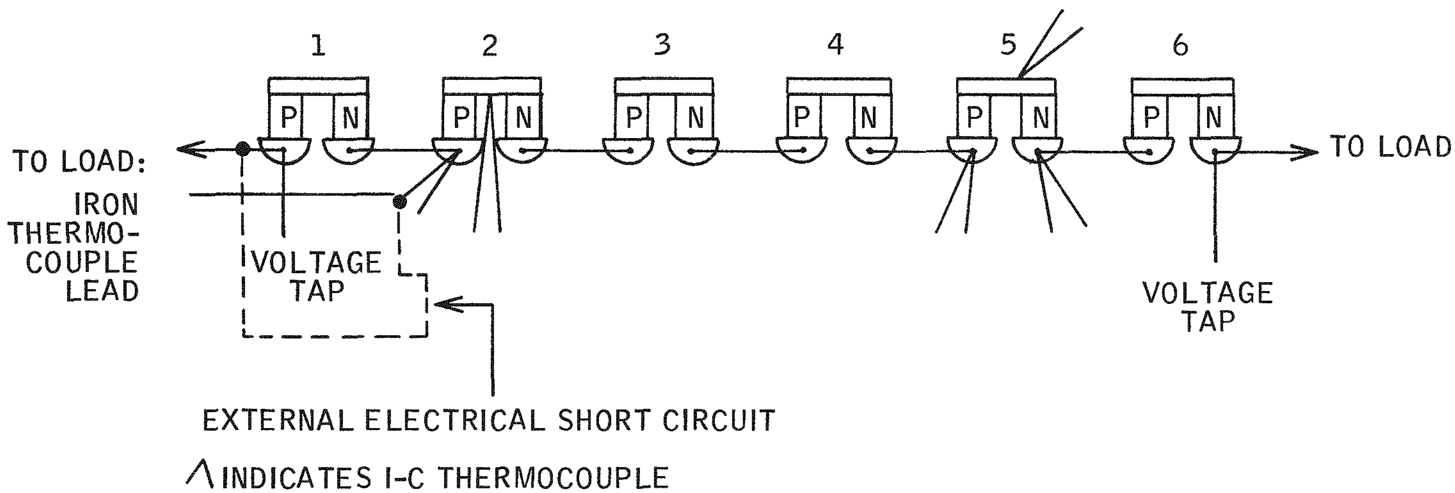

Figure 2-25. 6-Couple Module A4 Circuit Diagram

Prototype generators P5 through P7 operated satisfactorily during this past quarter. The only perturbation in the generator testing has been a regulator failure (January 27, 1969) which caused the hot and cold junction temperatures to increase approximately 270°F and 15°F respectively. See section 2. 5. 2. 2 for an explanation of this incident. It appears that there is a possibility of short-term effects from this incident. Investigation of Tables 2-13 through 2-15 showed that the resistance of the thermopiles has decreased approximately 2-3% after this incident. This resulted in an increase in power-out. This trend will be watched during the next quarter.

2. 5. 2 Phase II Thermoelectric Generators

2. 5. 2. 1 Performance Testing

A10D1

Thermoelectric generator A10D1 continued on test this past quarter. The leak in the generator appeared to be on the outlet side of the gas sample valve. To remedy this, the generator was backfilled to 25 psia, all tubing was removed, and the valve was plugged. This appears to have solved the problem.

During this past quarter, a failure occurred in the input power regulator for the SNAP-21 thermoelectric generators. Refer to section 2. 5. 2. 2 for a discussion of this incident.

Figures 2-26a through 2-26c show the performance curves for this generator. There was an approximate 7% drop in power-out this past quarter. The major cause for this is due to the increase in resistance. Also, there has been a decrease in Seebeck voltage. There have been no apparent short term effects from the malfunction of the voltage regulator.

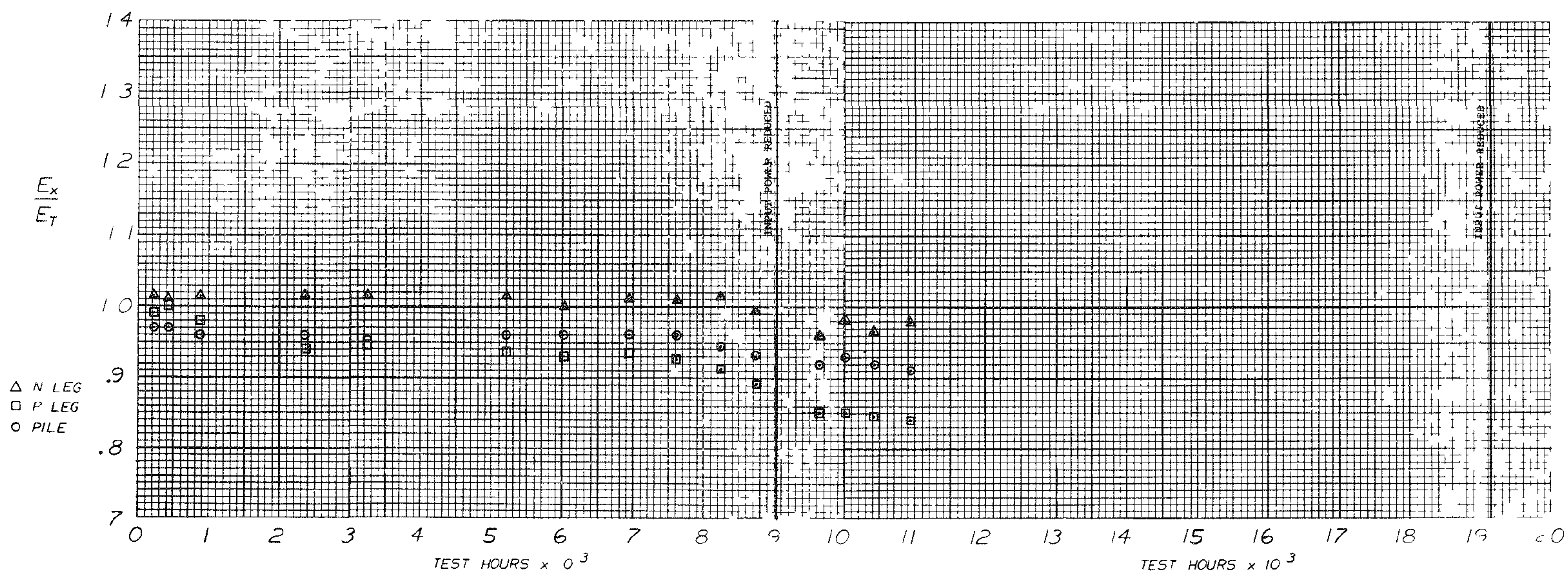

Figure 2-26a. SNAP-21 Thermoelectric Generator A10D1 Normalized Seebeck Voltage Ratio

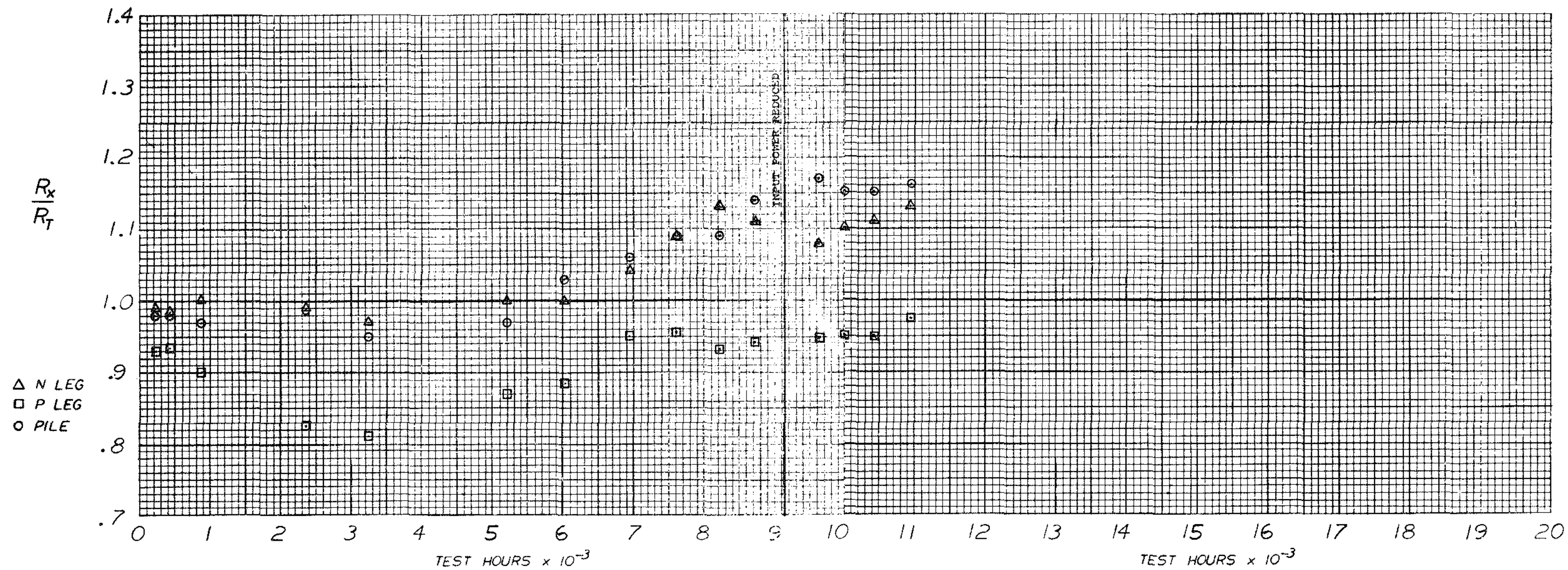

Figure 2-26b. SNAP-21 Thermoelectric Generator A10D1 Normalized Resistance Ratio

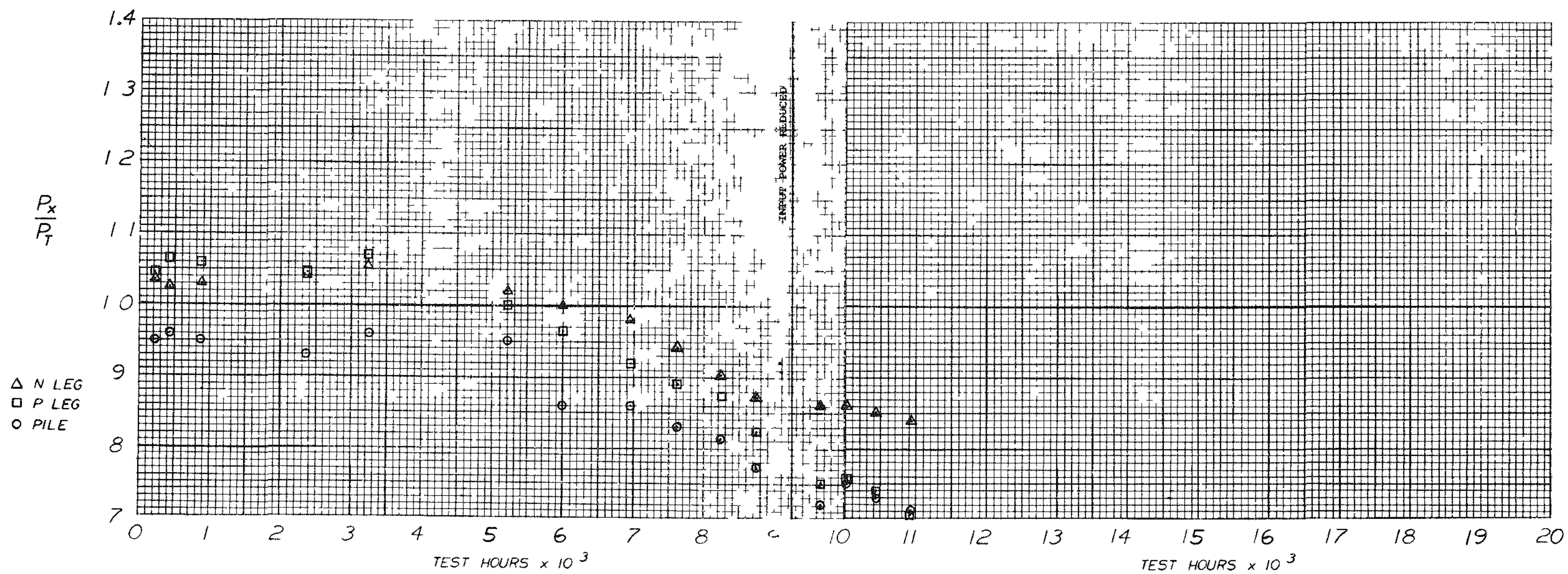

Figure 2-26c. SNAP-21 Thermoelectric Generator A10D1 Normalized Power Ratio

A10D2

During this past quarter, two incidents occurred while testing thermoelectric generator A10D2.

This first incident occurred on January 27, 1969 when the power regulator for the SNAP-21 thermoelectric generators malfunctioned. It caused the hot and cold buttons to increase a maximum of 222°F and 12°F respectively. For a discussion of this incident, refer to section 2.5.2.2.

The second incident occurred on the first of February when the hot frame heaters burned out. Because of this, the generator had to be removed from the test stand so that the heaters could be replaced. While off test, the external hot frame thermocouples were replaced. After replacing the heaters and thermocouples, the generator was put back on test.

Refer to section 2.5.2.3 for corrective action with regard to the thermoelectric generator heater failures.

Figures 2-27a through 2-27c show the performance curves for this thermoelectric generator. It can be seen that the power-out decreased this past quarter. The major cause for this is the drop in Seebeck voltage (~5% decrease this past quarter). It appears that the resistance has stabilized. There have been no apparent short term effects from the malfunction of the voltage regulator.

A10D4

Refer to paragraph 2.1.1.1 for evaluation of generator A10D4 performance.

A10D6

During this past quarter, generator A10D6 reached one year of testing. Because of the regulator failure (see section 2.5.2.2) on SNAP-21 thermoelectric generators, the simulated yearly isotope decay was delayed two weeks. On February 14, 1969, the power input was reduced to obtain a 20°F drop in hot button temperature.

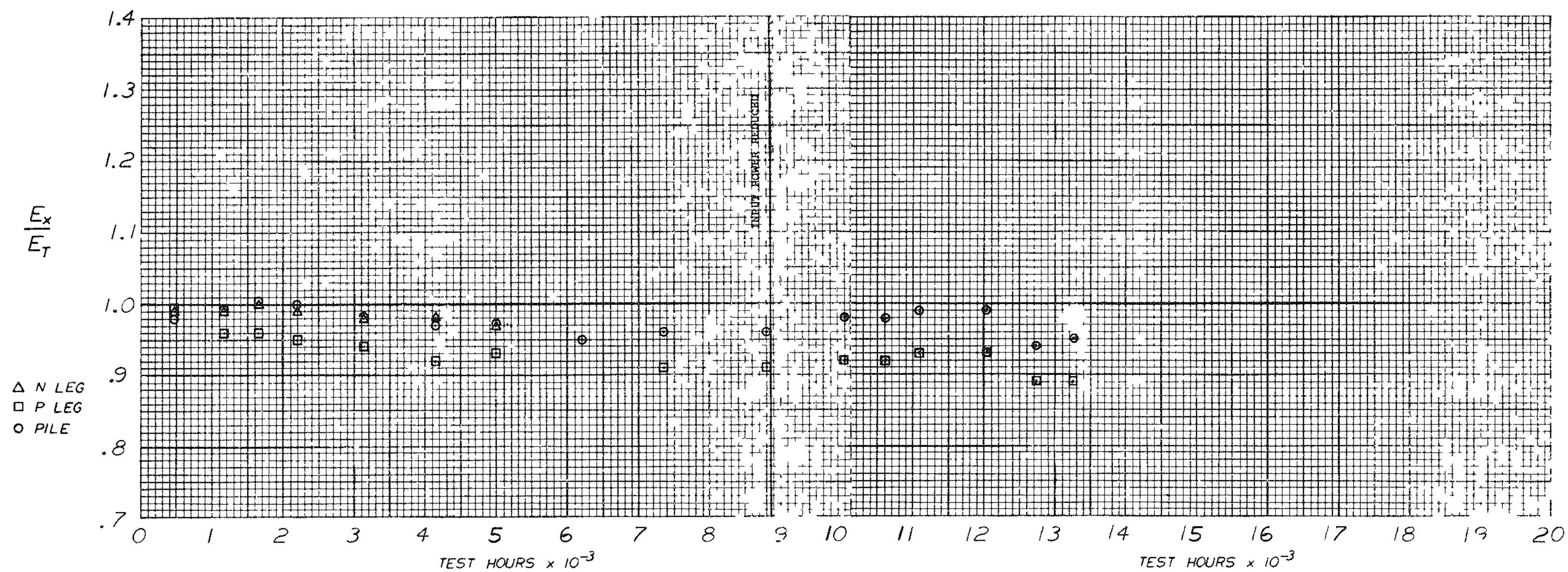

Figure 2-27a. SNAP-21 Thermoelectric Generator A10D2 Normalized Seebeck Voltage Ratio

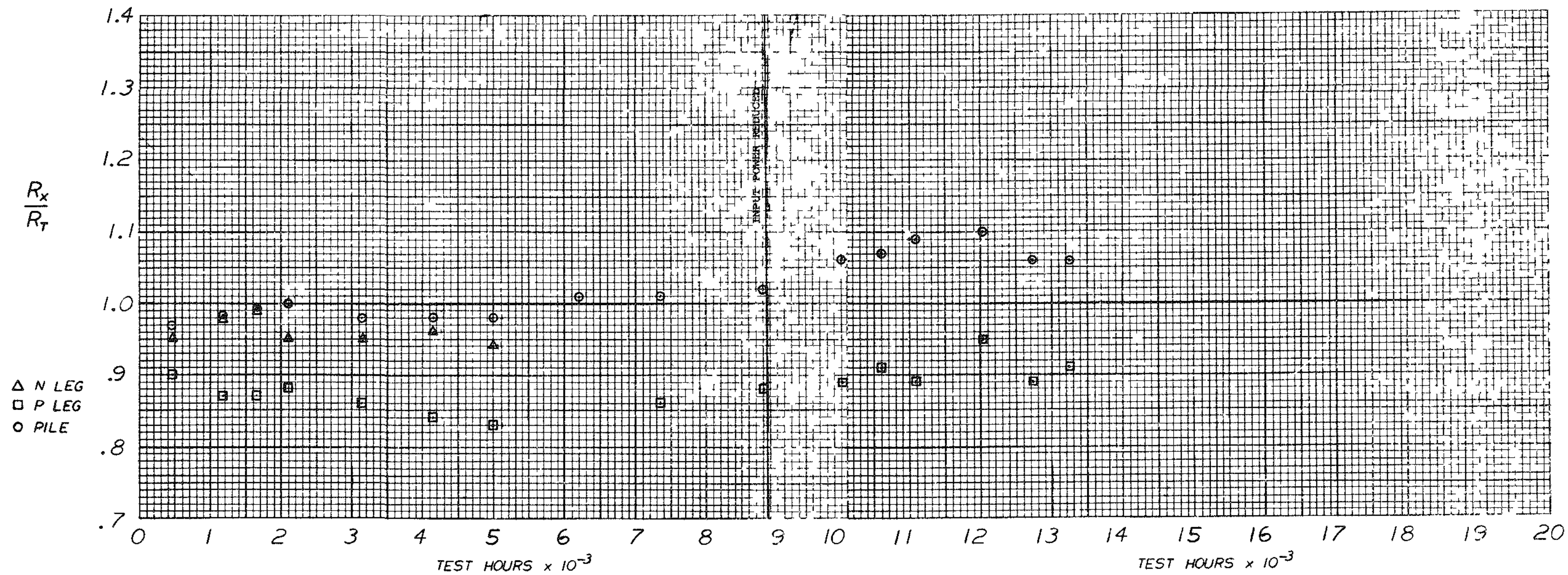

Figure 2-27b. SNAP-21 Thermoelectric Generator A10D2 Normalized Resistance Ratio

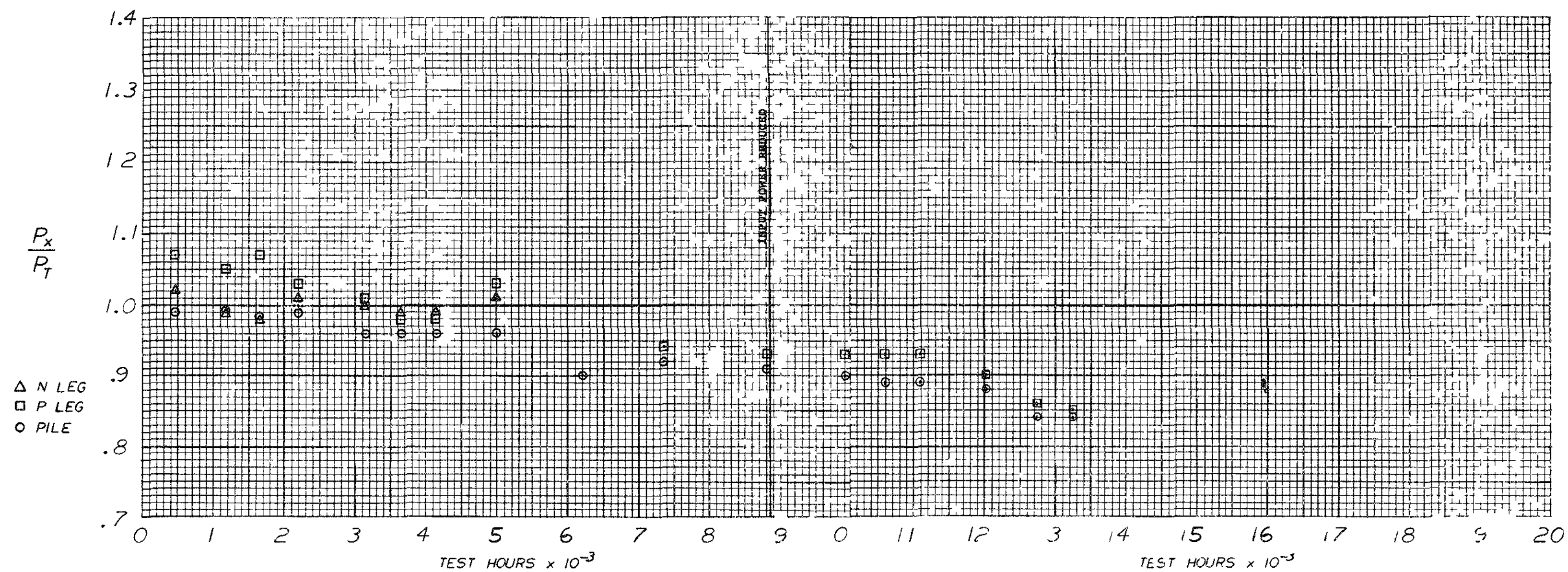

Figure 2-27c. SNAP-21 Thermoelectric Generator A10D2 Normalized Power Ratio

Figures 2-28a through 2-28c show the performance curves for this unit. From the curves, it can be seen that the performance for this thermoelectric generator has been stable this past quarter. There have been no apparent effects from the malfunction of the voltage regulator.

A10D7

During this past quarter, thermoelectric generator A10D7 reached one year of life testing. Power input was reduced on the 19th of January, 1969, to obtain a 20°F drop in hot button temperature.

Refer to section 2.5.2.2 for a discussion of the regulator failure on the SNAP-21 thermoelectric generators.

Figures 2-29a through 2-29c show performance curves for this unit. The P-leg continued to decrease in resistance. At the end of this report period, the resistance of the P-leg was at approximately the same value as at the start of test. Also, the N-leg and thermopile decreased slightly. The changes in Seebeck voltage and resistance caused the thermopile and N-legs power-out to stay approximately the same, while the P-leg power-out increased about 7%. There have been no apparent effects from the malfunction of the voltage regulator.

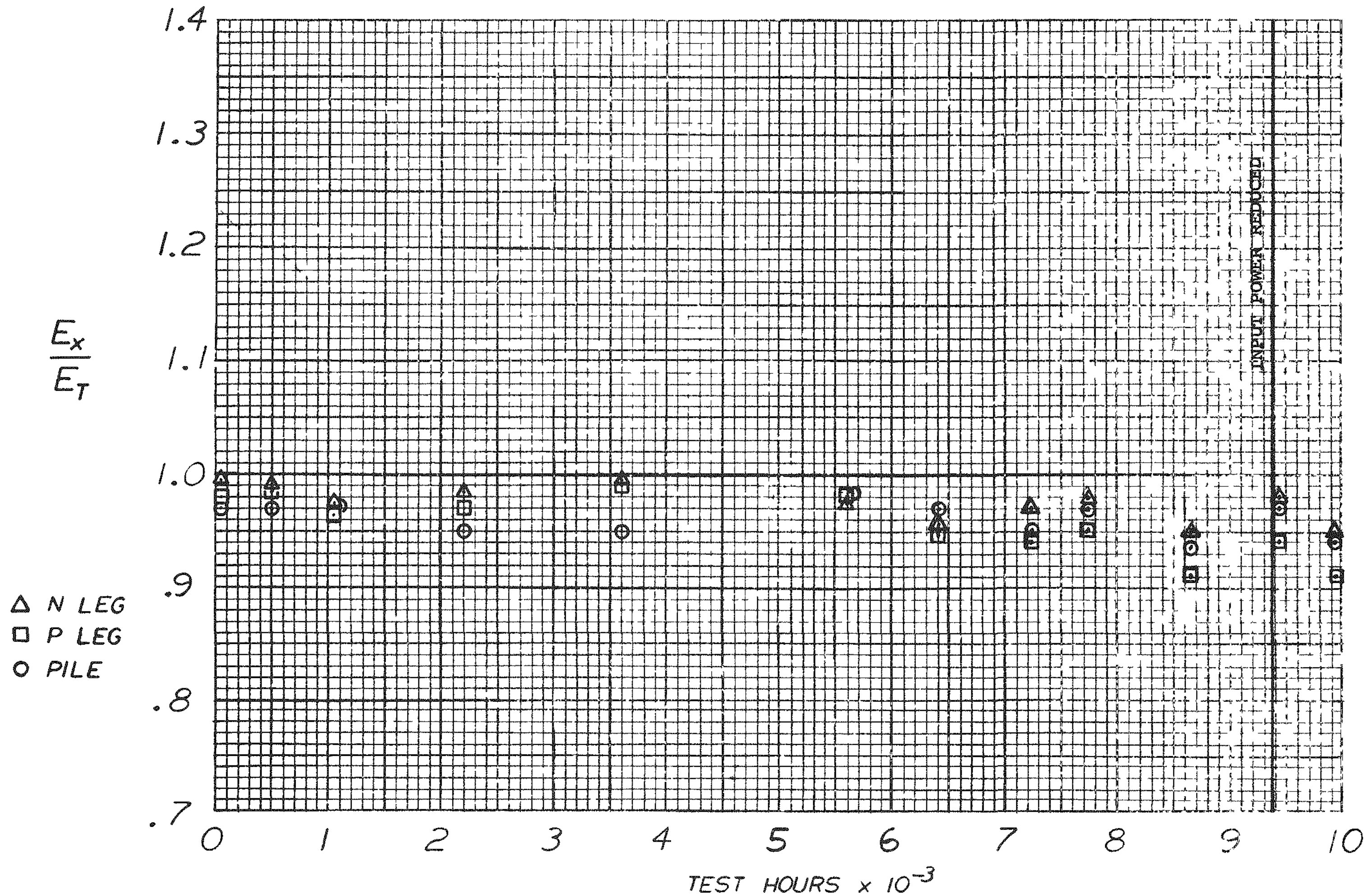

Figure 2-28a. SNAP-21 Thermoelectric Generator A10D6 Normalized Seebeck Voltage Ratio

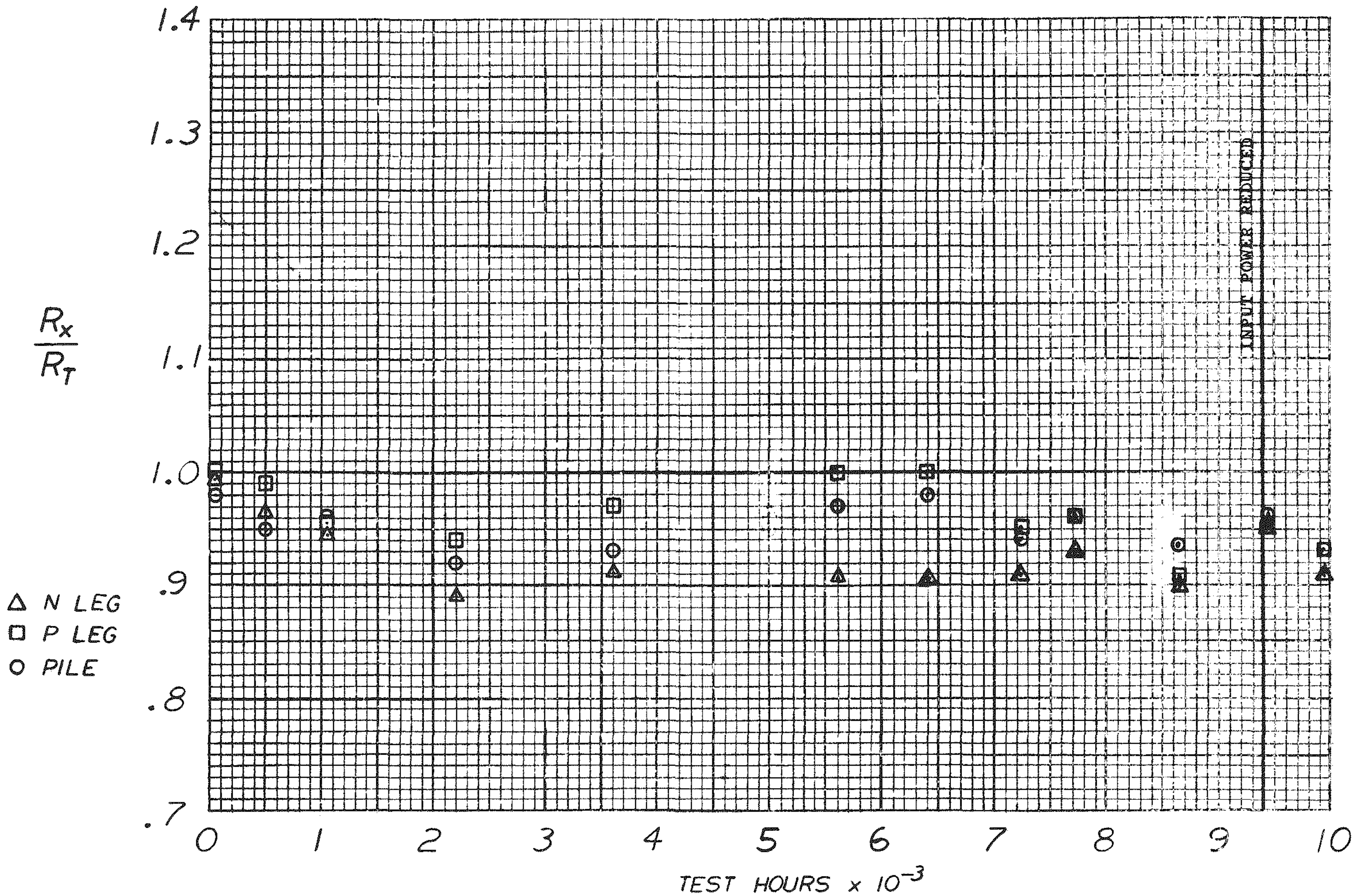

Figure 2-28b. SNAP-21 Thermoelectric Generator A10D6 Normalized Resistance Ratio

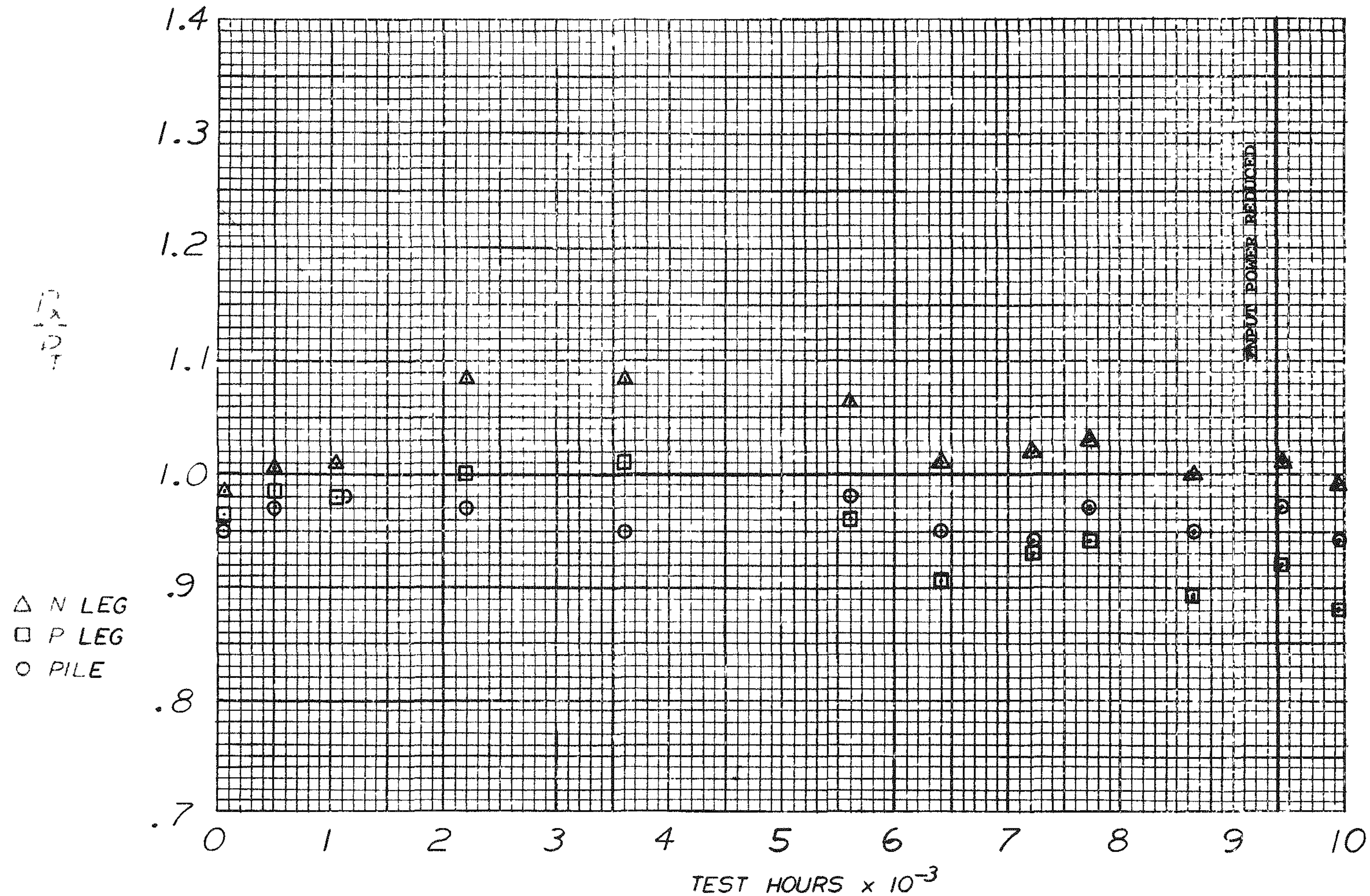

Figure 2-28c. SNAP-21 Thermoelectric Generator A10D6 Normalized Power Ratio

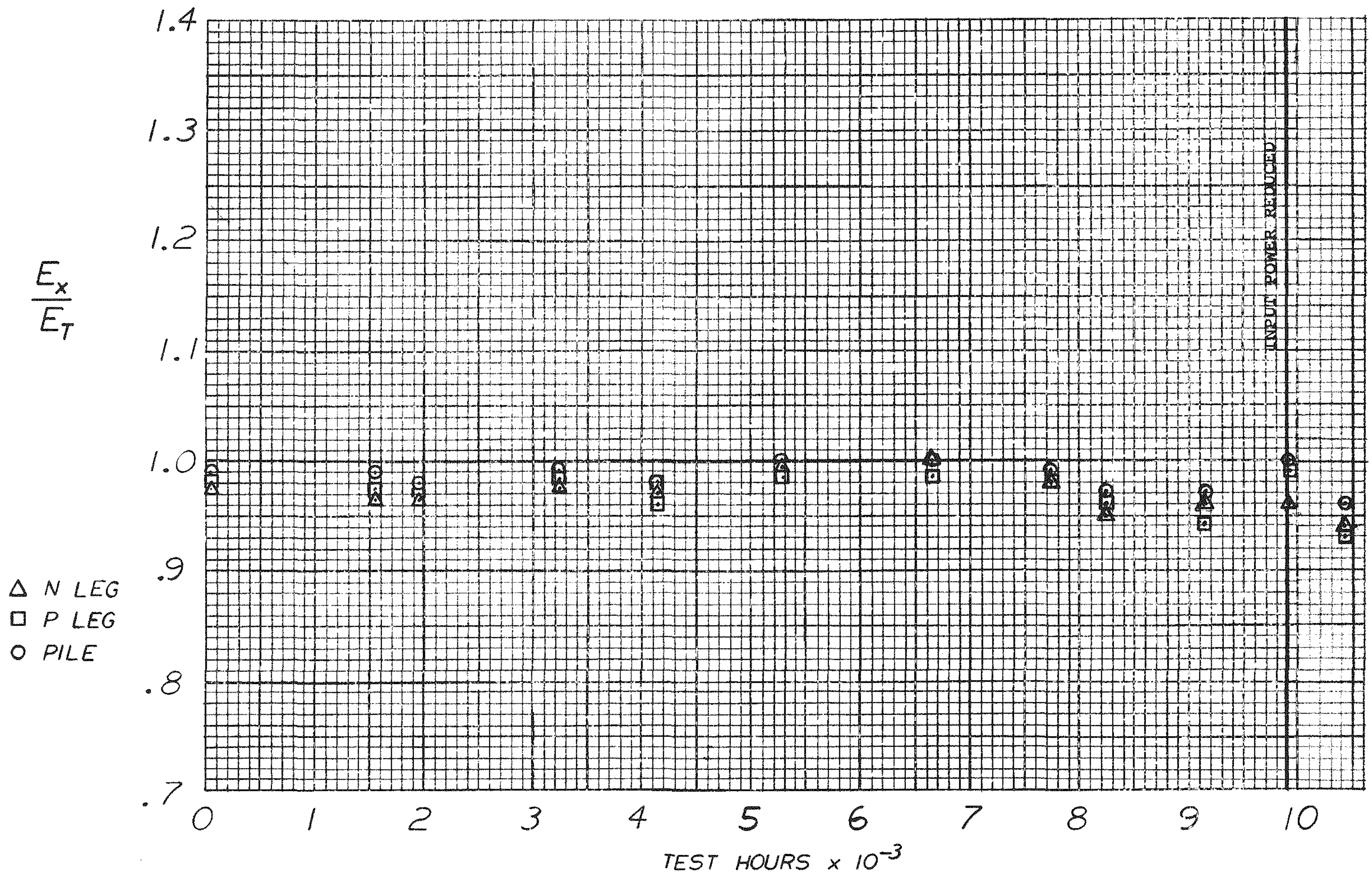

Figure 2-29a. SNAP-21 Thermoelectric Generator A10D7 Normalized Seebeck Voltage Ratio

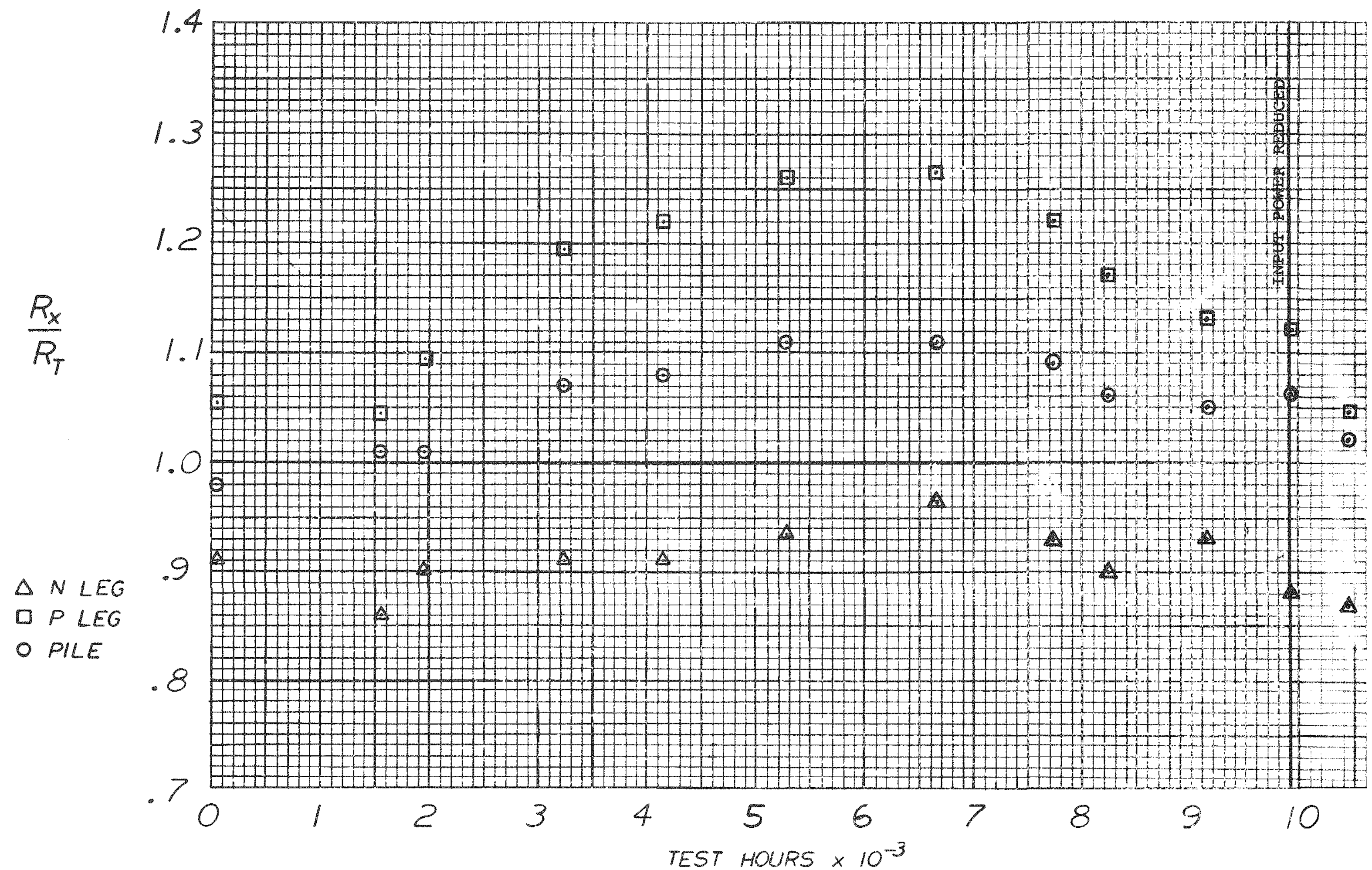

Figure 2-29b. SNAP-21 Thermoelectric Generator A10D7 Normalized Resistance Ratio

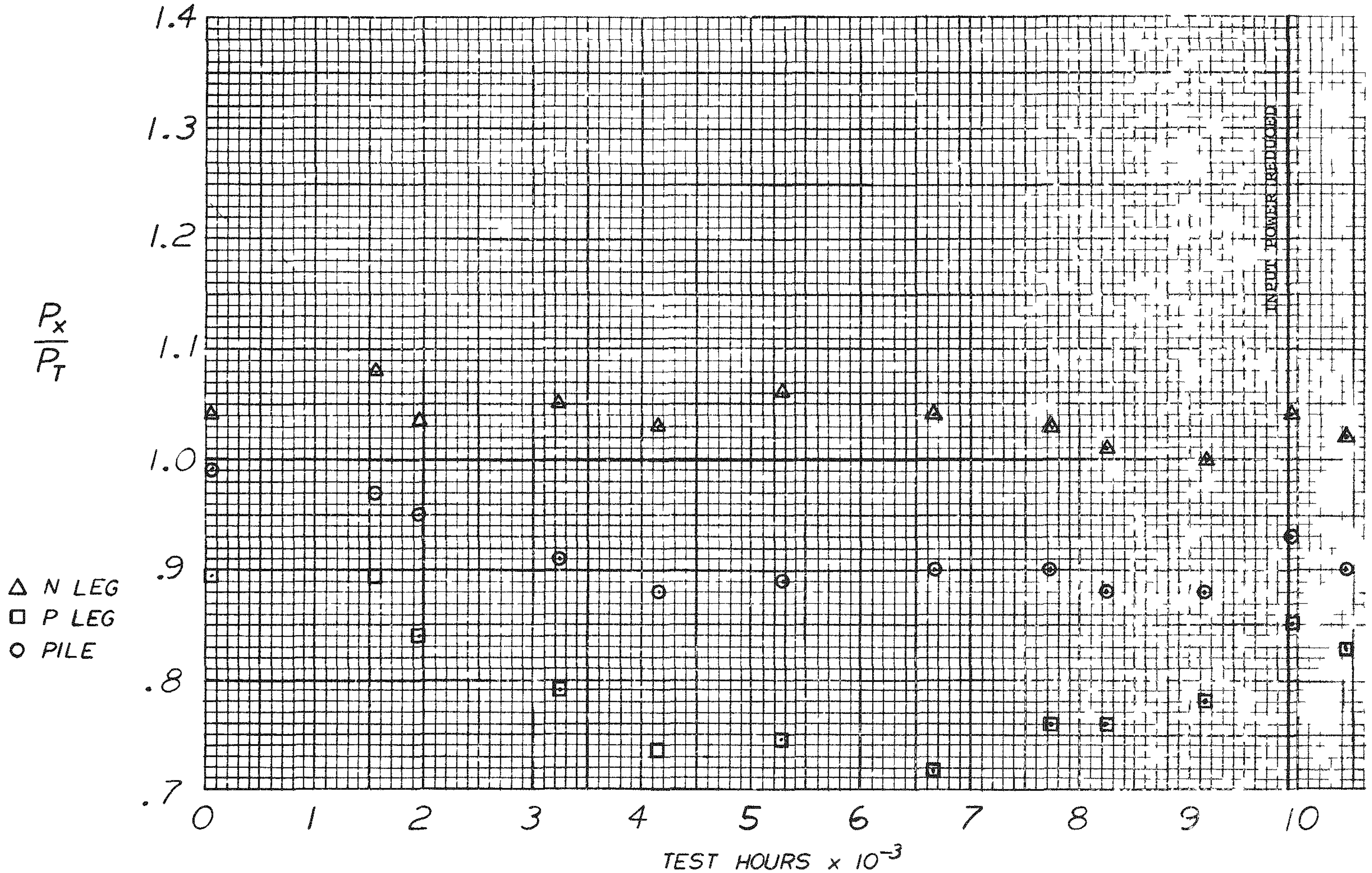

Figure 2-29c. SNAP-21 Thermoelectric Generator A10D7 Normalized Power Ratio

A10P1

Towards the latter part of this quarter, thermoelectric generator A10P1 was taken off test for integration with HTVIS B10DL6 which was also on long-term test. Shown in Figure 2-15 is a picture of the test set up. This set-up is identical to the efficiency test set-up.

Figure 2-30 shows the performance data for this generator. From the data it can be seen that the generator performance was stable this past quarter. There have been no apparent effects from the malfunction of the voltage regulator.

2.5.2.2 Voltage Regulator Failure

On 27 January 1969, at approximately 8:30 p.m., the voltage regulator (Sorenson Model ACR 15000) supplying power to the SNAP-21 thermoelectric generators sustained a voltage control malfunction resulting in a voltage increase.

The SNAP-21 modules experienced a 25% power input increase for approximately 12 hours. The external hot frame temperatures increased on an average of 220°F as a result of the power input increase. Maximum temperature excursion occurred at approximately 12:00 midnight (27 January 1969) and continued until the problem was discovered in the morning shortly before 10:00 a.m. (28 January 1969). Emergency procedures were implemented immediately to reduce the temperatures.

The data acquisition system scanned the temperatures every hour through the night. All data that exceeded the programmed limits were printed out. The internal hot frame and external cold frame temperatures were the only points with programmed limits.

Since these thermocouples have suffered degradation, it is difficult to determine the exact temperatures of all data points during the temperature excursion using the hourly scans of the data acquisition system.

The hot junction thermocouples in many cases have been open or invalid for some time, and the temperatures can only be found by calculation.

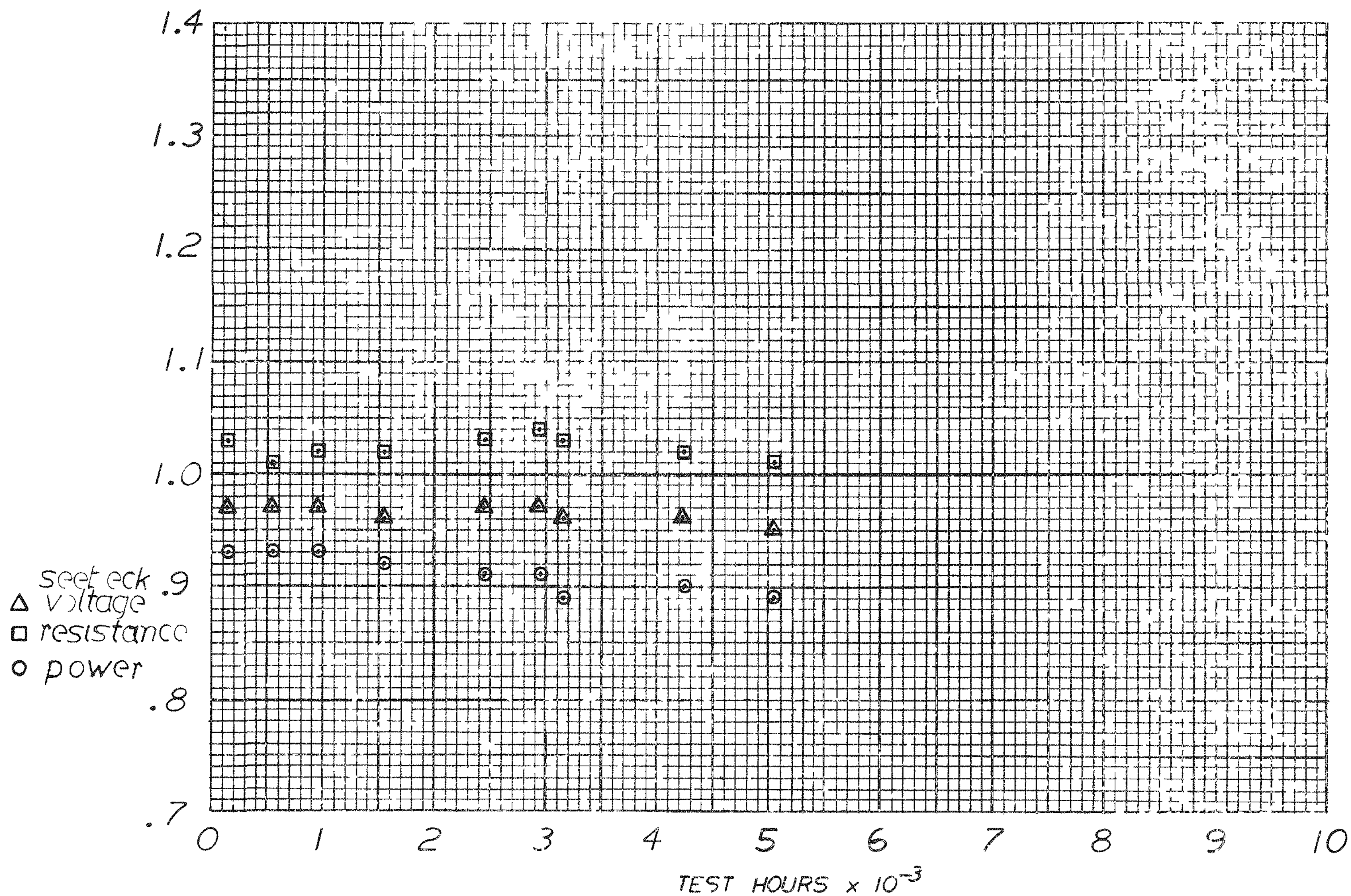

Figure 2-30. SNAP-21 Thermoelectric Generator A10P1 Normalized Data

The data shown in Tables 2-16 and 2-17 was taken from the data acquisition system log print-out taken at 1145 1-27-69 and 0945 1-28-69; this is indicative of the total temperature excursion.

The performance data in Table 2-18 gives the short-term effects on the SNAP-21 generators due to the power regulation failure.

No data is available on the Phase I prototypes since these are not integrated with the data acquisition system.

Observed and Potential Effects

Short-term performance comparisons indicate that none of the generators degraded significantly during the malfunction period.

Since there was no noted step function in the performance, it is not expected that any sublimation that occurred during the temperature excursion was significant enough to alter the long-term performance-time characteristics of the generators. However, other possible adverse effects of the increased temperature may have introduced additional degrading mechanisms into the thermopile. Possible degrading mechanisms are as follows:

1) Spalling of the iron plating from the electrodes: With the elevated temperature operation, spalling of the electrodes is possible. Copper from the electrodes could then possibly contaminate the PbTe material via vapor transport. Copper, being a known N-type doping agent in PbTe, will reduce the Seebeck coefficient and resistivity of N-material.

2) Sodium contamination of the N-legs from Min-K 1301 insulation: Min-K 1301 has approximately 0.4 atomic percent sodium. Sodium contamination of N-legs from modules operating near 1300°F has been observed on other programs. Sodium is a P-type doping agent and will raise the Seebeck coefficient and resistivity of the N-material. If the contamination is great enough, P-type phases may develop in the N-materials.

Table 2-16. SNAP-21 Generator Temperature Increase

Generator	Thermocouple	(Temperature °F) 1-27-69(1145)	1-28-69(0945)	(Increase)
A10D1	Avg Hot Frame (Ext)	1187	1405	218
	Avg Hot Frame (Int)	1137	1348	211
	Avg Hot Junction	1107	1305	198
	Avg Cold Junction	91	103	12
	Avg Cold Frame	68	73	5
A10D2	Avg Hot Frame (Ext)	1170	1374	204
	Avg Hot Frame (Int)	1120	1317	197
	Avg Hot Junction	1090	1261	171
	Avg Cold Junction	103	116	13
	Avg Cold Frame	68	73	5
A10D6	Avg Hot Frame (Ext)	1170	1402	232
	Avg Hot Frame (Int)	1103	1305	202
	Avg Hot Junction	1083	1271	188
	Avg Cold Junction	84	94	10
	Avg Cold Frame	64	67	3
A10D7	Avg Hot Frame (Ext)	1173	1389	216
	Avg Hot Frame (Int)	1111	1308	197
	Avg Hot Junction	1081	1265	184
	Avg Cold Junction	81	89	8
	Avg Cold Frame	69	74	5
A10P1	Avg Hot Frame (Ext)	1060	1290	230
	Avg Hot Junction (Est)	980	1180	200
	Avg Cold Junction (Est)	83	93	10
	Avg Cold Frame	55	59	4

Table 2-17. SNAP-21 Generator Power Input Increase

Generator	Power Input, watts (t)		Increase, watts (t)
	1-27-69(1145)	1-28-69(0945)	
A10D1	408	508	100
A10D2	320	400	80
A10D6	330	412	82
A10D7	388	484	96
A10P1	335	419	84

Table 2-18. SNAP-21 Generator Comparative Performance (Before and After Temperature Excursion)

Generator	Date	Test Time (hours)	Power In watts (t)	T_h (°F)	T_c (°F)	E (volts)	R (ohms)	P watts (e)	Pressure (psia)
A10D1	1/27/69	9,697	408	1108	91	10.36	2.09	12.83	22.0
	1/29/69	9,741	406	1095	91	10.16	1.92	13.47	21.5
A10D2	1/27/69	12,011	320	1090	103	10.66	2.11	13.41	22.6
	1/29/69	12,055	318	1083	102	10.64	1.91	14.79	22.6
A10D6	1/27/69	8,741	330	1083	84	9.14	1.41	14.83	24.3
	1/29/69	8,785	330	1081	83	9.16	1.40	14.95	24.3
A10D7	1/27/69	9,236	388	1081	81	10.79	1.82	15.92	21.4
	1/29/69	9,280	396	1099	81	11.12	1.85	16.57	21.5
A10P1	1/27/69	3,945	336	980	83	9.02	1.57	12.91	--
	1/29/69	3,989	334	965	84	8.97	1.52	13.18	--
Generator	**Date**	**Test Time (hours)**	**Power In watts (t)**	**T_{hf} (ext) (°F)**	**T_{cf} (°F)**	**E (volts)**	**R (ohms)**	**P watts (e)**	**Pressure (psia)**
P5	1/16/69	32,441	170	1078	63	9.88	2.33	10.47	--
	2/10/69	33,041	171	1073	62	9.88	2.24	10.92	--
P6	1/16/69	31,812	188	1055	73	9.83	2.47	9.80	--
	2/10/69	32,412	188	1054	71	9.83	2.40	10.07	--
P7	1/16/69	31,965	174	1081	83	9.88	2.57	9.48	--
	2/10/69	32,565	175	1082	82	9.90	2.53	9.68	--

T_h = Hot Junction Temp. T_c = Cold Junction Temp. T_{hf} = Hot Frame Temp. T_{cf} = Cold Frame Temp.

3) Other possible diffusion and chemical contamination problems (this would include the following possible problem areas):

(a) iron from the hot electrodes

(b) sulfur from the Min-K 1301

(c) boron compounds from the boron nitride materials.

a) Cause of Voltage Increase

The regulator voltage increase was caused by failure of a capacitor in the voltage regulator control circuit. This caused the voltage set-point to rise from 119V to 130V. The regulator has no over-voltage trip as such, however, the design is such that over-voltage of a gross nature will trip a circuit-breaker, resulting in a low output voltage. Hence, failure of a control component (like the capacitor which failed) can cause a significant voltage drift without resulting in trip-out to a lower voltage.

b) Corrective Action

The capacitors in regulator circuit boards have been replaced with highly reliable hermetic-sealed tantalum capacitors.

An RMS voltage drift sensing alarm has been installed. This consists of a heater with an attached thermocouple, which receives power from the voltage regulator (with a thermocouple sensing meter/relay activating an alarm). The method of operation is If the voltage output of the regulator increases, the temperature of the heater increases. When the temperature of the heater increases to the established set point of the sensing meter/relay, the alarm will be activated. Tests have proved that a 2-volt AC increase will energize the relay in less than 5 minutes. This system is only a temporary set-up until a reliable, permanent fail-safe alarm system can be completely evaluated and installed. The evaluation of other methods and hardware is underway at this time.

A special scan program tape for the data acquisition system has been completed, but two problems have delayed complete usage of the data acquisition system as a fail-safe alarm system for each test device. The first problem is with the data acquisition system linearizer. This component recently had a failure in the "k" circuit and has been returned to the factory for repair. Secondly, a delay has been encountered in delivery of the alarm mode relays.

A complete, integrated, test-lab, fail-safe, alarm system is presently under study to include all equipment, facilities, and test devices.

c) Heater Failure

As reported previously, there have been several thermoelectric generator test fixture heater failures. The major problem with the heaters used for generator testing is that the heater leads operate in the hot zone. This results in the leads failing through oxidiation. To correct for this, a dead space heater will replace those presently being used. This should permit the heater leads to run cooler resulting in longer life. Also, a thermal insulation will be placed in the interfaces between the test stand and the thermoelectric generator to limit the heat transfer to the thermoelectric generator cold frame from the heater block. See Figure 2-31.

2.6 POWER CONDITIONERS

2.6.1 Phase I Power Conditioners

Phase I electronic component testing continued this past quarter with the automatic selector switch, power conditioner MP-C, and regulators operating satisfactorily. Tables 2-19 through 2-22 are the life data for these electronic units. As can be seen, the performance for these units has been stable.

2.6.2 Phase II Power Conditioners

Tables 2-23 and 2-24 are the performance data for power conditioners H10D3 and H10D6. As can be seen, the performance for these units has been stable this past report period.

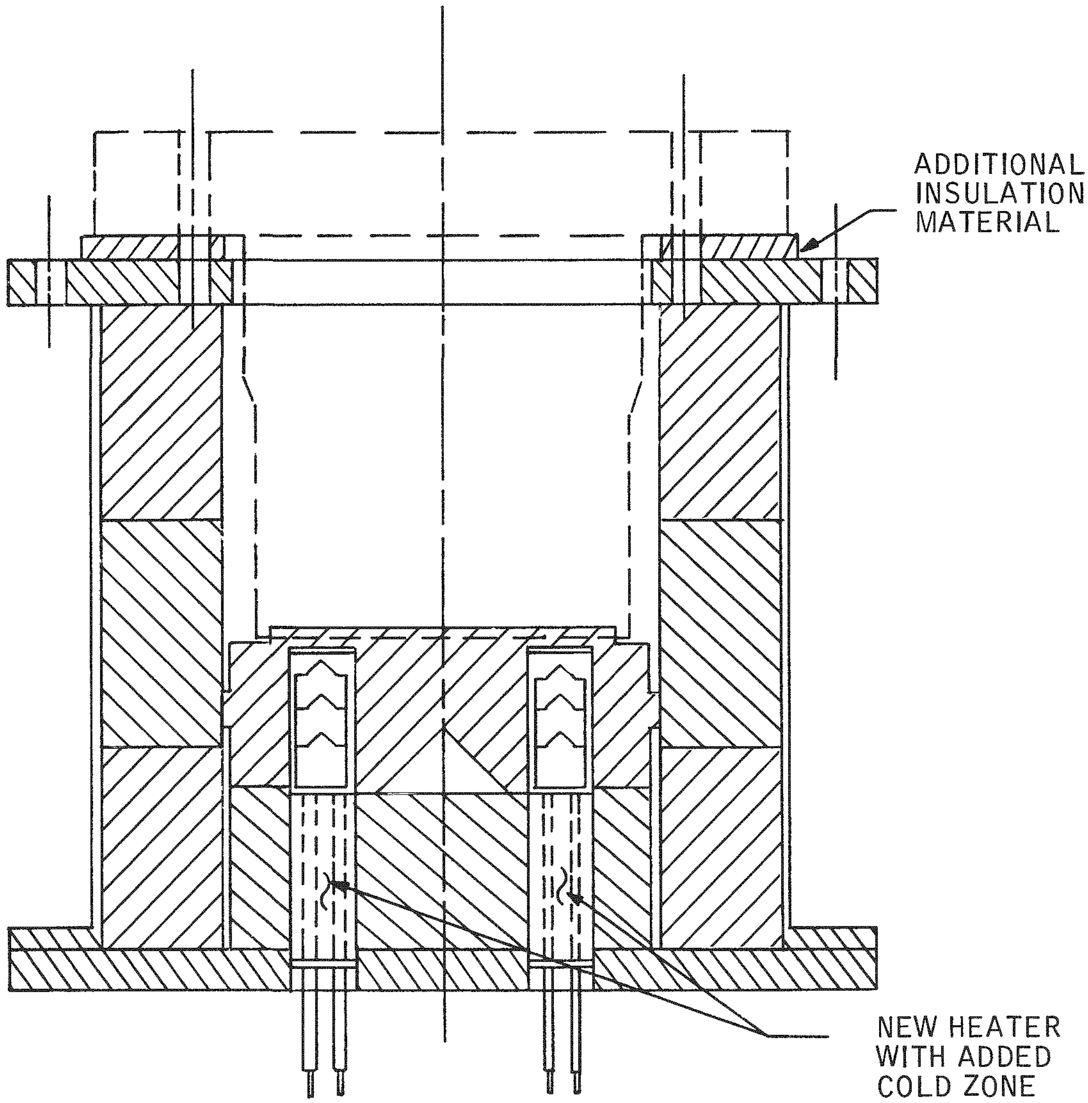

Figure 2-31. Revised Configuration of Test Fixture Showing the New, Dead-Space Heaters

Table 2-19. Phase I Regulator Test Fixture Performance Data

Operating Hours	TRIO-LAB Regulators				High Power Regulator-A HPR-A	
	A Output (vdc)	C Output (vdc)	D Output (vdc)	F Output (vdc)	Output (vdc)	Operating Hours
18,369	21.75	21.86	22.49	21.93	26.78	17,552
18,729	21.72	21.79	22.47	21.90	26.77	17,912
19,257	21.72	21.78	22.46	21.89	26.80	18,440
19,401	21.72	21.78	22.46	21.88	26.81	18,584
19,881	21.54	21.63	22.41	21.88	26.46	19,064
20,265	21.53	21.55	22.42	21.90	26.47	19,448
20,673	21.53	21.46	22.42	21.88	26.51	19,856
21,117	21.49	21.39	22.40	21.84	26.51	20,360
21,161	21.52	21.37	22.39	21.85	26.51	21,344
22,617	21.60	20.79	22.40	21.88	26.48	21,800
23,145	21.46	21.45	22.35	21.82	26.45	22,328
23,769	21.46	21.13	22.31	21.82	26.36	22,952
24,297	21.35	21.52	22.41	21.82	26.31	23,480
24,777	21.43	20.93	22.33	21.76	26.34	23,960
25,137	21.49	21.00	22.36	21.83	26.47	24,320
25,449	21.49	21.00	22.39	21.84	26.53	24,632
25,929	21.50	20.97	22.39	21.83	26.56	25,112
26,381	21.51	20.95	22.40	21.84	26.60	25,564
26,693	21.74	21.81	22.46	21.92	26.93	25,876
28,061	21.52	21.30	22.41	21.83	26.52	27,244
28,541	21.51	21.27	22.38	21.81	26.56	27,724
29,525	21.48	21.00	22.33	21.75	26.52	28,708
30,773	21.46	21.01	22.31	21.75	26.52	29,956
31,733	21.48	20.82	22.32	21.76	26.53	30,916
32,189	21.49	20.28	22.33	21.80	26.51	31,372
33,029	21.51	20.25	22.36	21.78	26.55	32,212
33,941	21.61	21.07	22.39	21.81	26.73	33,124
34,541	21.70	21.73	22.39	21.83	26.78	33,724
35,405	21.70	21.74	22.40	21.85	26.85	34,588
36,317	21.71	21.74	22.41	21.86	26.87	35,500
37,325	21.70	21.74	22.40	21.84	26.86	36,508

Table 2-20. Performance of Phase I Power Conditioner MP-C

Converter Performance Power Conditioner	E_I (volts)	I_I (amps)	P_I (watts)	E_o (volts)	I_o (amps)	P_o (watts)	Efficiency %	Hours on Test	Notes
MP-C	4.913	2.395	11.809	24.00	0.436	10.464	88.61	15,783	
	4.908	2.360	11.606	24.00	0.429	10.296	88.71	16,143	
	4.909	2.374	11 757	24.00	0.432	10.368	88.19	16,671	
	4.910	2.378	11.779	24.00	0.433	10.392	88.22	16,815	
	4.906	2.372	11.740	24.00	0.432	10.368	88.31	17,295	
	4.905	2.374	11.747	24.00	0.432	10.368	88.26	17,679	
	4.904	2.353	11.642	24.00	0.428	10.272	88.23	17,087	
	4.909	2.389	11.831	24.00	0.439	10,416	88.04	18,591	
	4.912	2.395	11 867	24.00	0.436	10.464	88.18	19,575	
	4,913	2.396	11,878	24.00	0.436	10.464	88.10	20,031	
	4.910	2.375	11.764	24.00	0.432	10.368	88.13	20,559	
	4.908	2.371	11.740	24.00	0.431	10.344	88.11	21,183	
	4.909	2.375	11.762	24.00	0.432	10.368	88.15	21,811	
	4.909	2.376	11.767	24.00	0.432	10.368	88.11	22,098	
	4.910	2.375	11.764	24.00	0.432	10.368	88.13	22,485	
	4.912	2.403	11.907	24.00	0.438	10.512	88.28	22,770	
	4.911	2.377	11.776	24.00	0.433	10.380	88.92	23,250	
	4.909	2.357	11.674	24.00	0.428	10.270	87.99	24,066	Note: Unit accidentally shut down. Discovered on 12/22/67. Power restored 12/22/67.
	4.908	2.368	11.725	24.00	0.431	10.344	88.22	25,434	
	4.908	2.368	11.725	24.00	0.430	10.320	88.02	25,914	
	4.908	2.374	11.755	24.00	0.432	10.368	88.21	26,898	
	4.908	2.376	11.764	24.00	0.432	10.368	88.13	28,146	
	4.910	2.378	11.779	24.00	0.433	10.384	88.16	29,106	
	4.910	2.395	11.862	24.00	0.435	10.440	88.01	29,562	
	4.909	2.395	11.860	24.00	0.435	10.440	88.03	30,402	
	4.907	2.375	11.757	24.00	0.432	10.368	88.18	31.314	
	4.905	2.373	11.743	24.00	0.434	10.416	88.70	31,914	
	4.904	2.371	11.730	24.00	0.431	10.344	88.18	32,778	
	4.907	2.381	11.780	24.00	0.433	10.392	88.21	34,698	

Table 2-21. Phase I Automatic Selector Switch Performance Data

Notes	Hours	Output Voltage	
		Conditioner MP-A (vdc)	Conditioner MP-D (vdc)
	13,583	24.54	24.59
	13,943	24.55	24.60
	14,471	24.56	24.60
	14,615	24.55	24.59
Note: System turned off from 4/24/67 to 6/6/67	15,095	24.62	24.58
	15,479	24.62	24.58
	15,887	24.50	24.59
	16,343	24.46	24.58
	16,799	24.45	24.57
	17,327	24.47	24.55
	17,951	24.50	24.55
	18,479	24.47	24.59
	18,959	24.47	24.57
	19,319	24.48	24.59
	19,631	24.48	24.58
	20,111	24.47	24.58
	20,687	24.45	24.56
	20,999	24.48	24.56
	22,367	24.49	24.60
Note: At 22,367 hours system shut down to install into cabinet type mount (2/28/67).	22,895	24.49	24.56
	24,119	24.49	24.57
	24,719	24.50	24.57
Note: 8/27/68 unit put back on test.	25,583	24.51	24.58
	26,495	24.48	24.55
	27,503	24.48	24.56

Table 2-22. Phase I Regulator Performance Data

Operating Hours	No-Load Voltage (vdc)
15,783	24.54
16,143	24.54
16,671	24.54
16,815	24.53
17,295	24.54
17,679	24.54
18,087	24.53
18,591	24.53
19,575	24.52
20,031	24.52
20,559	24.51
21,183	24.52
21,811	24.52
22,098	24.51
22,485	24.51
22,770	24.50
23,250	24.51
24,066	24.51
25,434	24.49
25,914	24.48
26,898	24.52
28,146	24.52
29,106	24.52
29,562	24.52
30,402	24.51
31,314	24.52
31,914	24.52
32,778	24.52
34,698	24.52

Table 2-23. Power Conditioner H10D3 Performance Data

E_I Primary (volts)	I_I Primary (amps)	P_I Primary (watts)	E_I Bias (volts)	I_I Bias (amps)	P_I Bias (watts)	E_o (volts)	I_o (amps)	P_o (watts)	Efficiency (%)	Temp. (°F)	Test* Hours
5.06	2.17	11.02	0.646	0.132	0.085	23.77	0.424	10.08	90.77	82	1296
5.06	2.17	11.00	0.657	0.132	0.085	23.76	0.423	10.05	90.66	82	1413
5.08	2.18	11.07	0.658	0.134	0.087	23.80	0.422	10.04	89.99	82	1576
5.08	2.18	11.07	0.647	0.132	0.085	23.81	0.422	10.05	90.09	80	1894
5.08	2.18	11.07	0.648	0 132	0.086	23.83	0.422	10.06	90.18	81	2106
5.08	2.18	11.07	0.648	0.134	0.087	23.82	0.422	10.05	90.10	86	2904
5.08	2.18	11.07	0.647	0 134	0.087	23.81	0.422	10.05	90.07	86	3575
5.08	2.18	11.07	0.648	0.134	0.087	23.82	0.422	10.05	90.07	86	4244
5.08	2.18	11.07	0.648	0.134	0.087	23.83	0.422	10.06	90.17	86	5058
5.08	2.18	11.07	0.648	0.134	0.087	23.82	0.422	10.05	90.08	87	5928
5.08	2.18	11.07	0.648	0.134	0.087	23.83	0.422	10.06	90.17	87	6476

*Includes 1241 hours of short-term tests.

Table 2-24. Power Conditioner H10D6 Performance Data

E_I Primary (volts)	I_I Primary (amps)	P_I Primary (watts)	E_I Bias (volts)	I_I Bias (amps)	P_I Bias (watts)	E_o (volts)	I_o (amps)	P_o (watts)	Efficiency (%)	Temp (°F)	Test* Hours
4 81	2 35	11 30	0 646	0 122	0 079	24 00	0 430	10 32	90 69	82	1296
4 81	2 35	11 30	0 646	0 122	0 079	24 00	0 430	10 32	90 69	82	1437
4 82	2 35	11 33	0 648	0 122	0 079	24 08	0 425	10 23	89 67	82	1600
4 83	2 35	11 35	0 648	0 122	0 079	24 20	0 430	10 41	91 08	80	1968
4 83	2 35	11 35	0 648	0 122	0 079	24 09	0 425	10 24	89 60	81	2278
4 82	2 35	11 33	0 648	0 122	0 079	24 07	0 425	10 23	89 67	87	2904
4 82	2 35	11 33	0 647	0 122	0 079	24 07	0 425	10 23	89 67	86	3575
4 82	2 35	11 33	0 648	0 122	0 079	24 07	0 425	10 24	89 75	87	4244
4.82	2.35	11.33	0.648	0.122	0.079	24.08	0.425	10.23	89.67	87	5058
4.82	2.35	11.33	0.647	0.122	0.079	24.07	0.430	10.35	90.72	88	5928
4 82	2.35	11.33	0.648	0.122	0.079	24.10	0.425	10.24	89.75	87	6476

Includes 1271 hours of short-term tests.

2.7 ELECTRICAL RECEPTACLE AND STRAIN RELIEF PLUG

No effort was expended in this area during the report period.

2.8 PRESSURE VESSEL

No effort was expended in this area during this report period.

2.9 NRDL SYSTEM TESTING

A handling adapter was designed for the stainless steel pressure vessel which was fabricated during Phase I and will be used as a dummy system for handling trials by NRDL. This handling adapter will simulate the adapter used with the final system. The dummy system handling trials are scheduled to take place at San Clemente Island, California on April 1 and 2, 1969. 3M Company personnel will be present to witness the dummy system implantment.

3.0 TASK II – 20-WATT SYSTEM

3.0 TASK II - 20-WATT SYSTEM

Preliminary planning and scheduling was initiated in anticipation of starting Task II.

In order to provide a sounder basis for selection of a 20-watt design for continued development effort, a Concept Definition Program has been prepared. This includes both a review of problem areas intrinsic to each of the two conceptual design candidates and definition of selected analysis and of evaluations to be performed. A thermoelectric materials development effort has been outlined providing concurrent system development with the potential for incorporating improved TE materials properties.

4.0 PLANNED EFFORT FOR NEXT QUARTER

4.0 PLANNED EFFORT FOR NEXT QUARTER

- The Final Development Test Plan for SNAP-21 Fueled Systems will be updated, and revision sheets will be reissued.
- Complete Final Design Description.
- Complete Final Safety Analysis Report.
- Complete dynamic test Appendix on Engineering Analysis of Insulation System B10D4.
- Complete Operational Safety Analysis.
- Complete updating Task I system drawings.
- Restart Task II.
- Complete Task II Conceptual Design Definition study.
- Initiate alternate materials evaluation study.
- Continue investigation and analysis of system S10D3 low performance.
- Ship systems S10P1, S10P2 and S10P3 to NRDL for implantment in the ocean off San Clemente Island.
- Complete thermal and electrical characterization of system S10P3.
- Complete assembly, fueling and dynamic test of system S10P4.
- Complete insulation systems B10DL7 and B10DL8.
- Assist NAVSHIPS R&D Center with assembly of 10-couple module number 5.
- Continue testing Phase I and Phase II thermoelectric generators.
- Continue long-term test of Phase II power conditioners.

Blank page

Appendix A

INNER LINER FABRICATION USING HYDROFORMING TECHNIQUES FOR THE NECK TUBE SECTION

Appendix A

INNER LINER FABRICATION USING HYDROFORMING TECHNIQUES FOR THE NECK TUBE SECTION

To supplement the brief background delineated herein, additional background history may be obtained through the normal Quarterly, Monthly and Topical reports (Report No. MMM 3691-40, "Engineering Analysis of High Temperature Vacuum Insulation System B10D4") is particularly pertinent.

A major component in the High Temperature Vacuum Insulation System used in the SNAP-21 10-watt system is the inner liner. The inner liner serves as the receptacle for the isotope fuel source, as the upper attachment point for the biological shield, and as the top enclosure weld for maintenance of a pressure of less than 10 microns for a life of five years. Figure A-1 shows the components of the vacuum insulation system.

This appendix is concerned with the inner liner, as shown in Figure A-1, and in particular, with the neck tube portion.

Hastelloy-X was selected as the material for this application because of its excellent resistance to oxidation at operating temperatures, a coefficient of thermal expansion that is slightly greater than that of the U-8 w/o Mo shield material, good high temperature mechanical properties, and its good welding characteristics.

Inner liners used for the SNAP-21 Phase I liners were machined from solution annealed Hastelloy-X bar stock. At that time, no special requirements were imposed.

At the start of the Phase II program, a detailed thermal and structural analysis was performed with development tests conducted to verify predicted design values. This analysis confirmed that Hastelloy-X was the right material selection.

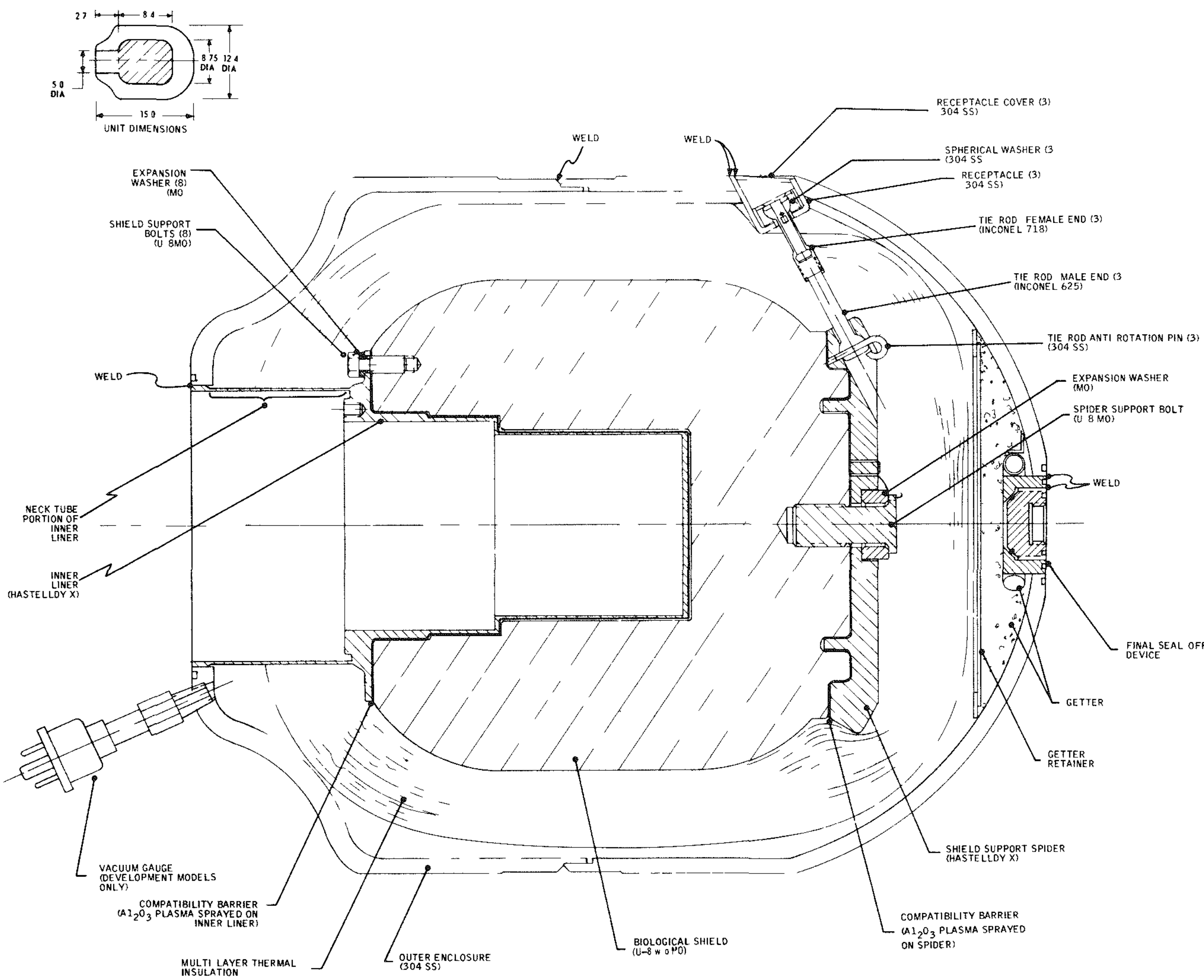

Figure A-1. SNAP-21 High Temperature Vacuum Insulation System

At the start of Phase II, four inner liners were machined from solution annealed bar stock. To eliminate some of the costly machining time, forging a rough shape was tried. This did not prove successful since the available tooling used was not adequate to do a good job. The first run of material was scrapped. The final forgings were given a basic blocking operation and then rough machined prior to finish machining.

At about the same time that the forgings were completed and rough machined, one of the earlier bar stock machined inner liners failed in shear buckling during the dynamic testing of an insulation system. Later, a neck tube section of one of the forged inner liners developed a small leak during the processing of the insulation system.

The above events lead to a more thorough investigation of the inner liners as a part of a complete evaluation of the insulation systems. These studies showed that all liners had a very large grain size with some grains extending completely across the neck tube wall which is 0.012 – 0.013 inch thick. The material also contained carbides and other phases which were segregated and branded. (See Report No. MMM 3691-40.) Since this is more of a general fabrication technique report, specific hardware identity will not be used.

Fabrication Survey

Because of the above difficulties and the loss of two more insulation systems during dynamic testing, it became necessary to fabricate additional inner liners. The presence of the large grains and heavily segregated and banded structures noted during the Engineering Analysis pointed out the need for a fabrication survey to determine the feasibility of developing other techniques capable of producing better metallurgical properties in the neck tube section of the inner liner. For scheduler reasons, it was also necessary to start machining liners from solution annealed bar stock. The fabrication techniques investigated were as follows:

- Hydroforming
- High energy rate forming
- Shape or closed die forging

- Tubing and plate construction
- Ring forging
- Machining from bar stock

Based on schedule and fabrication costs, it was apparent that hydroforming techniques would be best adaptable to our program and produce a neck tube area with the best metallurgical structure.

A hydroformed neck tube section could also be welded to the bottom section of the machined inner liner.

Development Program

After determining that a hydroformed neck tube (electron beam welded to a machined lower section) was the best approach, a development program was initiated to determine the feasibility of hydroforming Hastelloy-X to the desired shape necessary to obtain a ring equivalent to a neck tube section. Figure A-2 shows the basic manufacturing sequence.

The basic development sections of the program consisted of the following:

- Hydroform cups from different sheet stock thicknesses.
- Obtain neck tube sections by removing top and bottom of cups.
- Develop electron beam welding of neck tube sections to lower inner liner sections.
- Develop annealing times and temperatures to be used.
- Develop a non-destructive test program for assuring final quality levels.
- Run a metallographic study on all phases of the program.

Hastelloy-X sheet stock, per AMS 5536, in 0.090" and 0.125" thick stock was ordered for our first feasibility study. This stock was cut into 12" diameter

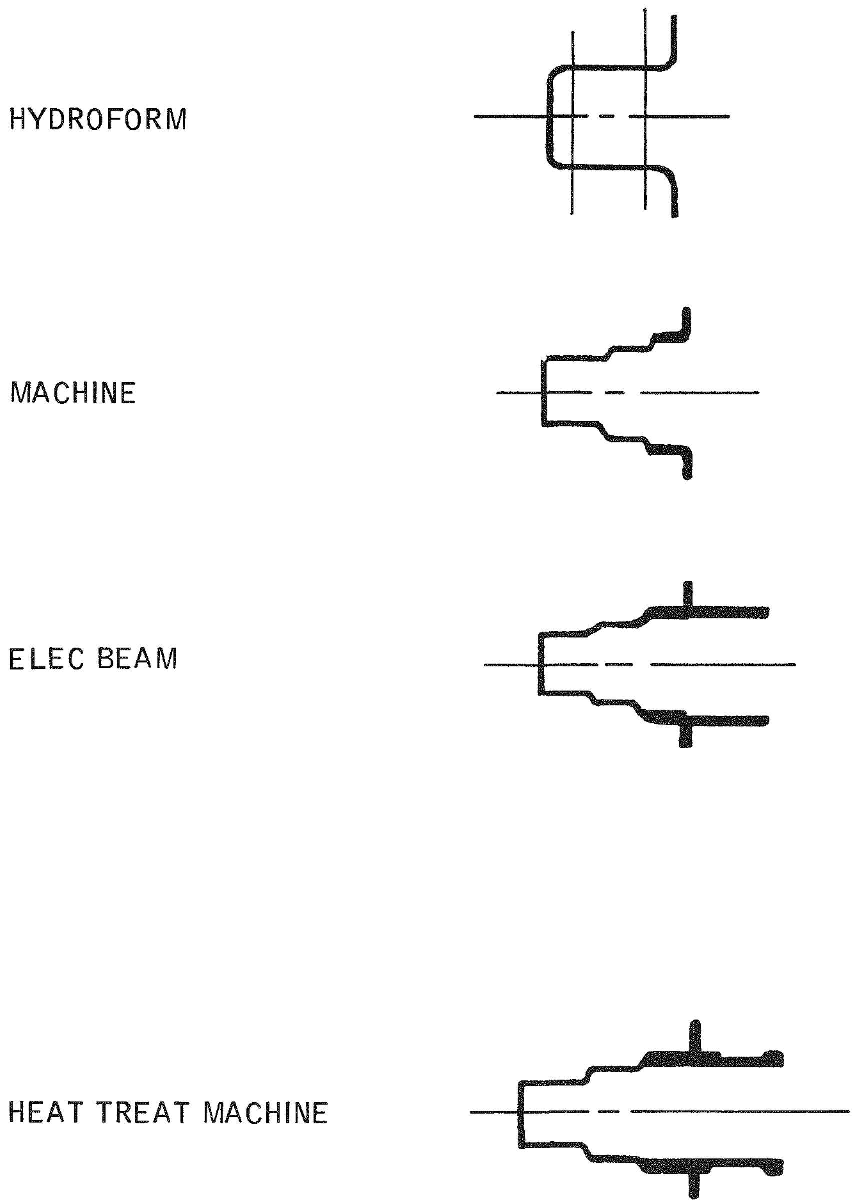

Figure A-2. Basic Manufacturing Sequence circles which was the maximum size allowable for the hydroforming equipment used. Four pieces of each size were hydroformed by a local vendor using an in-house set of dies which were close to the neck tube ID dimensions. A clamping force of 8000 psi was exerted on the sheet stock which was placed between a metal die and a rubber backup plate. A force of 14, 500 psi then forced the male die into the hydraulic fluid backed rubber plate forming the cup around the die. Various depths of cupping were tried to determine when cracking or tearing would take place. This did not happen on the limited number of samples available. Table A-I shows the average dimensional tolerances obtained on the hydroformed cups. Figure A-3 shows the cup shape formed and dimensional locations. During hydroforming a thinning of the material takes place at the closed end or top of the cup, while a thickening takes place at the open end or the bottom of the cup. Because of the material and cupping depth variation on this feasibility study, hydroforming dimensions varied more than will be seen in the production run.

Three of each size of the hydroformed cups had the top and bottom ends removed to obtain rings to be used for further work. After removing both ends of the cups, the out-of-roundness condition increased up to approximately 0.012".

Weld samples to which the rings were electron beam welded were obtained from scrap inner liners which had the neck tube and part of the flange removed. The production weld configuration will be as shown in Figure A-4. The rings and scrap inner liners which had received weld preparation by machining were cleaned by washing in chlorothane and acetone wiped and assembled for welding. The rings were hand pressed onto the liners and held in place by a strap bolted across the open end and into the liner biological plug holes. The welding parameters are given in Table A-II.

Because of the good fit up of the machined weld joint, it was difficult to find and track the joint. It was noted during welding that the joint was missed on one liner. Production weld preparation will contain a small chamfer on the joint so that location and tracking will be easier. Figures S-65, S-95, S-93, S-93A, S-106 and S-107 in Attachment I show the sectioned welds. Figures S-93 and S-93A show a crack which developed due to excessive stresses caused by too deep a weld zone. The production welds will be broadened and the depth controlled to about 10 – 15% deeper than the joint thickness. Samples will be run prior to the production parts.

Table A-I. Average Dimensional Tolerances Obtained on Hydroformed Cups

Male Die Dimensions

Die End – 4.989" OD to 4.991"OD
0.002 Out-of-Round

OD of Cup

0.125" Stock

Top Average – 5.233"
Bottom Average – 5.273"

0.909 Stock

Top Average – 5.175"
Bottom Average – 5.203"

ID of Cup

0.125" Stock

Top Average – 4.996"
Bottom Average – 5.009"

0.090" Stock

Top Average – 4.998"
Bottom Average – 5.004"

Wall Thickness

0.125" Stock

Top Average – 0.111"
Bottom Average – 0.129"

0.090" Stock

Top Average – 0.085"
Bottom Average – 0.098"

Out-of-Roundness of Cup

0.125" – 0.008" to 0.009"
0.090" – 0.005" to 0.008"

NOTE: Average Starting Sheet Stock Thickness – 0.125" and 0.095".

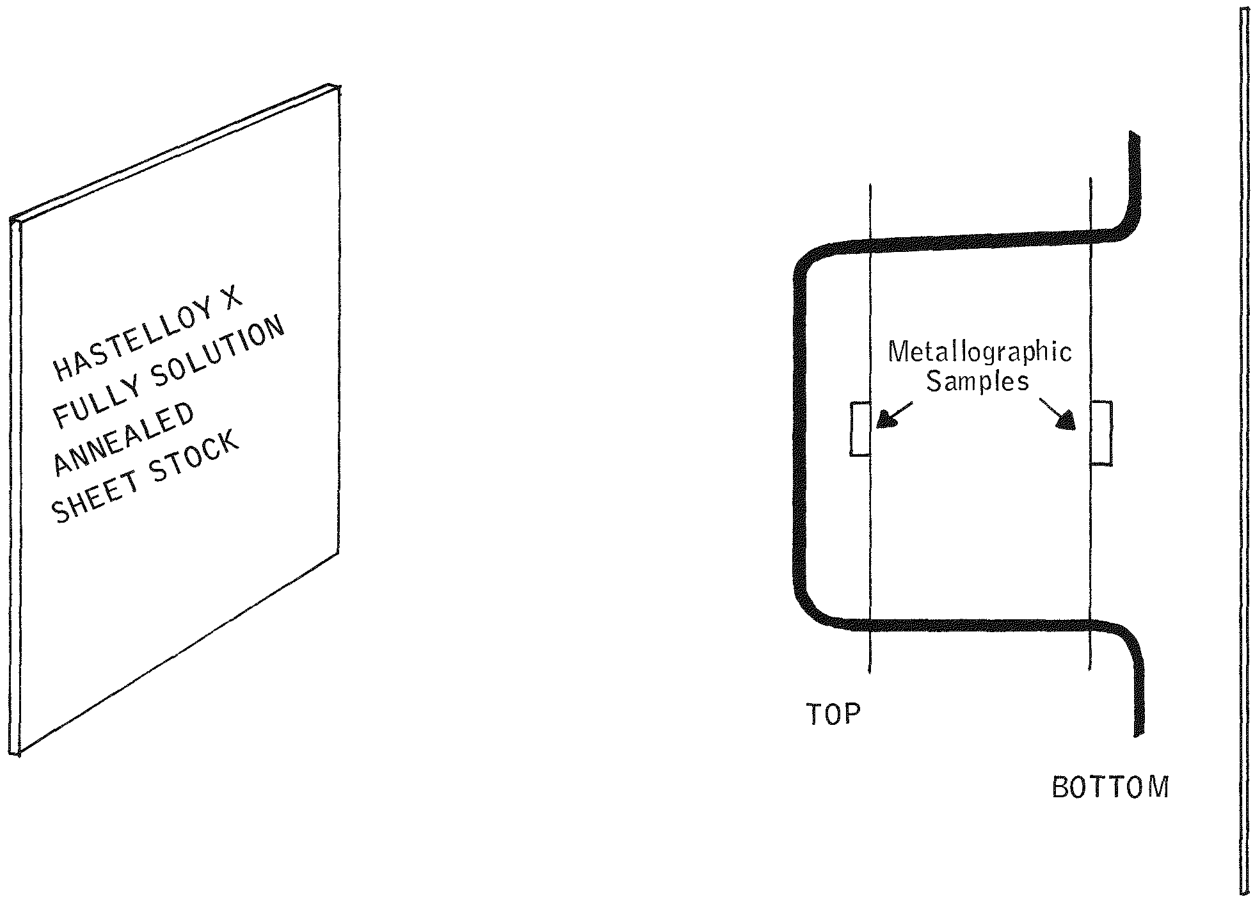

Figure A-3. Cup Shape Formed and Dimensional Locations

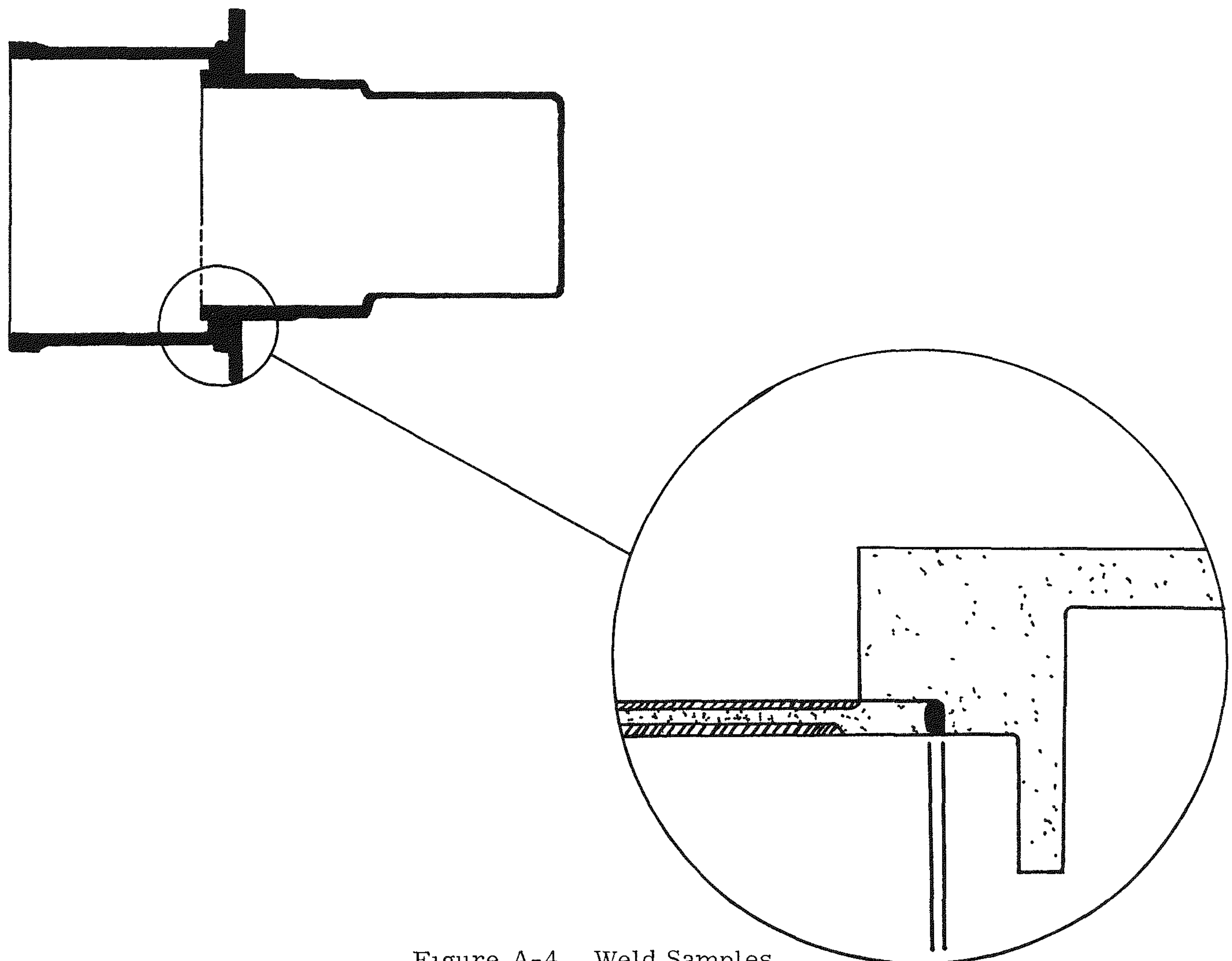

Figure A-4. Weld Samples

Table A-II. Welding Parameters

ELECTRON BEAM WELDING SCHEDULE

PART DESCRIPTION PART NUMBER	884-43-1	DRAWING NUMBER	3M Co. PD-37-4017	DATE	1-22-69
ROTATING SOURCE	Sciaky Dyne Drive	TABLE MOVEMENT	Stationary		
TABLE NUMBER	2596-1	FIXTURE NUMBER	Chuck Assy.	ADDITIONAL TOOLS	2, 1/4-20 Bolts & Hold down Bar

MATERIAL	TYPE	Hastelloy "X"	TYPE	Hastelloy "X"	TYPE		FILLER WIRE	TYPE	None
	GAGE	0.090	GAGE	0.125	GAGE			SIZE	

JOINT DESC.	Modified Butt	NO. TABS REQUIRED	None	WELD TYPE	Circumferential

GUN SET-UP			
FILAMENT TO CATHODE	0.353	SPACER	0.200
GUN TO WORK DISTANCE	2 In.	FILAMENT	250 ma

GUN DISTANCE FRONT TO BACK		
1st Setting	2nd Setting	3rd Setting
4th Setting	5th Setting	6th Setting
7th Setting	8th Setting	9th Setting

OPERATOR'S CONTROL CONSOLE	
X-AXIS DRIVE	DRIVE SPEED ADJUST
Forward	28.0
MODE SELECTION	HIGH VOLTAGE
Continuous	Unlock
Manual	26 Kv
Beam Align: 4.20	

SCOPE CONTROL PANEL			
HIGH VOLTAGE		MOTOR	
Slope	14 Kv	Initial	N/A
Slope Rate	20%	Final	N/A
Start Delay	0 – 0.75	Start Delay	0 – 0.75
% of Delay	60	% of Delay	10

GUN POWER METER PANEL			
BEAM CURRENT	85	MULTIPLIER	X2
DIVIDE BY TEN	No	HIGH VOLTAGE	13
MULTIPLIER	X1	WORK MOTION	28.0
FOCUS CURRENT	4.5	GUN FILAMENT	45
FILAMENT ADJUST	62 Approx.		

VACUUM CONTROL PANEL		
POPPET VALVE	Open	VACUUM Stand By
VACUUM SYSTEM	Automatic	
WELDING PRESSURE	LIGHT ON	
EVACUATE CHAMBER	LIGHT ON	
SEQUENCE ON	INITIAL START	
WELDING PRESSURE GAUGE	10^{-4} Min.	

26 Kv ~ 85 ma ~ 68.5 ipm

Inner Liner, Insulation System

JOINT DIAGRAM

Various solution annealing times and temperatures were given to samples of every operation so that a complete metallographic study could be made of the changes taking place. Of specific interest to this study was the change in grain size and the change in the amount, size and location of carbides and other phases in the material. Figures S-47 through S-10D4 in Attachment I show this complete history. The material description, treatment and grain size is listed under each figure and in Table A-III.

Annealing of the electron beam welded part just prior to machining was discussed with Union Carbide personnel. Since the goal of this development program was to maintain a small grain size, Union Carbide recommended that the inner liner be annealed at 1950°F. Some recent work has been done with a lower solution annealing temperature specifically for maintaining small grains. Two development liners were given this treatment, and the metallographic structure is shown in Figures S-104A, B, C and D. Figure A-5 depicts the minimum grain size in each section of the inner liner expected in the production liners.

After solution annealing, the out-of-roundness condition increased by 2 – 4 mils. This condition was difficult to check because we were using scrap liners which were in various stages of manufacture. It was difficult to come back to the same "0" point each time. The neck tube section was machined to approximately final dimension on one liner. The study showed that final dimensions could be met. A small amount of effort was expended on surface finish. Abrasive impregnated nylon wheels were tried which gave a surface finish of about 12 rms. Hand finishing with abrasive paper produced a 4 – 8 rms surface finish. Figure A-6 is a drawing of the final machined inner liner.

After machining, the parts were given a fluorescent penetrant inspection for surface defects. None were detected. The parts also passed a rigid helium leak test which indicated no leaks. The liners were then taken to Larpin Company in Milwaukee, Wisconsin, for development radiography. A non-destructive test was required to determine weld quality. Defects which might compromise the weld integrity are lack of fusion, porosity or cracking which might be internally present. The x-ray film shows indications of porosity and line type defects, which could be lack of fusion or a missed weld joint. Figures S-65, S-93, S-93A, S-106 and S-107 in Attachment I, show the metallographic cross section through the defect areas as shown on the radiographs. This shows that radiography is a valid NDT for assuring the quality of the electron beam weld.

Table A-III. Materials

Sample Designation	Material Thickness	Material Condition	Sample Location	Additional Heat Treatment	ASTM Grain Size	Remarks
S-47	0.125	As Received Sheet Stock			4 – 5	
S-50	0.090	As Received Sheet Stock			5-1/2 – 6-1/2	
S-47A	0.125	As Received Sheet Stock				
S-50A	0.090	As Received Sheet Stock				
S-60	0.125	As Received Sheet Stock		10 min. at 2150°F W.Q.	4-1/2 – 5-1/2	
S-62	0.090	As Received Sheet Stock		10 min. at 2150°F W.Q.	5-1/2 – 6-1/2	
S-64	0.090	As Received Sheet Stock		20 min. at 2150°F W.Q.	4 – 6	
S-91	0.125	As Received Sheet Stock		10 min. at 2050°F W.Q.	4 – 5-1/2	
S-92	0.090	As Received Sheet Stock		10 min. at 2050°F W.Q.	5 – 7	
S-98	0.125	As Received Sheet Stock		10 min. at 1950°F W.Q.	4 – 5-1/2	

Table A-III. Materials (Continued)

Sample Designation	Material Thickness	Material Condition	Sample Location	Additional Heat Treatment	ASTM Grain Size	Remarks
S-97	0.090	As Received Sheet Stock		10 min. at 1950°F W. Q.	5 – 7	
S-56	0.090	Hydroformed	#7 – Top		5-1/2 – 6-1/2	
S-57	0.090	Hydroformed	#7 – Bottom		6 – 7	
S-56A	0.090	Hydroformed	#7 – Top			
S-57A	0.090	Hydroformed	#7 – Bottom			
S-58	0.125	Hydroformed	#8 – Top		4 – 5-1/2	
S-59	0.125	Hydroformed	#8 – Bottom		4-1/2 – 6	
S-58A	0.125	Hydroformed	#8 – Top			
S-59A	0.125	Hydroformed	#8 – Bottom			
S-99	0.090	Hydroformed	#7 – Top	10 min. at 2150°F W. Q.	4 – 5	
S-100	0.090	Hydroformed	#7 – Bottom	10 min. at 2150°F W. Q.	4-1/2 – 6	
S-102	0.125	Hydroformed	#8 – Top	10 min. at 2150°F W. Q.	3 – 5	

Table A-III. Materials (Continued)

Sample Designation	Material Thickness	Material Condition	Sample Location	Additional Heat Treatment	ASTM Grain Size	Remarks
S-101	0.125	Hydroformed	#8 – Bottom	10 min. at 2150°F W. Q.	3-1/2 – 5	
S-88	0.090	Hydroformed	#7 – Top	10 min. at 2050°F W. Q.	6 – 7-1/2	
S-87	0.090	Hydroformed	#7 – Bottom	10 min. at 2050°F W. Q.	6 – 7-1/2	
S-89	0.125	Hydroformed	#8 – Top	10 min. at 2050°F W. Q.	4-1/2 – 6	
S-90	0.125	Hydroformed	#8 – Bottom	10 min. at 2050°F W. Q.	Severely worked indeterminate sample questionable	
S-80	0.090	Hydroformed	#7 – Top	10 min. at 1950°F W. Q.	5 – 7	
S-79	0.090	Hydroformed	#7 – Bottom	10 min. at 1950°F W. Q.	5 – 7	
S-82	0.125	Hydroformed	#8 – Top	10 min. at 1950°F W. Q.	4-1/2 – 6	

Table A-III. Materials (Continued)

Sample Designation	Material Thickness	Material Condition	Sample Location	Additional Heat Treatment	ASTM Grain Size	Remarks
S-81	0.125	Hydroformed	#8 — Bottom	10 min. at 1950°F W. Q.	4-1/2 — 6	
S-104A		Hydroformed	Upper Section of Machined Neck Tube	Solution Annealed at 1950°F for 10 min. and W. Q.	6 — 8	
S-104B		Hydroformed	Upper Section of Machined Neck Tube	Solution Annealed at 1950°F for 10 min. and W. Q.		
S-104C		Hydroformed	Thin Section of Neck Tube	Solution Annealed at 1950°F for 10 min. and W. Q.	6 — 8	
S-104D		Hydroformed	Thin Section of Neck Tube	Solution Annealed at 1950°F for 10 min. and W. Q.		
S-65		Electron Beam Welded	Inner Liner #2	Solution Annealed at 1950°F for 10 min. and W. Q.		

Table A-III. Materials (Continued)

Sample Designation	Material Thickness	Material Condition	Sample Location	Additional Heat Treatment	ASTM Grain Size	Remarks
S-95		Electron Beam Welded	Inner Liner #1	Solution Annealed at 1950°F for 10 min. and W. Q.		
S-93		Electron Beam Welded	Inner Liner #3	Solution Annealed at 1950°F for 10 min. and W. Q.		
S-93A		Electron Beam Welded	Inner Liner #3	Solution Annealed at 1950°F for 10 min. and W. Q.		
S-106		Electron Beam Welded	Inner Liner #3	Solution Annealed at 1950°F for 10 min. and W. Q.		
S-107		Electron Beam Welded	Inner Liner #3	Solution Annealed at 1950°F for 10 min. and W. Q.		

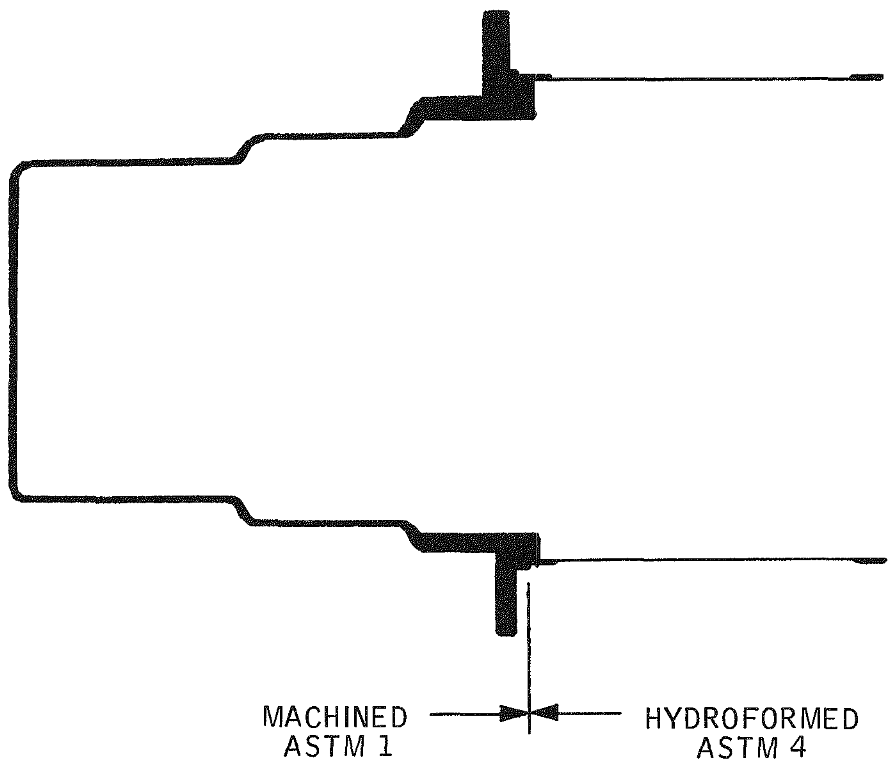

Figure A-5. Minimum Grain Size

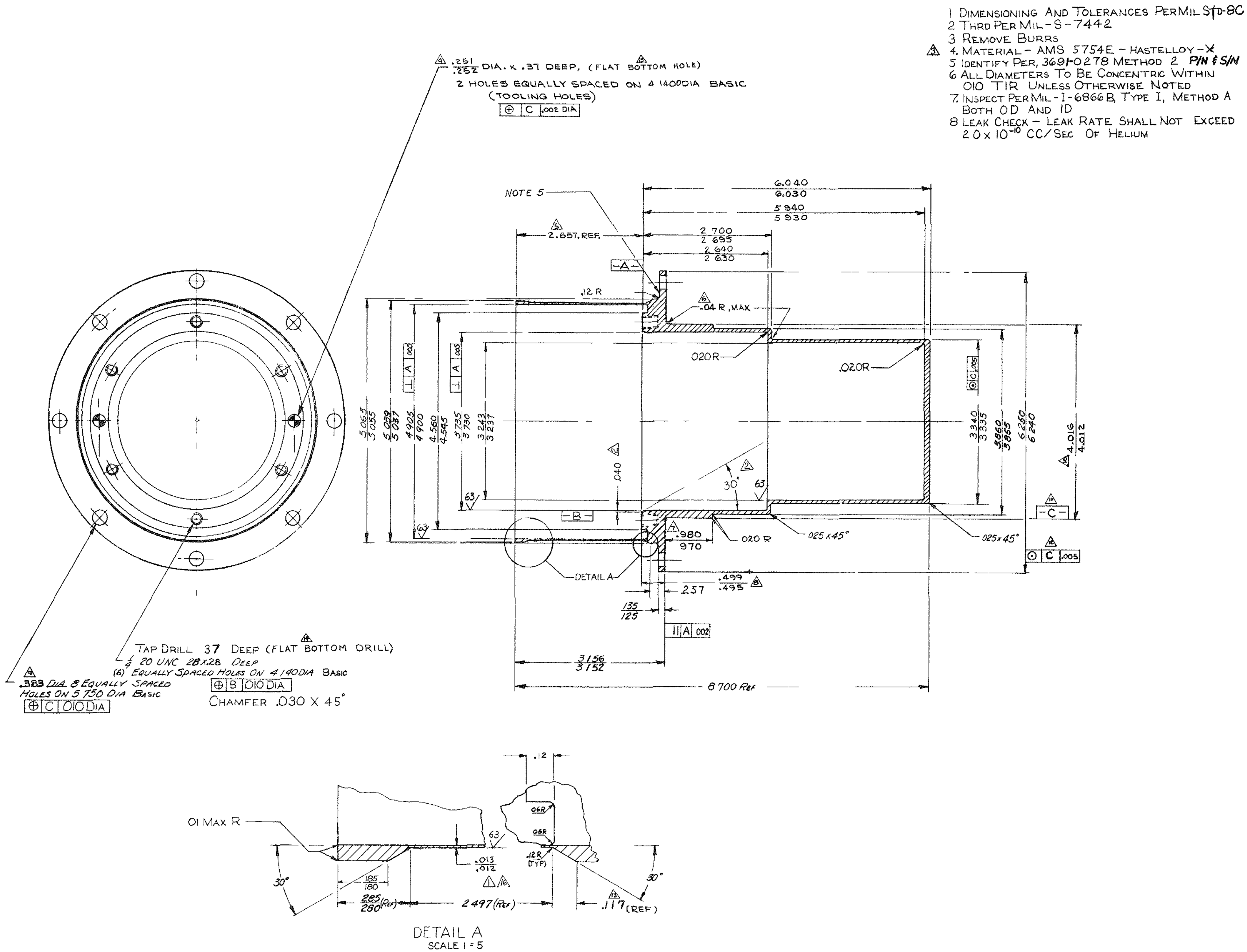

Figure A-6. Inner Liner, Insulation System

Conclusion

After reviewing the complete metallographic history, as shown in Attachment I, the following conclusions can be reached:

- Neck tube sections can be fabricated by hydroforming techniques.
- The grain size of hydroformed neck tube sections can be kept finer than an ASTM #4.
- Carbides and other phases can be kept well dispersed and small through the use of sheet stock, hydroforming techniques, and proper solution annealing temperatures.
- Solution annealing can be accomplished at 1950°F.
- Radiography, penetrant inspection, and helium leak test are adequate quality assurance checks for good quality parts.
- Dimensional distortion can be kept within allowable machining dimensions.

Recommendations

The following recommendations are made regarding the balance of the SNAP-21, Phase I, 10-watt system. Two additional inner liners can be made by the following techniques and procedures:

- Machine the lower section of the inner liner from bar stock.
- Hydroform the neck tube section of the inner liner.
- Electron beam weld the hydroformed ring to the inner liner.
- Solution anneal at 1975°F for approximately 20 minutes.
- Machine neck tube section for radiography.

- Radiograph welds, fluorescent penetrant inspect welds and helium leak test liner.
- Machine neck tube section per drawing PD-37-4017.
- Helium leak test and dimensional inspection.

The following recommendations are made for future designs of a similar nature and application:

- Investigate the use of seam welded tubing for both the lower section and neck tube section of the inner liners.
- Investigate the use of plate stock for the center section.
- Investigate other types of welding such as TIG welding and inertia welding.

ATTACHMENT I
TO
APPENDIX A

Microstructures of Hastelloy-X Obtained During the Hydroforming Development Program

The location, condition of sample, magnification and grain size is given for each microstructure. All solution annealed samples were water quenched. All samples have been electrolytically etched in 10 percent oxalic acid with the exception of Figures S-65, S-95, S-93, S-93A, S-106 and S-107, which were swab etched with a HCl, HNo_3 and $CuSO_4$ solution.

100X

Figure S-47. 0. 125 Thick — As Received Sheet
ASTM Grain Size 4-5

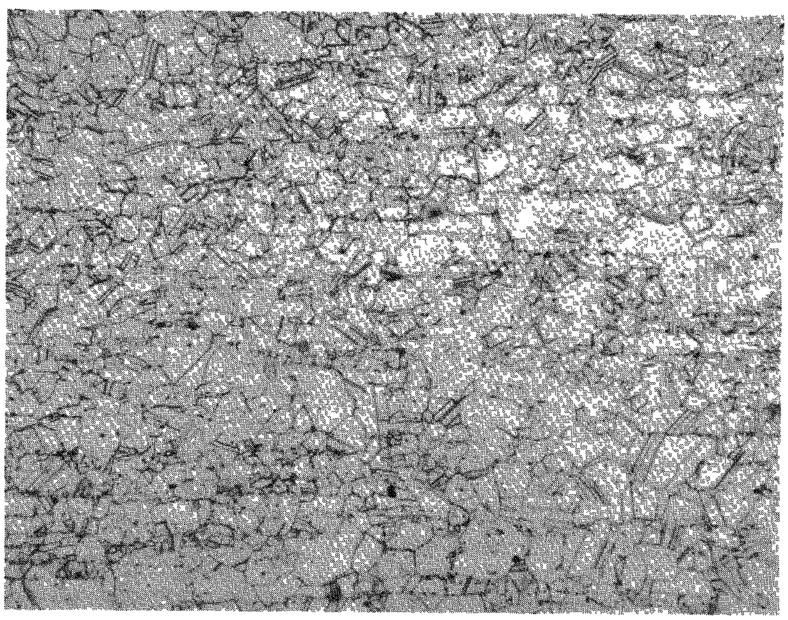

100X

Figure S-50. 0. 090 Thick — As Received Sheet
ASTM Grain Size 5-1/2-6-1/2

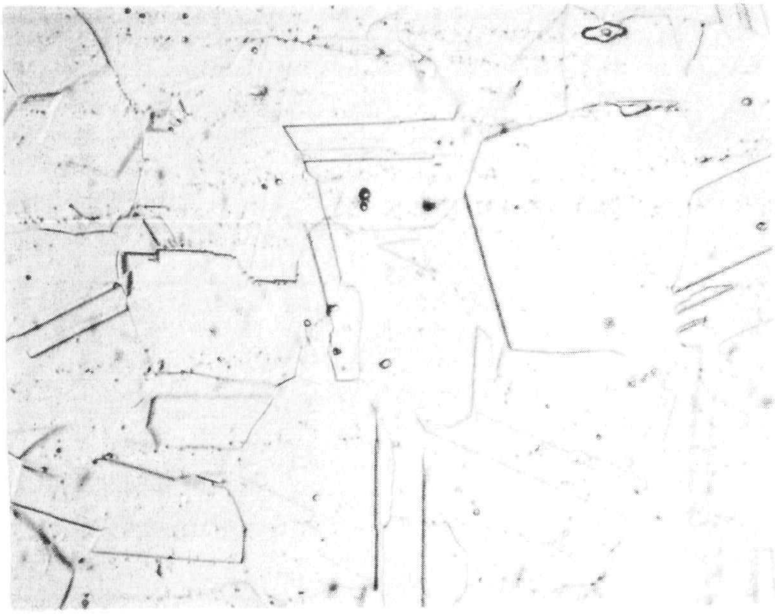

400X

Figure S-47A. 0.125 Thick — As Received Sheet

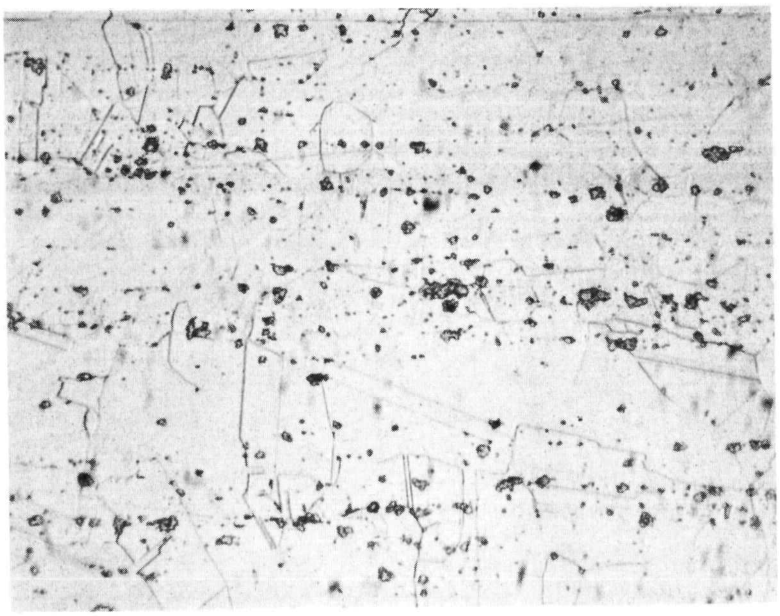

400X

Figure S-50A. 0.090 Thick — As Received Sheet

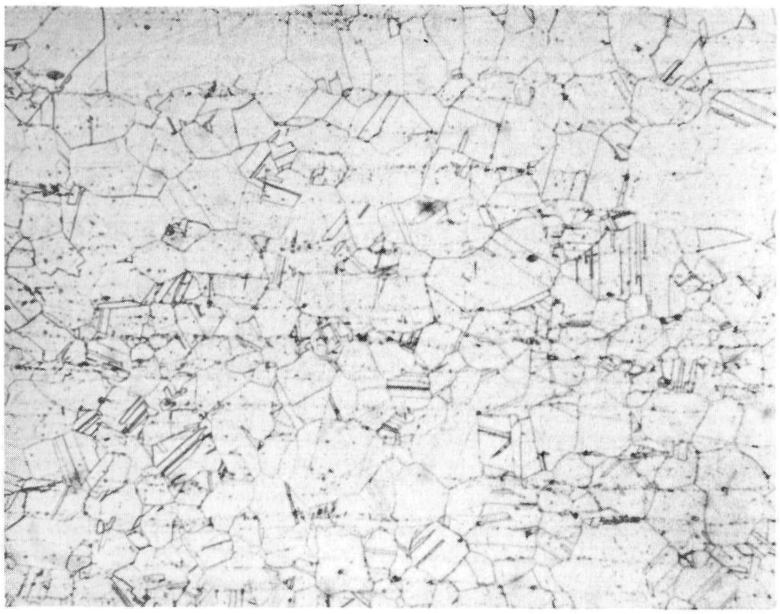

100X

Figure S-60. 0.125 Thick — As Received Sheet
Sol'n Annealed at 2150°F for 10 Min
ASTM Grain Size 4-1/2-5-1/2

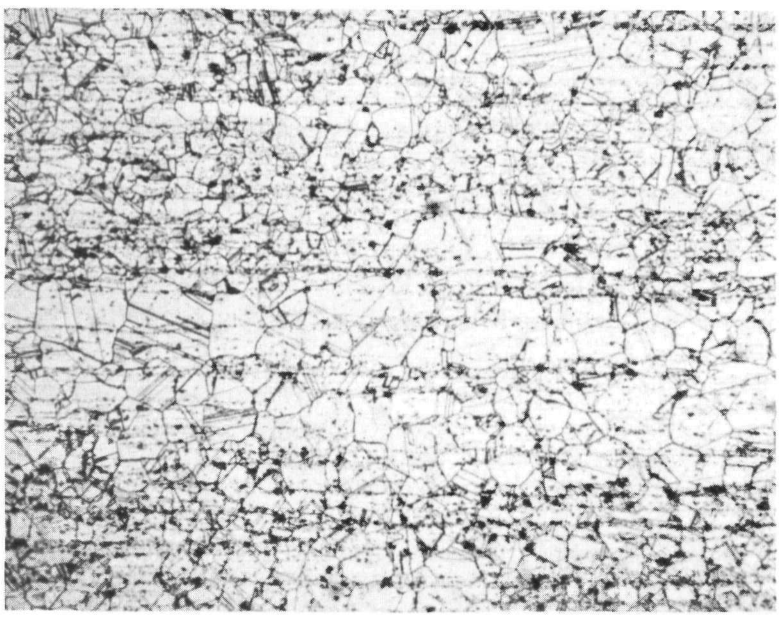

100X

Figure S-62. 0.090 Thick — As Received Sheet
Sol'n Annealed at 2150°F for 10 Min
ASTM Grain Size 5-1/2-6-1/2

100X

Figure S-64. 0.090 Thick — As Received Sheet
Sol'n Annealed at 2150°F for 20 Min
ASTM Grain Size 4-6

100X

Figure S-91. 0.125 Thick — As Received Sheet
Sol'n Annealed at 2050°F for 10 Min
ASTM Grain Size 4-5-1/2

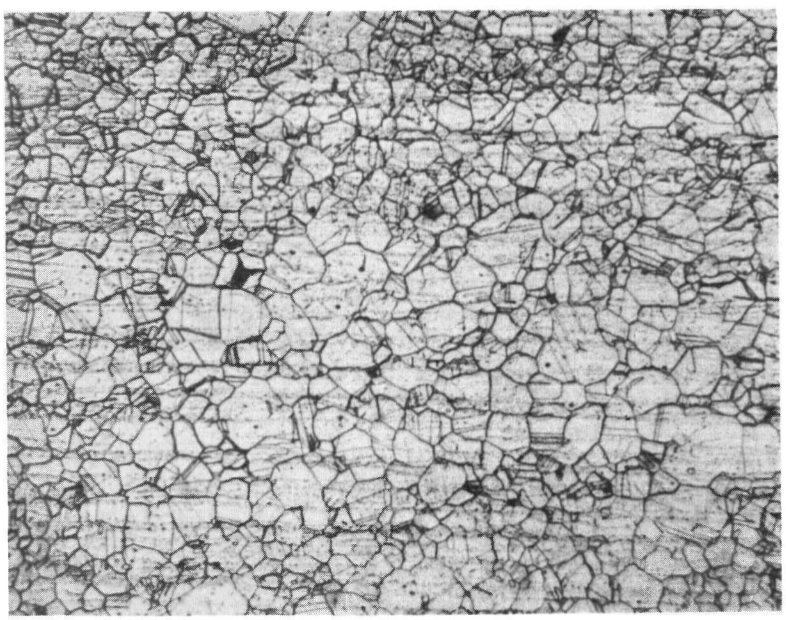

100X

Figure S-92. 0.090 Thick — As Received Sheet
Sol'n Annealed at 2050°F for 10 Min
ASTM Grain Size 5-7

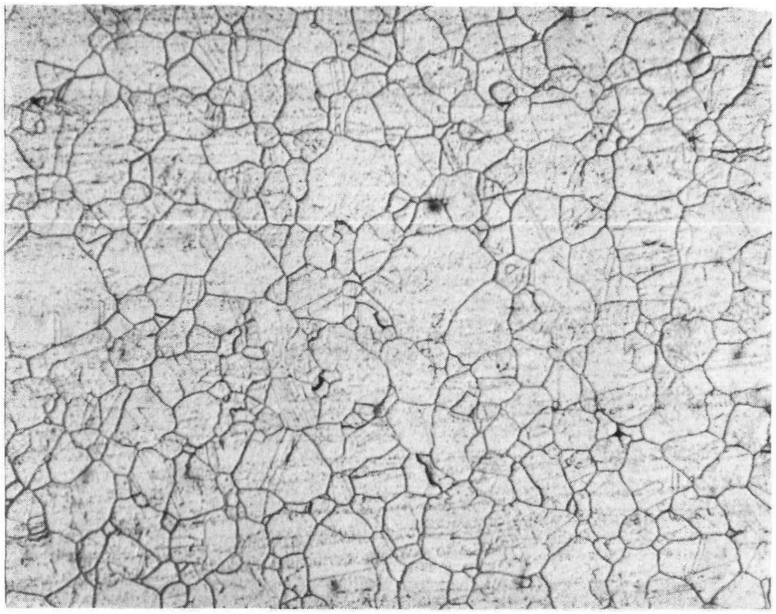

100X

Figure S-98. 0.125 Thick – As Received Sheet
Sol'n Annealed at 1950°F for 10 Min
ASTM Grain Size 4-5-1/2

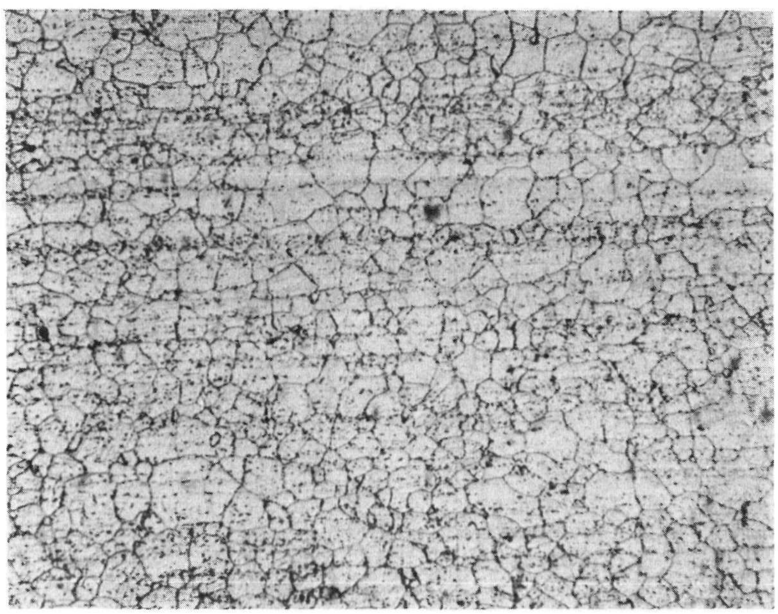

100X

Figure S-97. 0.090 Thick – As Received Sheet
Sol'n Annealed at 1950°F for 10 Min
ASTM Grain Size 5-7

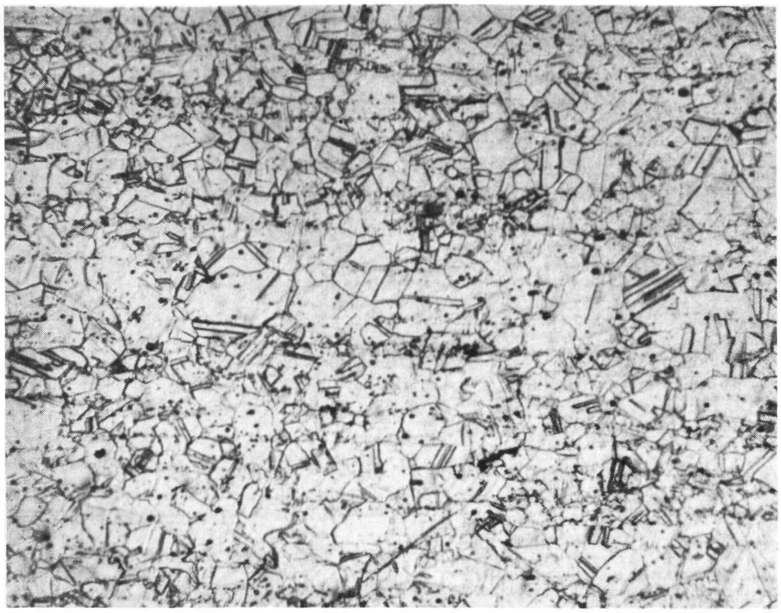

100X

Figure S-56. 0.090 Thick — Hydroformed
#7 — Top
ASTM Grain Size 5-1/2-6-1/2

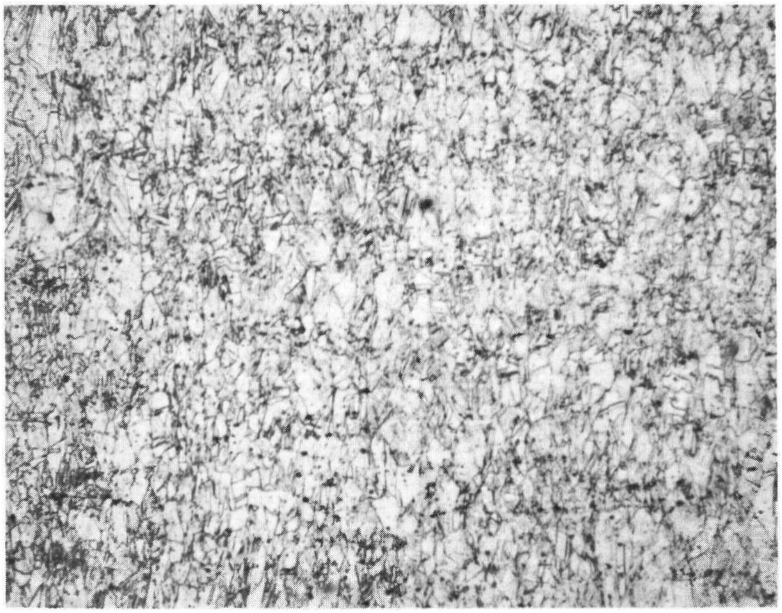

100X

Figure S-57. 0.090 Thick — Hydroformed
#7 — Bottom
ASTM Grain Size 6-7

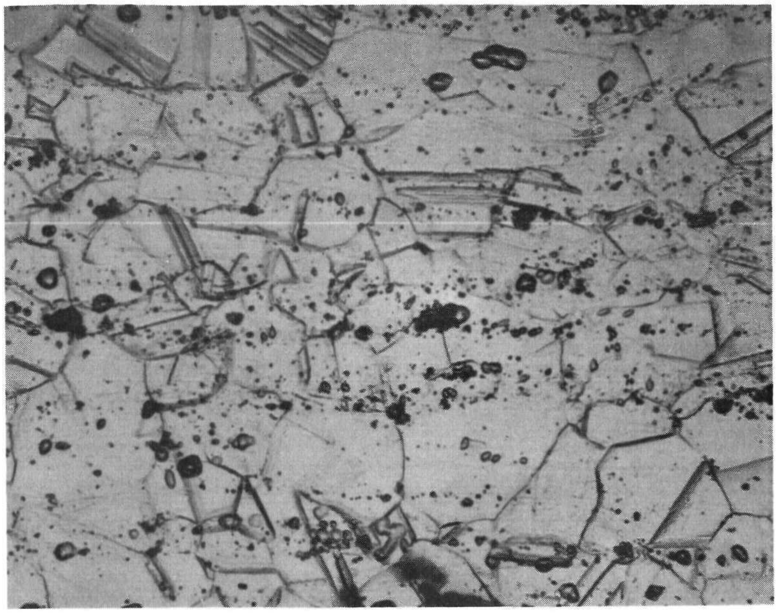

400X

Figure S-56A. 0.090 Thick — Hydroformed
#7 — Top

400X

Figure S-57A. 0.090 Thick — Hydroformed
#7 — Bottom

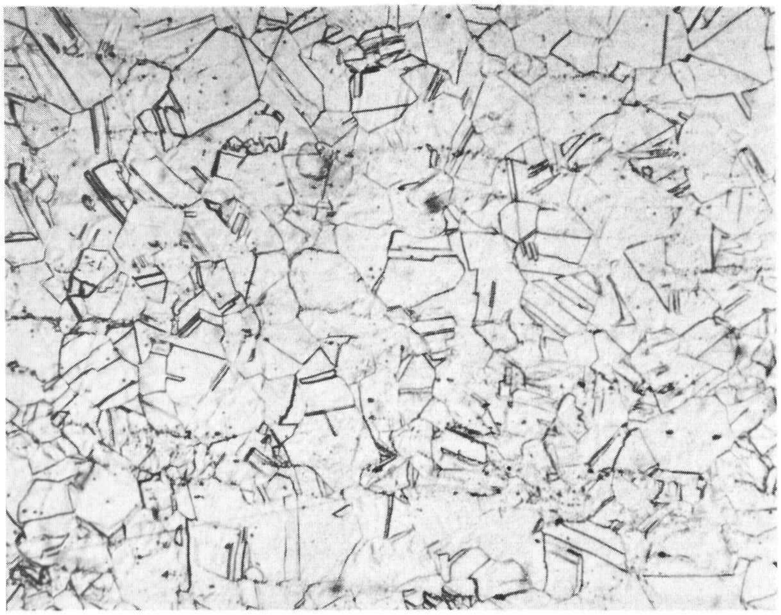

100X

Figure S-58. 0.125 Thick — Hydroformed
#8 — Top
ASTM Grain Size 4-5-1/2

100X

Figure S-59. 0.125 Thick — Hydroformed
#8 — Bottom
ASTM Grain Size 4-1/2-6

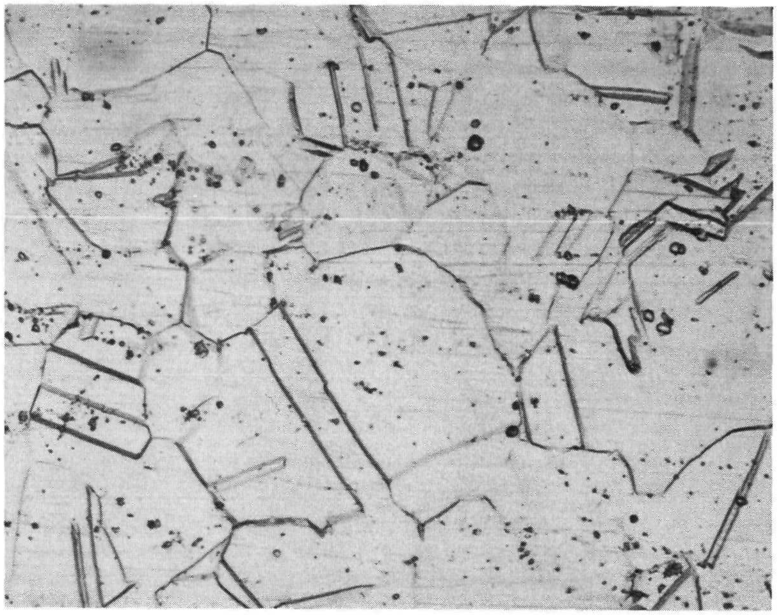

400X

Figure S-58A. 0.125 Thick – Hydroformed
#8 – Top

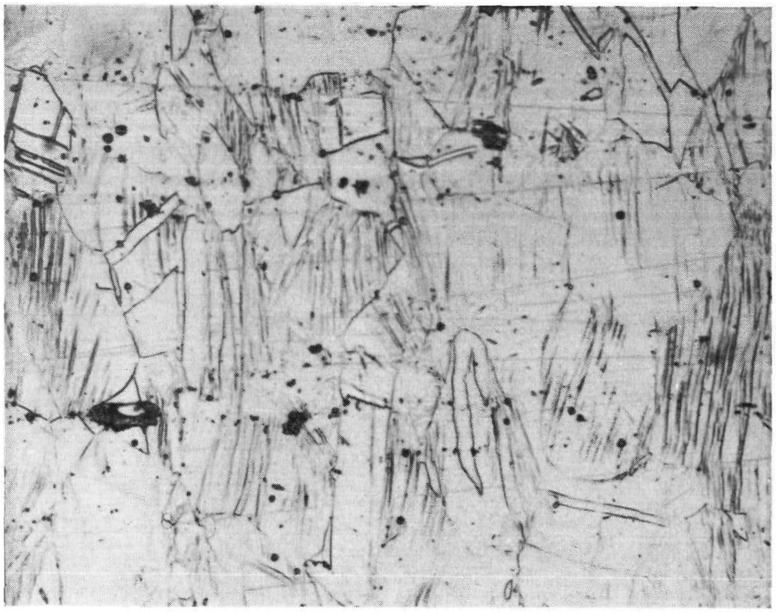

400X

Figure S-59A. 0.125 Thick – Hydroformed
#8 – Bottom

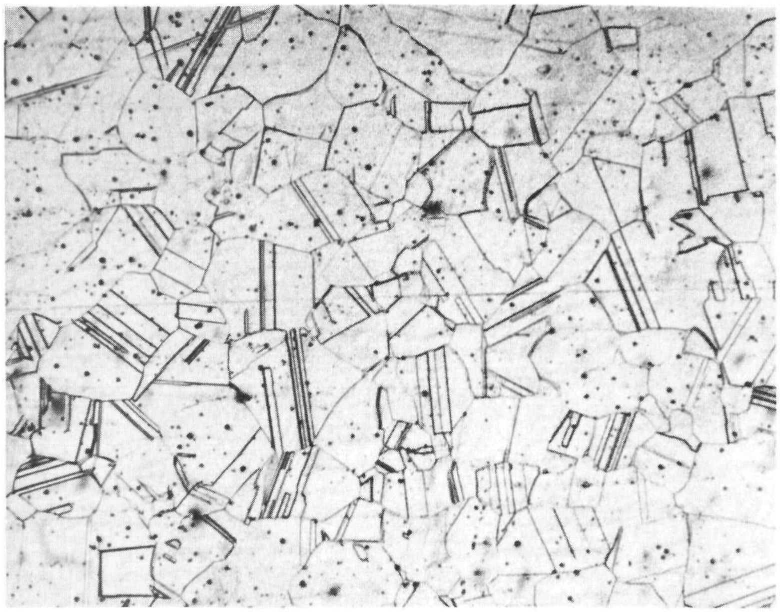

100X

Figure S-99. 0.090 Thick — Hydroformed
#7 — Top
Sol'n Annealed at 2150°F for 10 Min
ASTM Grain Size 4-5

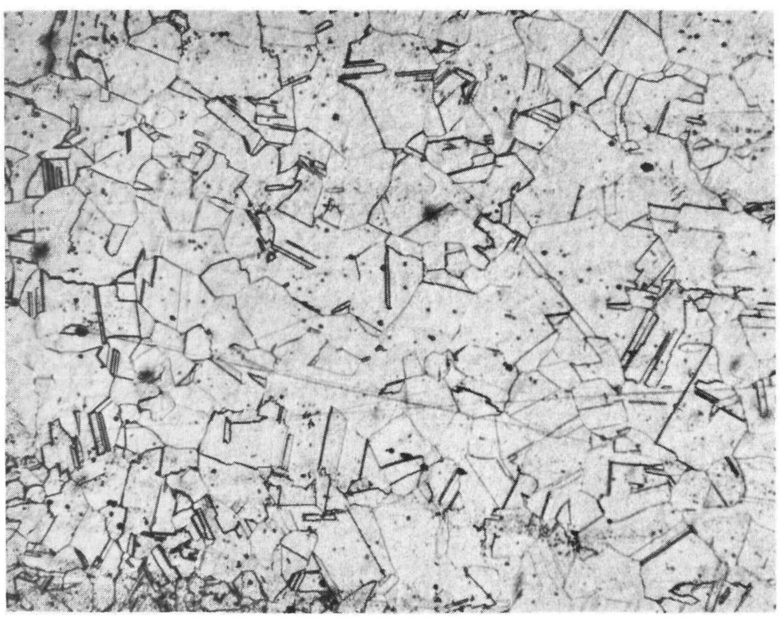

100X

Figure S-100. 0.090 Thick — Hydroformed
#7 — Bottom
Sol'n Annealed at 2150°F for 10 Min
ASTM Grain Size 4-1/2-6

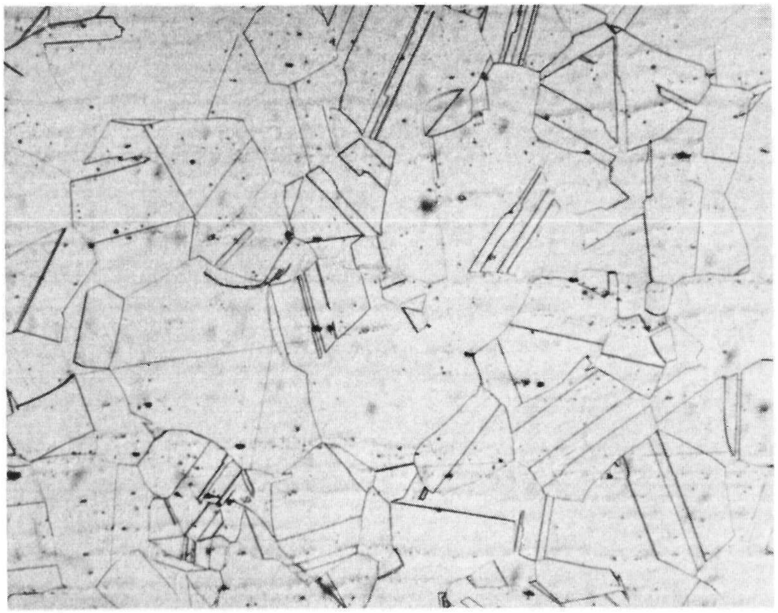

100X

Figure S-102. 0. 125 Thick — Hydroformed
#8 — Top
Sol'n Annealed at 2150°F for 10 Min
ASTM Grain Size 3-5

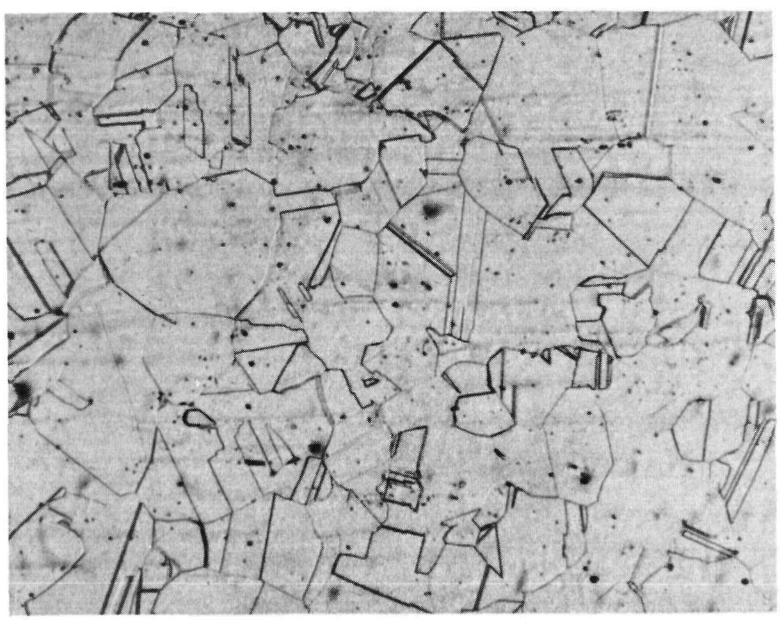

100X

Figure S-101. 0. 125 Thick — Hydroformed
#8 — Bottom
Sol'n Annealed at 2150°F for 10 Min
ASTM Grain Size 3-1/2-5

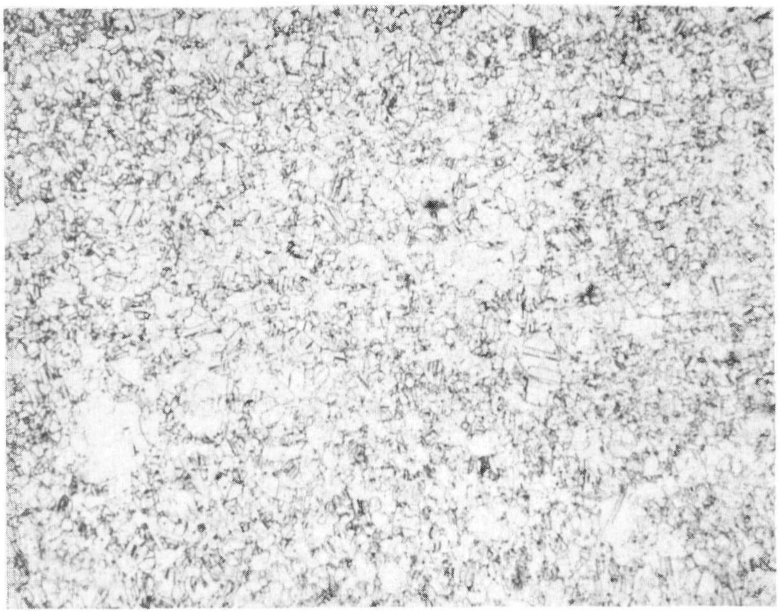

100X

Figure S-88. 0.090 Thick — Hydroformed
#7 — Top
Sol'n Annealed at 2050°F for 10 Min
ASTM Grain Size 6-7-1/2

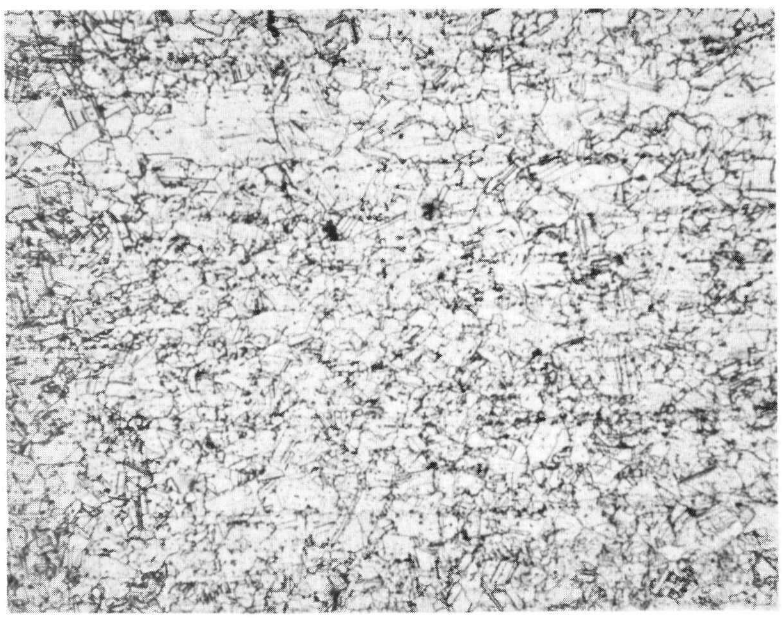

100X

Figure S-87. 0.090 Thick — Hydroformed
#7 — Bottom
Sol'n Annealed at 2050°F for 10 Min
ASTM Grain Size 6-7-1/2

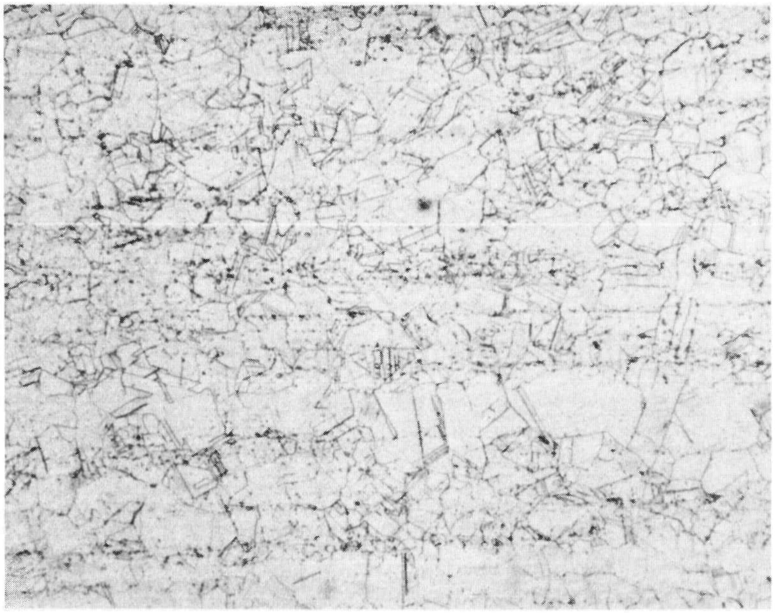

100X

Figure S-89. 0. 125 Thick — Hydroformed
#8 — Top
Sol'n Annealed at 2050°F for 10 Min
ASTM Grain Size 4-1/2-6

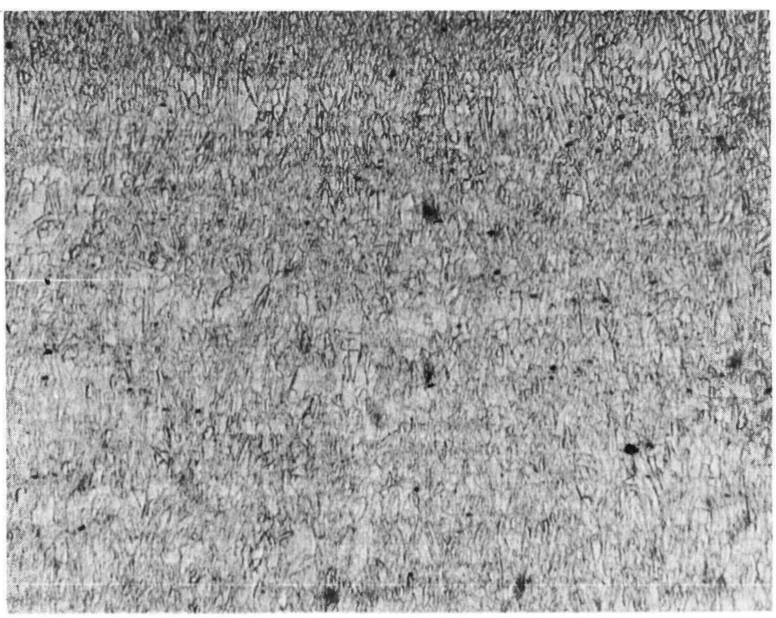

100X

Figure S-90. 0. 125 Thick — Hydroformed
#8 — Bottom
Sol'n Annealed at 2050°F for 10 Min
ASTM Grain Size — Severely Worked
Indeterminate

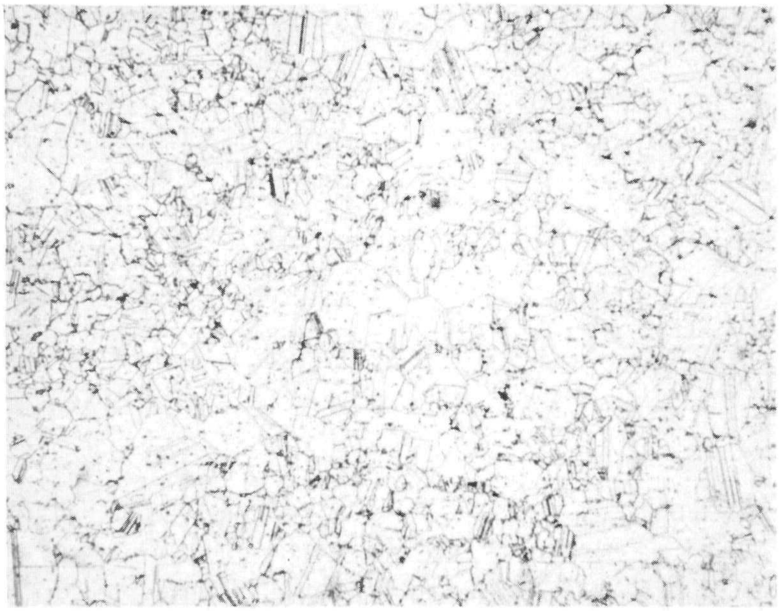

100X

Figure S-80. 0.090 Thick – Hydroformed
#7 – Top
Sol'n Annealed at 1950°F for 10 Min
ASTM Grain Size 5-7

100X

Figure S-79. 0.090 Thick – Hydroformed
#7 – Bottom
Sol'n Annealed at 1950°F for 10 Min
ASTM Grain Size 5-7

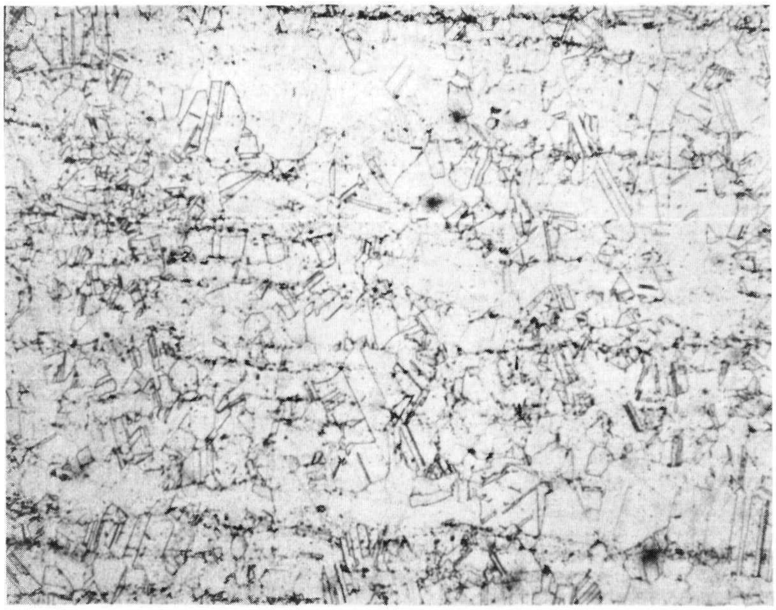

100X

Figure S-82. 0. 125 Thick — Hydroformed
#8 — Top
Sol'n Annealed at 1950°F for 10 Min
ASTM Grain Size 4-1/2-6

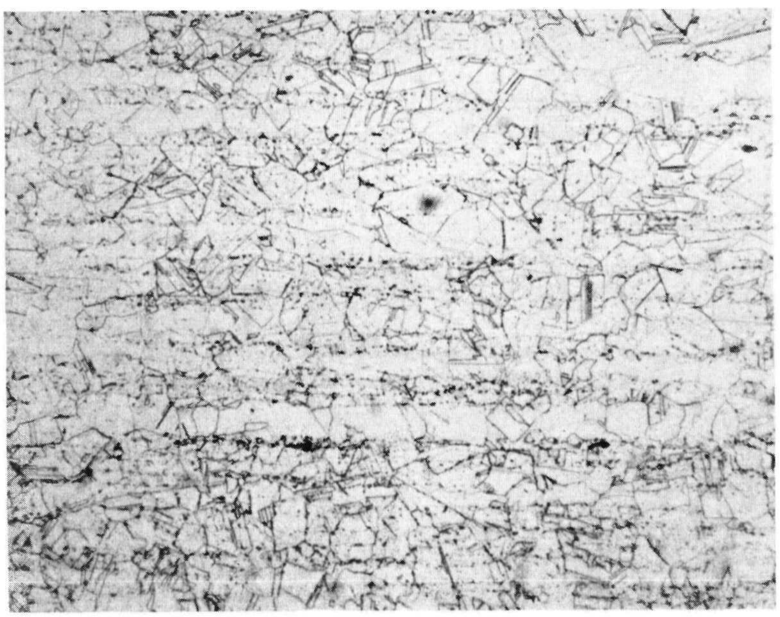

100X

Figure S-81. 0. 125 Thick — Hydroformed
#8 — Bottom
Sol'n Annealed at 1950°F for 10 Min
ASTM Grain Size 4-1/2-6

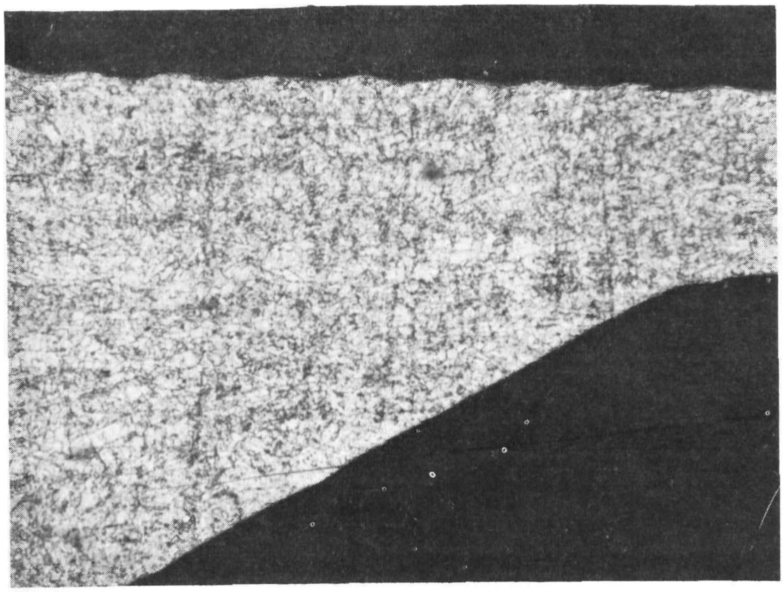

100X

Figure S-104A. Hydroformed – Electron Beam Welded
Sol'n Annealed at 1950°F for 10 Min
and Water Quenched
Upper Section – ASTM Grain Size 6-8

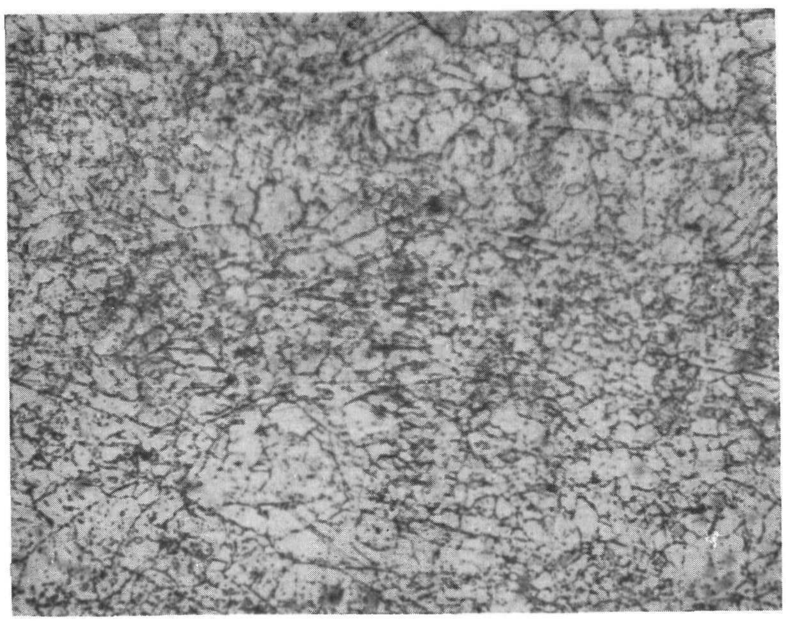

400X

Figure S-104B. Same Treatment as S-104A Upper Section

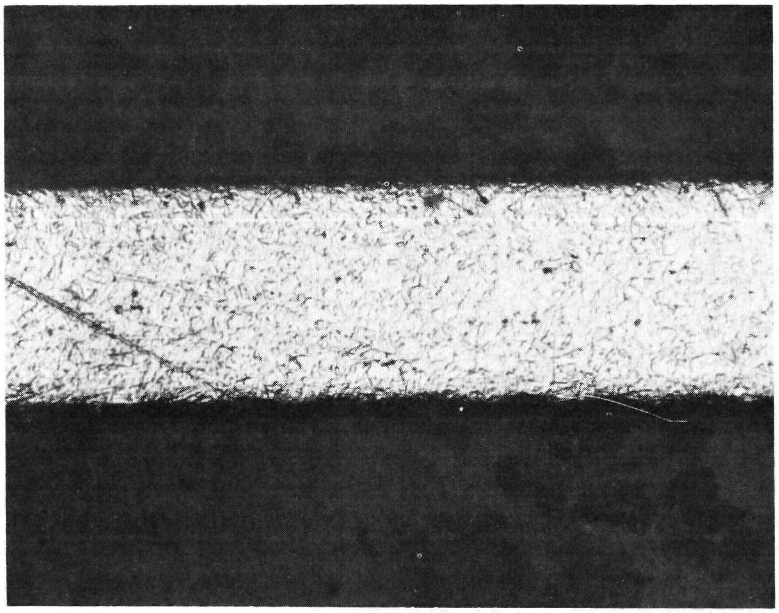

100X

Figure S-104C. Same Treatment as S-104A
Thin Section (0.013")
ASTM Grain Size 6-8

400X

Figure S-104D. Same Treatment as S-104A
Thin Section

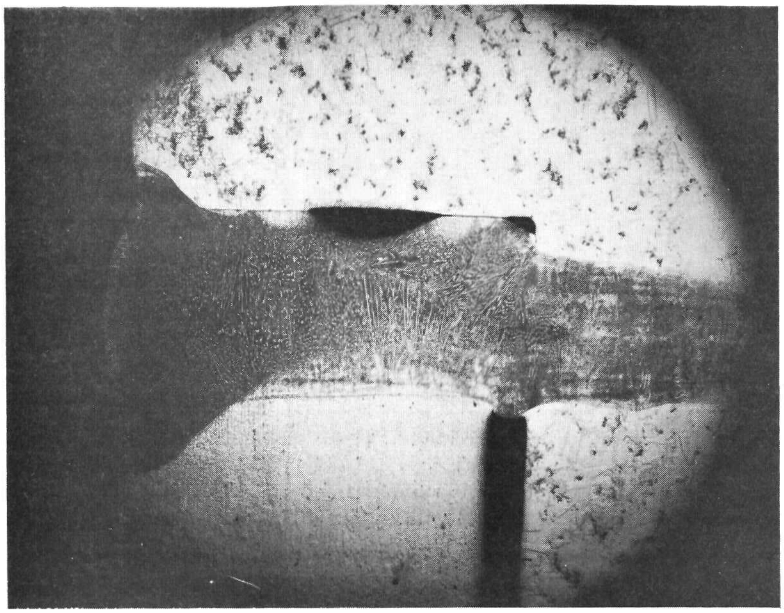

16X

Figure S-65. Inner Liner #2
Electron Beam Welded Joint Showing the Results of an Improperly Located Beam on the Weld Joint

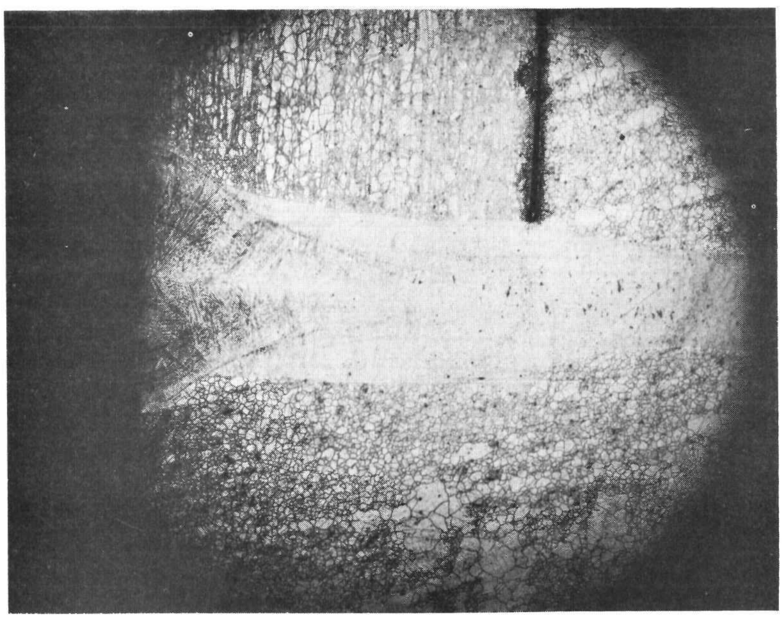

16X

Figure S-95. Inner Liner #1
Example of Satisfactory Weld Joint

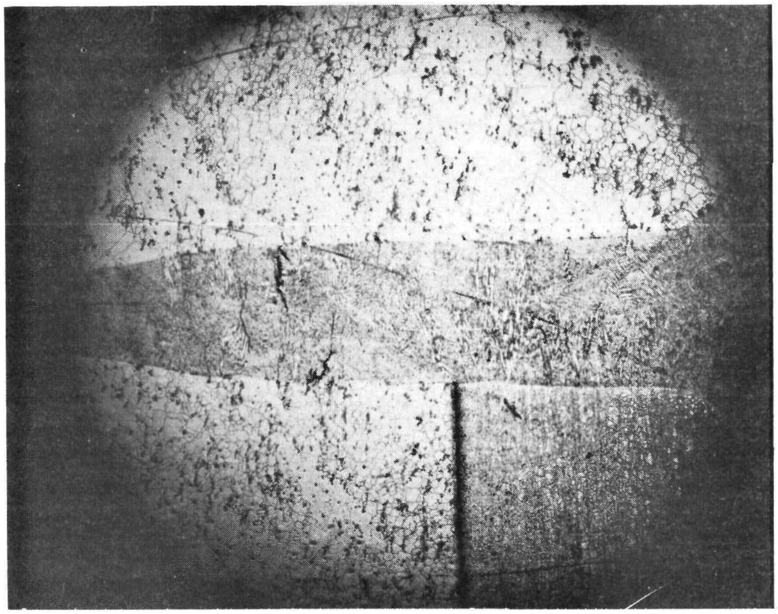

16X

Figure S-93. Inner Liner #3
Electron Beam Welded Joint Showing Stress Cracking in the Weld Zone that Penetrated Too Deeply into the Base Material

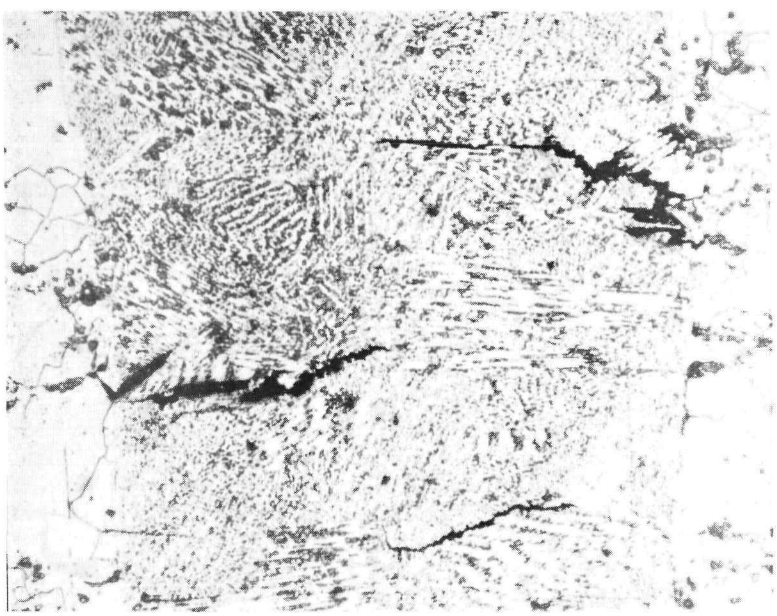

100X

Figure S-93A. Magnified View of the Cracked Area Shown in Figure S-93. Note that the Cracks Appear to Extend into the Grain Boundaries of the Base Material

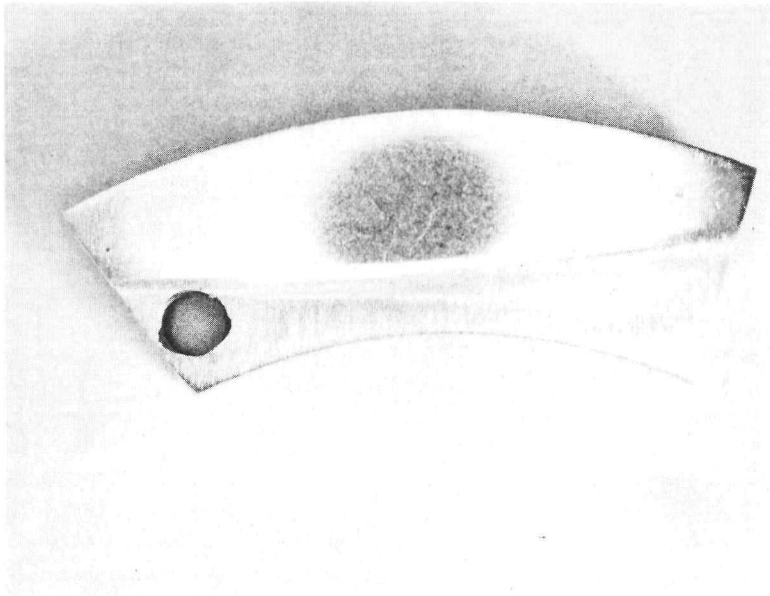

2X

Figure S-106. Inner Liner #3 — Sample #1
Cross Section Showing Porosity
as Indicated by Radiography
Porosity Size -
0. 030 x 0. 028 Max Porosity
0. 012 x 0. 017 Min Porosity

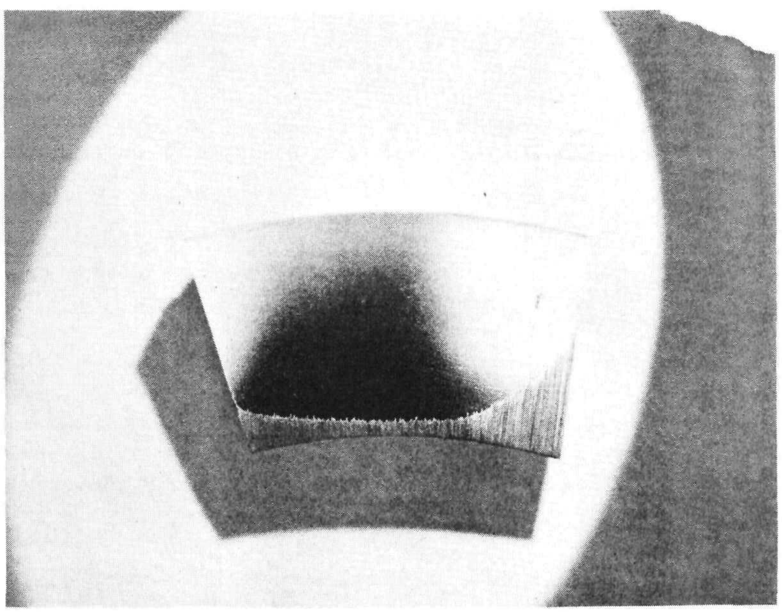

2X

Figure S-107. Inner Liner #3 — Sample #2
Cross Section Showing Porosity
as Indicated by Radiography
Porosity Size -
0. 014 x 0. 0465 Max Porosity